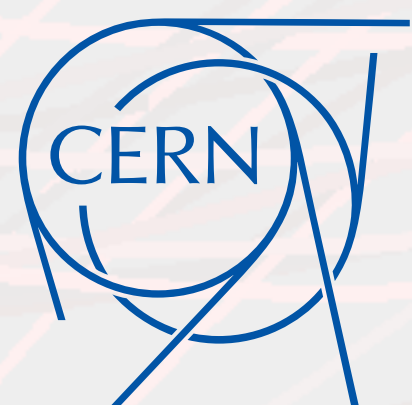
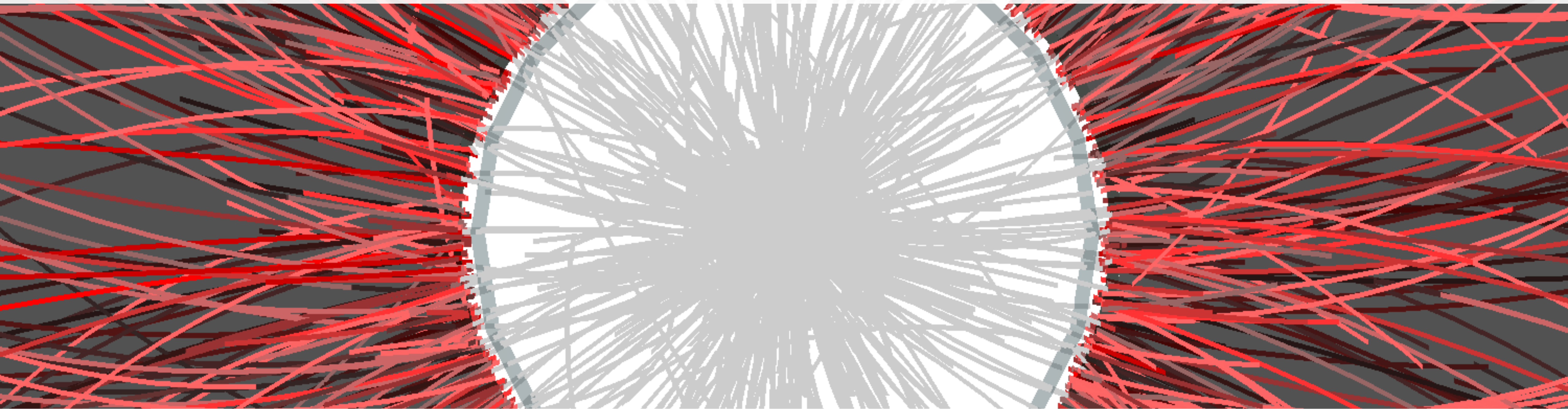


Measurements of hadronic interactions between light and charm hadrons with femtoscopy

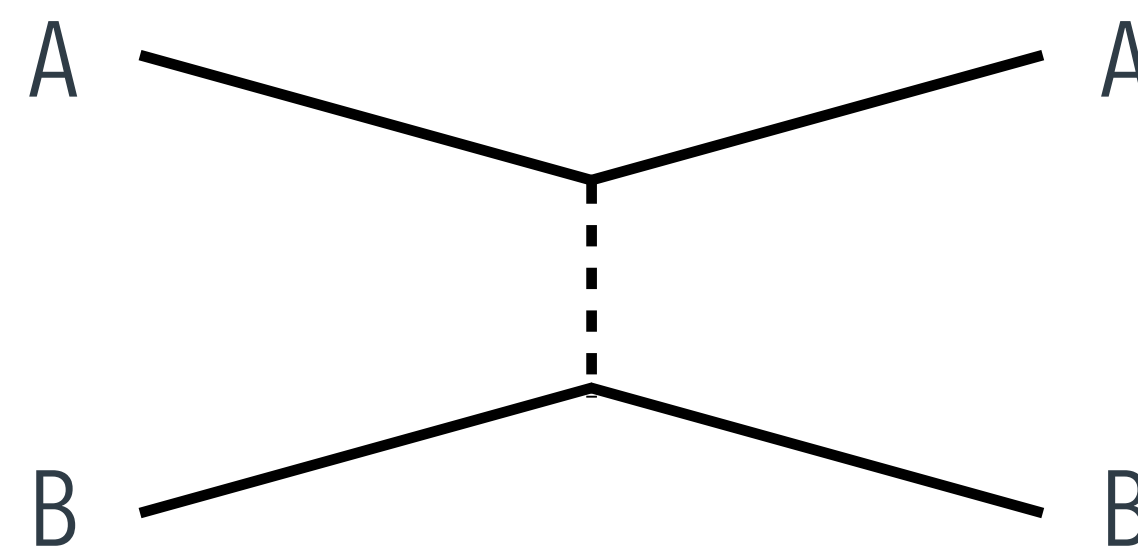


Fabrizio Grosa
CERN

GDR-QCD, GDR-Inf and Gluodynamics workshop
Spectroscopy in decays & in femtosopic correlations
Orsay, Paris | 16–17 December 2024

- Physics motivations for **D-meson – hadron femtoscopy**
 - Study **residual strong interaction**
 - Assess role of **hadronic phase in heavy-ion collisions**
- **Measurements of D-meson – hadron interactions** from ALICE
 - Study residual strong interaction
- Future perspectives
 - Interaction between charm baryons and nucleons to investigate the possible existence of **charmed nuclei**
 - Interaction between two charm hadrons to study nature of **recently discovered exotic states**

- Traditional method to study hadron-hadron interaction: **scattering experiments**



S. Navas et al. (PDG), PRD 110 (2024) 030001

Hadron	$c\tau$ (μm)
D^0	121
D^+	312
D_s^+	150
Λ_c^+	63

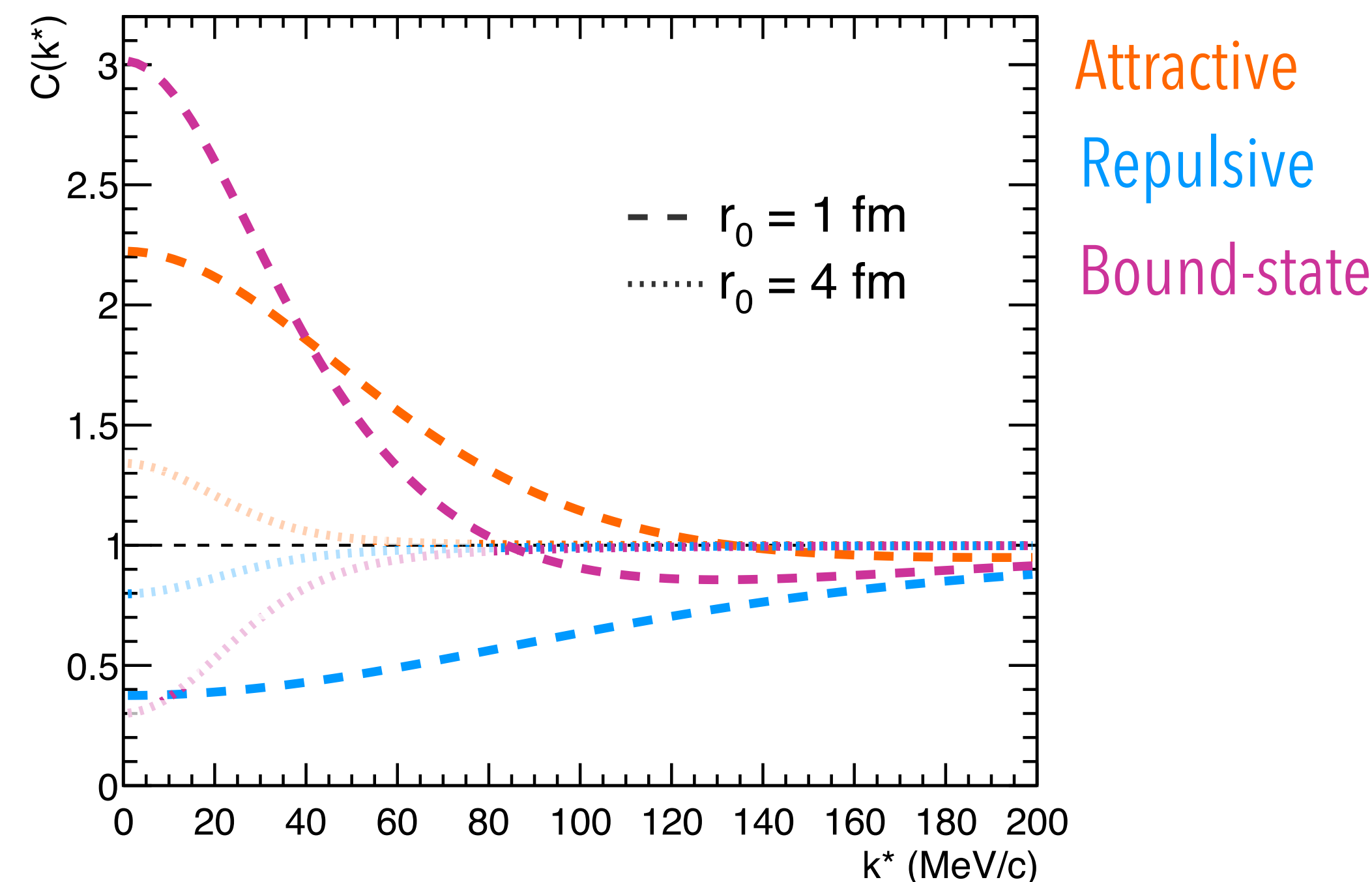
- Experimental challenge in case of **charm hadrons** due to their short lifetime
 → **Femtoscopy** is a very powerful tool to study hadron interaction at colliders

$$C(\vec{k}^*) = \underbrace{\mathcal{N} \frac{N_{\text{same}}^{\text{pairs}}(k^*)}{N_{\text{mixed}}^{\text{pairs}}(k^*)}}_{\text{Experiment}} = \underbrace{\int S(\vec{r}^*) |\psi(\vec{k}^*, \vec{r}^*)|^2 d^3 r^*}_{\text{Theory}}$$

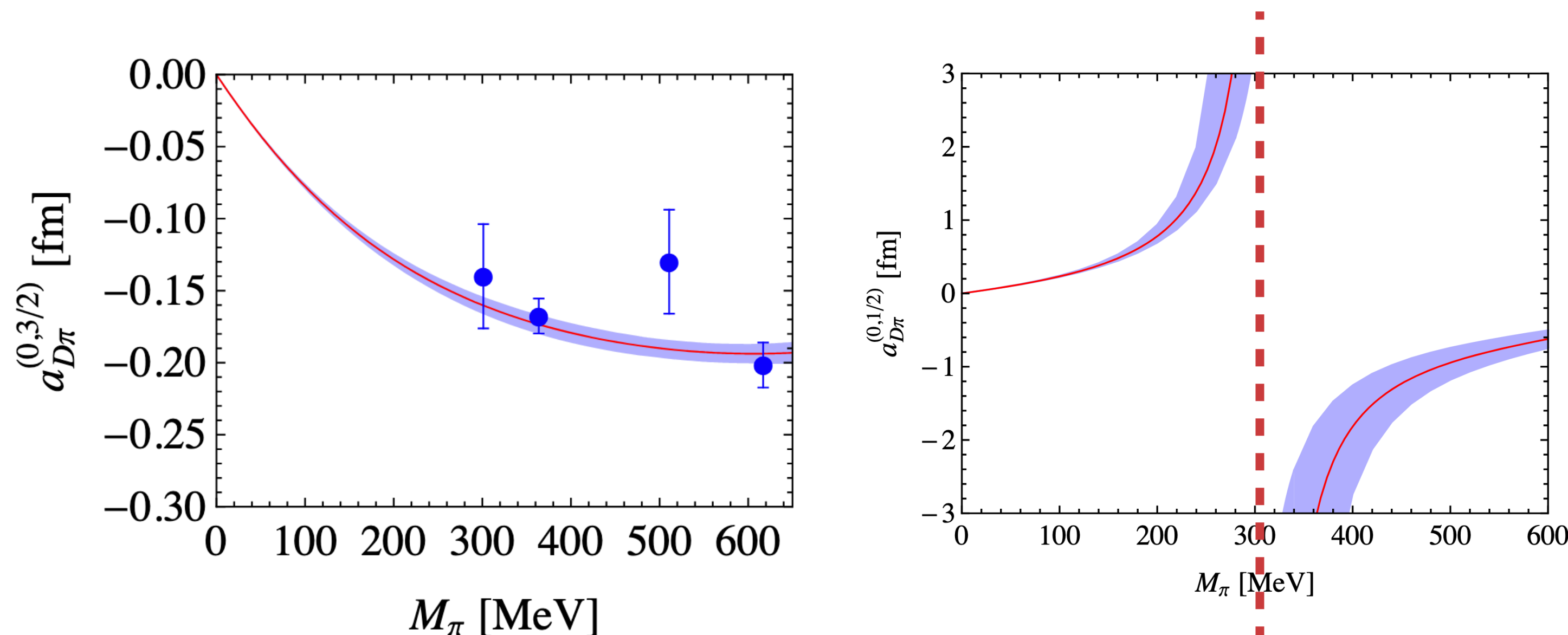
Koonin-Pratt equation

M. Lisa, S. Pratt et al, Ann.Rev.Nucl.Part.Sci. 55 (2005) 357–402

where $\vec{k}^* = \frac{\vec{p}_a^* - \vec{p}_b^*}{2}$ is in the rest frame of the particle pair



- Theory predictions based on **lattice QCD calculations** for the determination of low energy constants (i.e. **scattering length a**) + **unitarized chiral perturbation theory** for the extrapolation to the physical pion mass



- Example: $D\pi$ interaction via two isospin channels
 - ➔ $I = 3/2$ purely elastic
 - ➔ $I = 1/2$ inelastic, with several **coupled channels**

Strangeness

$(0, \frac{1}{2})$

↑
Isospin

$D\pi \rightarrow D\pi$

$D\eta \rightarrow D\eta$

$D_s\bar{K} \rightarrow D_s\bar{K}$

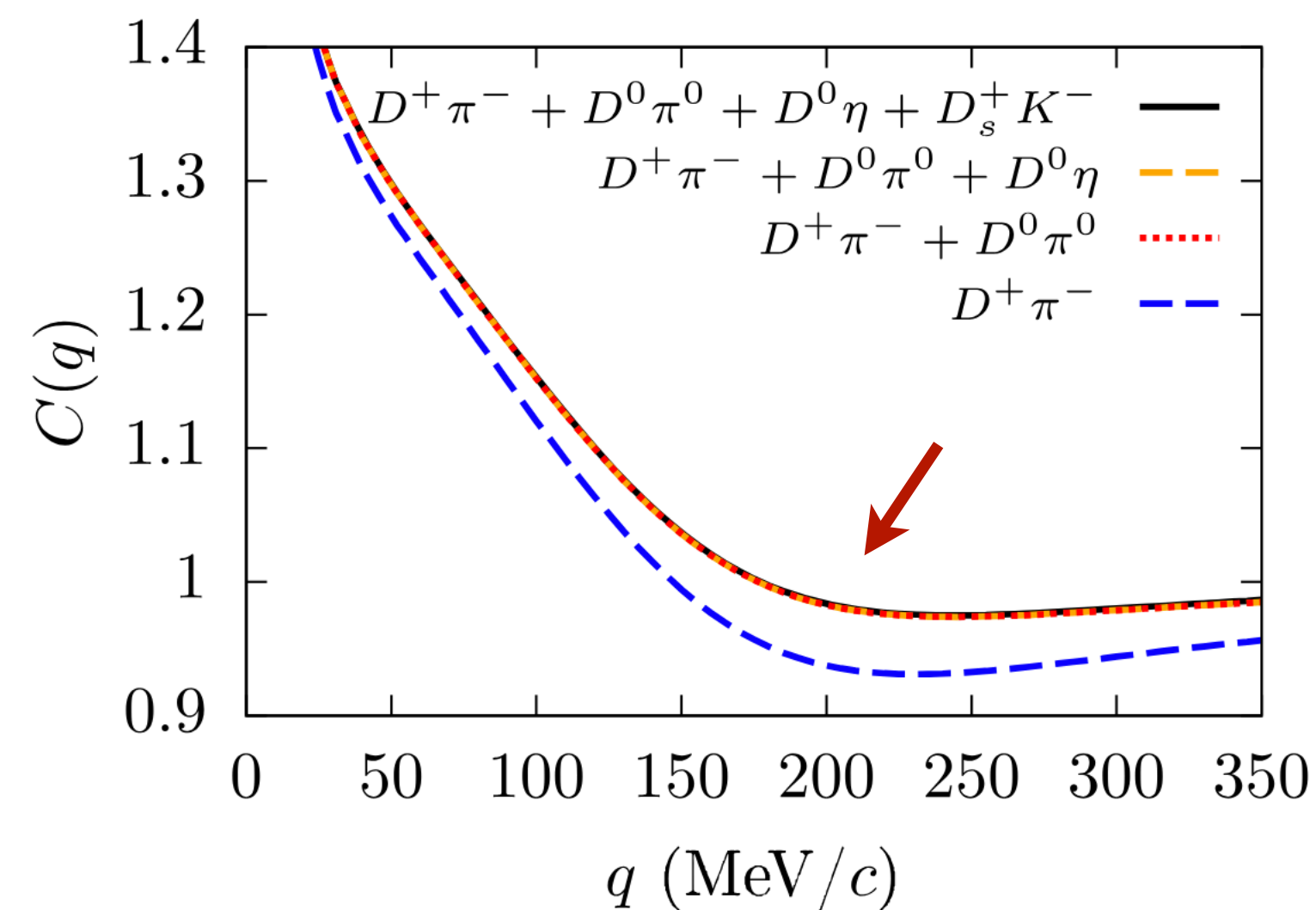
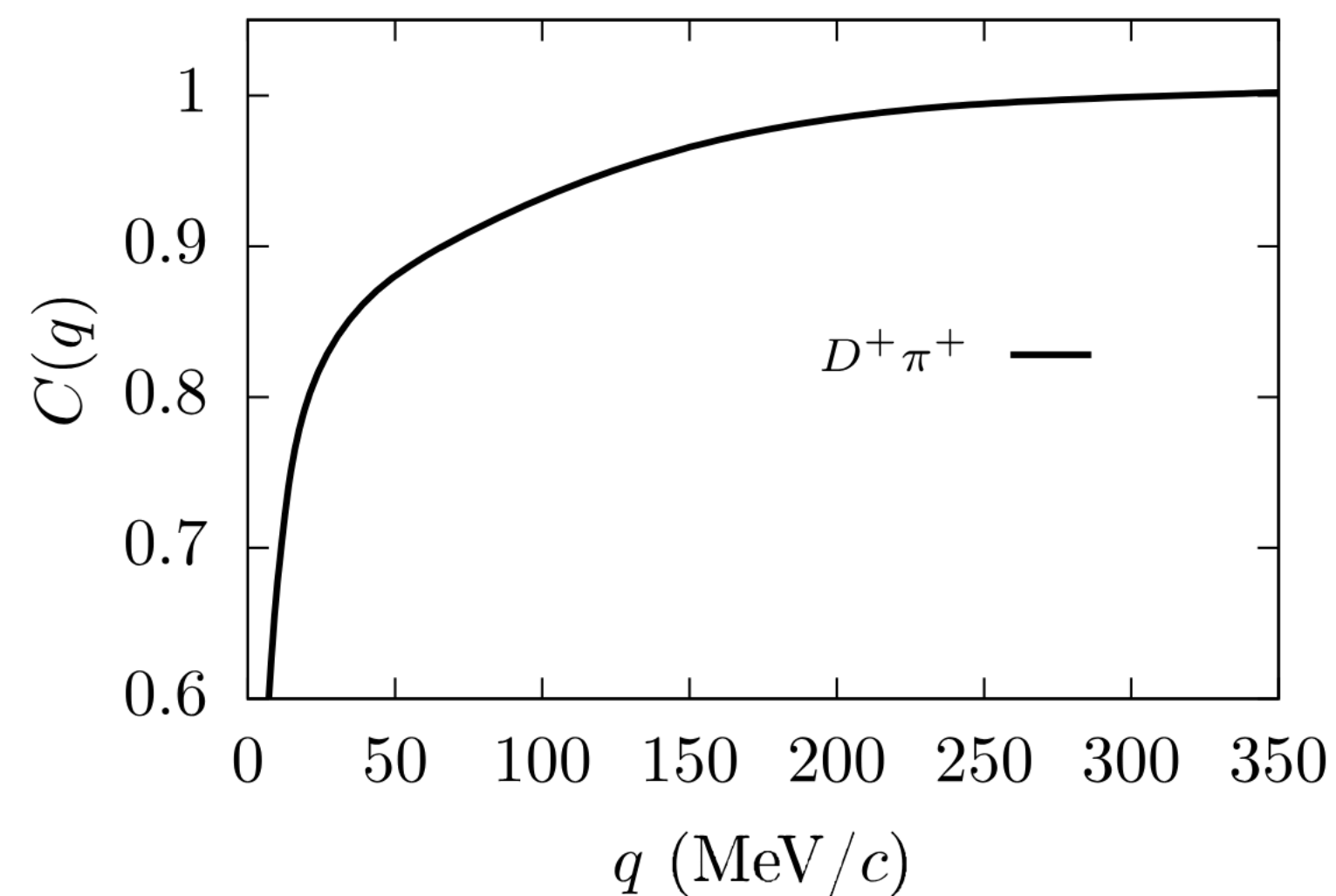
$D\eta \rightarrow D\pi$

$D_s\bar{K} \rightarrow D\pi$

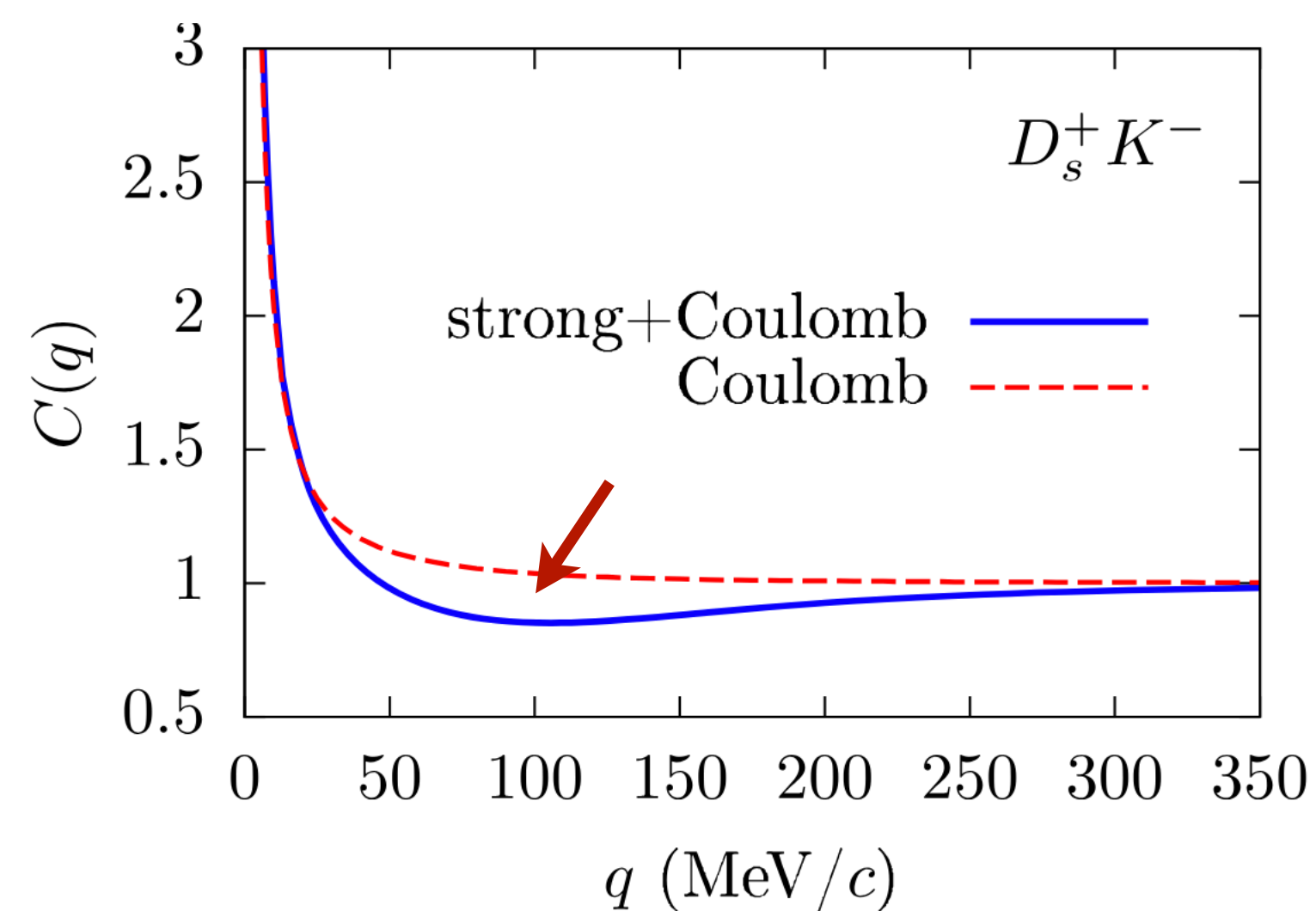
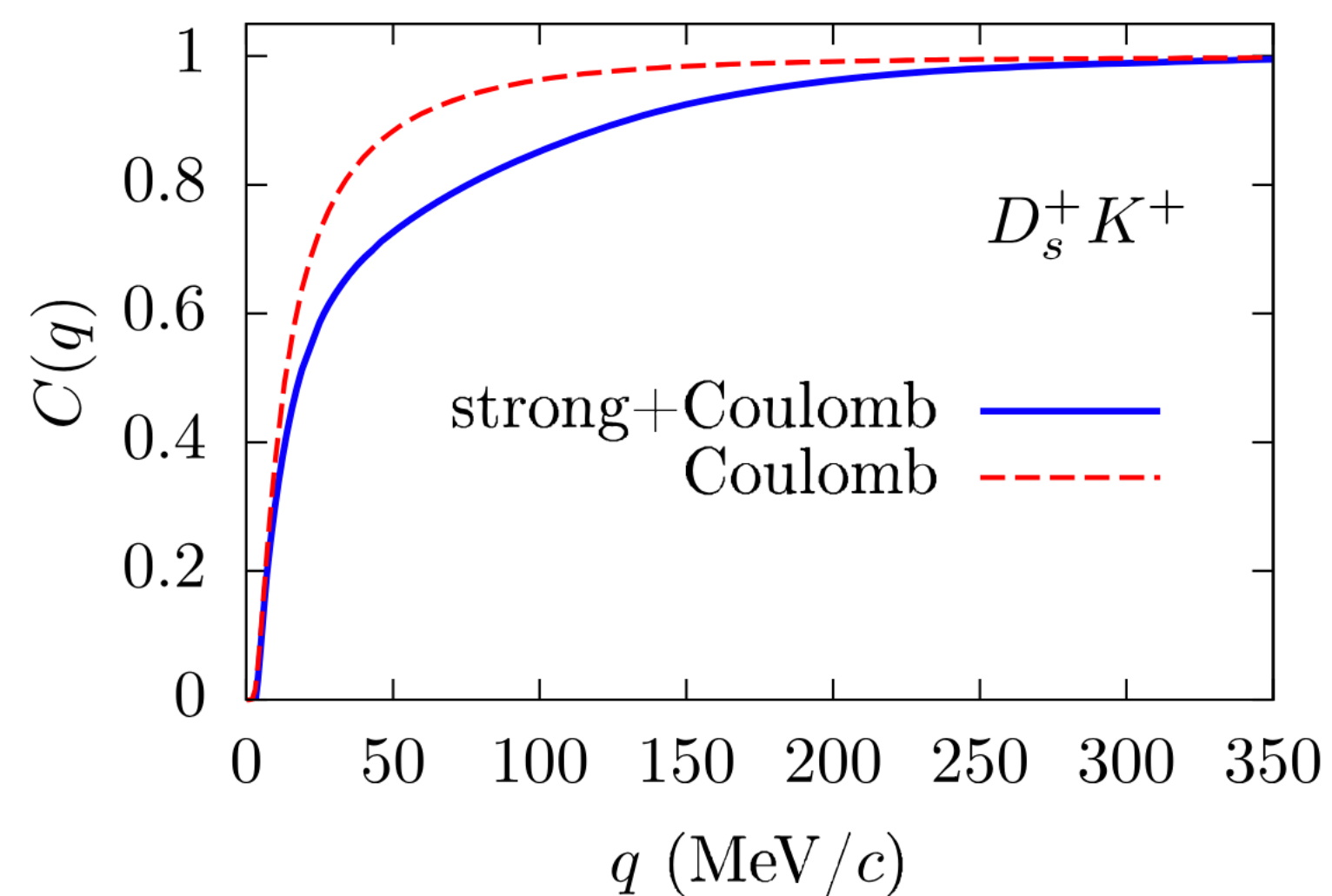
$D_s\bar{K} \rightarrow D\eta$

- Inelastic interactions might also lead to the formation of dynamical / molecular states
 - ➔ I.e. $D_0^*(2300)$ in unitarized chiral perturbation theory, is a two-pole structure dynamically formed by $D\pi$ and $D_s\bar{K}$ interactions
 - ➔ **Impact the correlation function** measured with femtoscopy

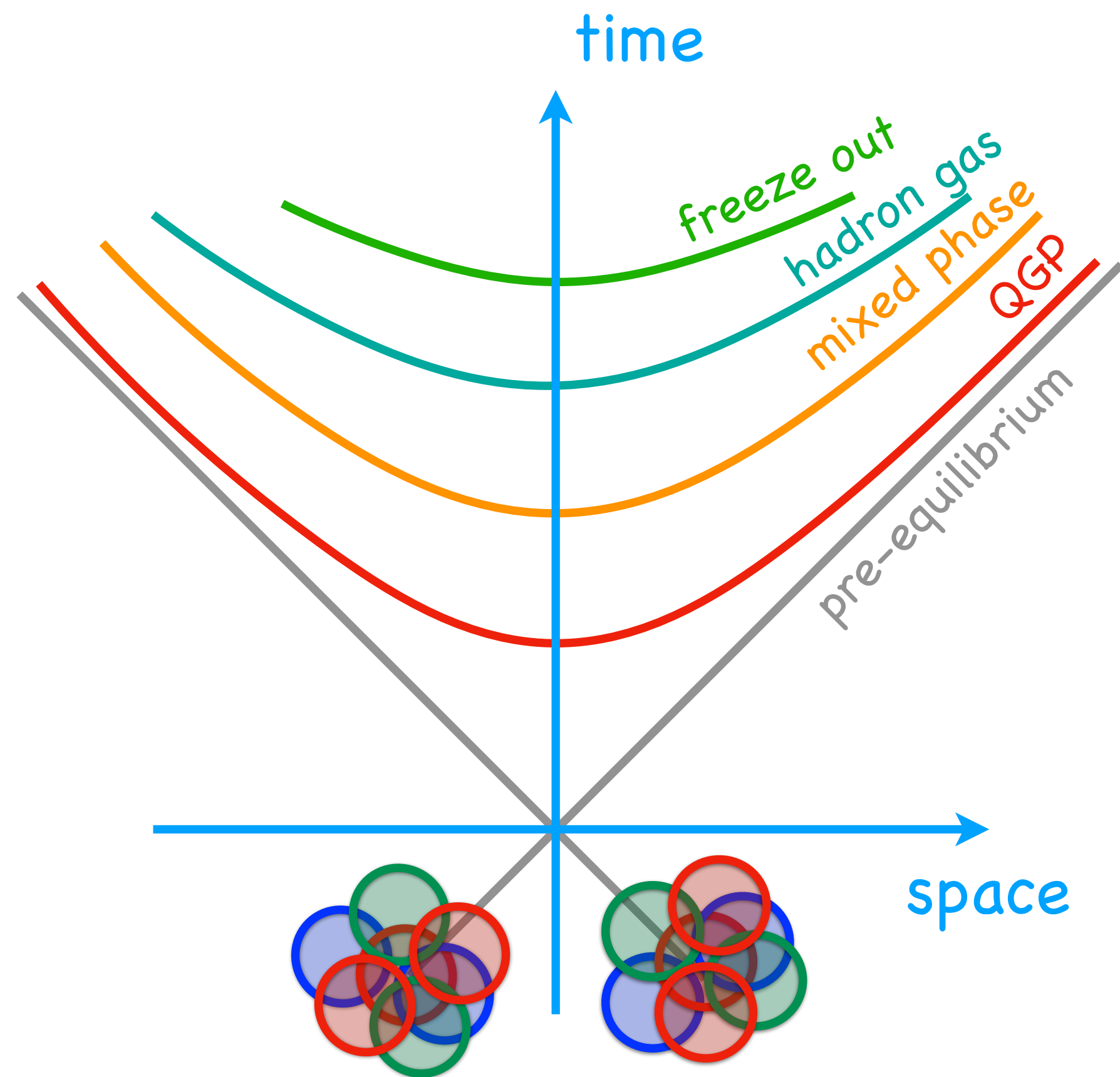
J.M. Torres-Rincon et al, PRD 108 (2023) 096008



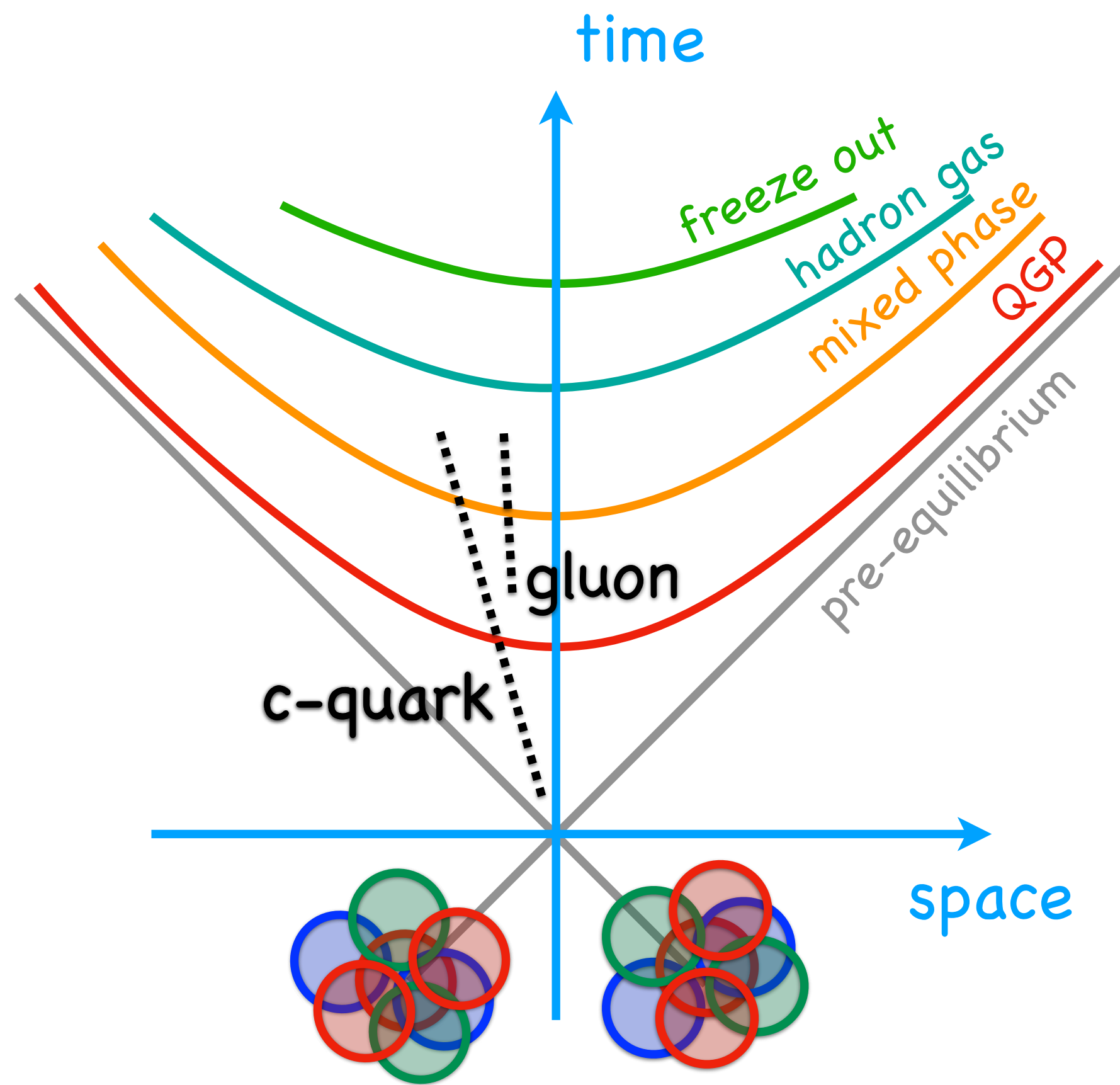
- In the $D\pi$ correlation function expected sizeable effect due to couple channels
- ➔ Depletion around 200 MeV due to quasi-bound state (first pole of $D_0^*(2300)$) compensated by couple channels



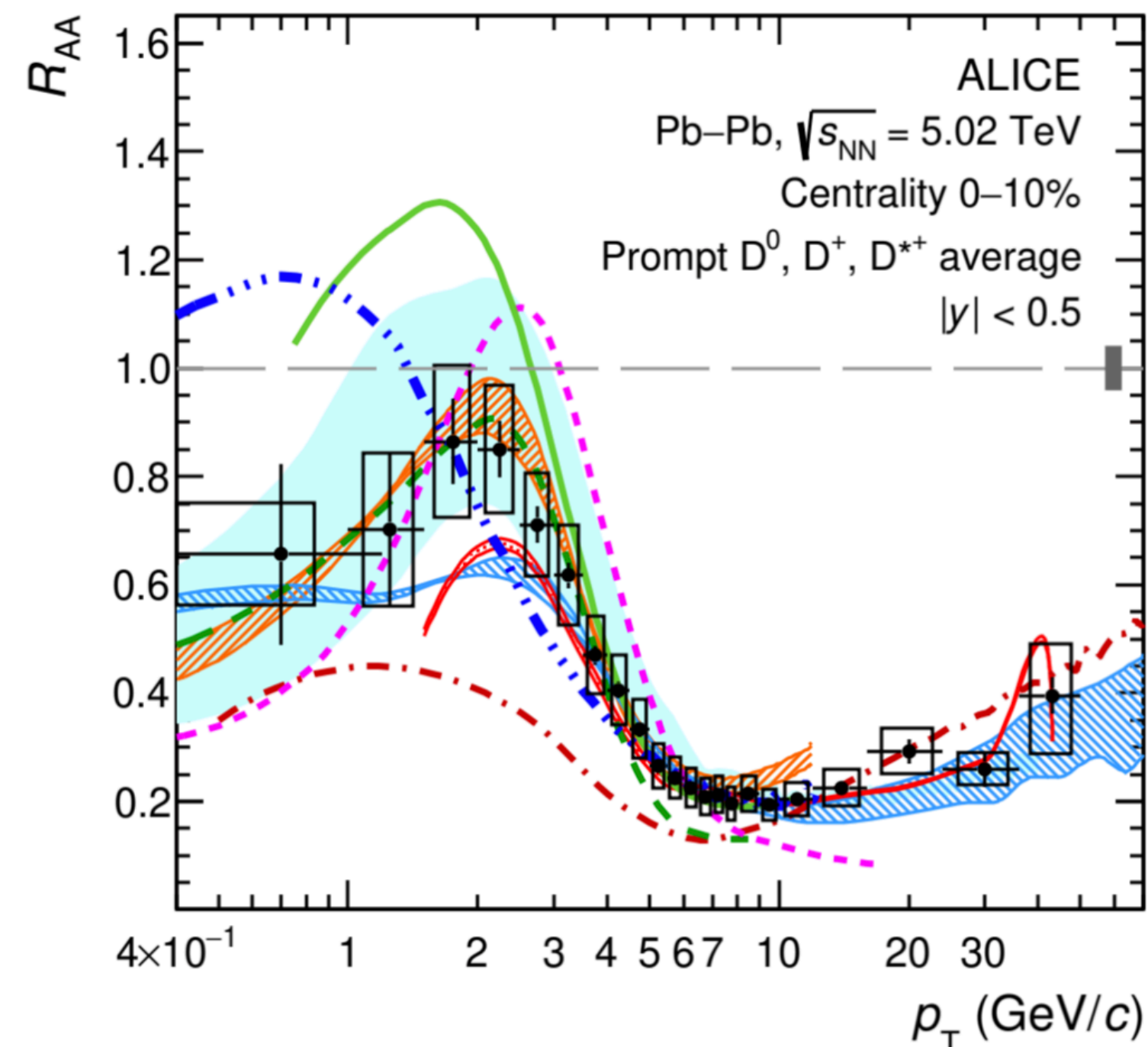
- Similar depletion expected in $D_s\bar{K}$ correlation function due to the second pole



- QCD calculations on lattice predict a phase transition from the ordinary nuclear matter to a **colour-deconfined medium**, called **quark-gluon plasma** (QGP)
 - created in **ultra-relativistic heavy-ion collisions**
 - **very high energy density $\varepsilon > 15 \text{ GeV}/\text{fm}^3$**
 - after a pre-equilibrium phase **expands hydrodynamically**



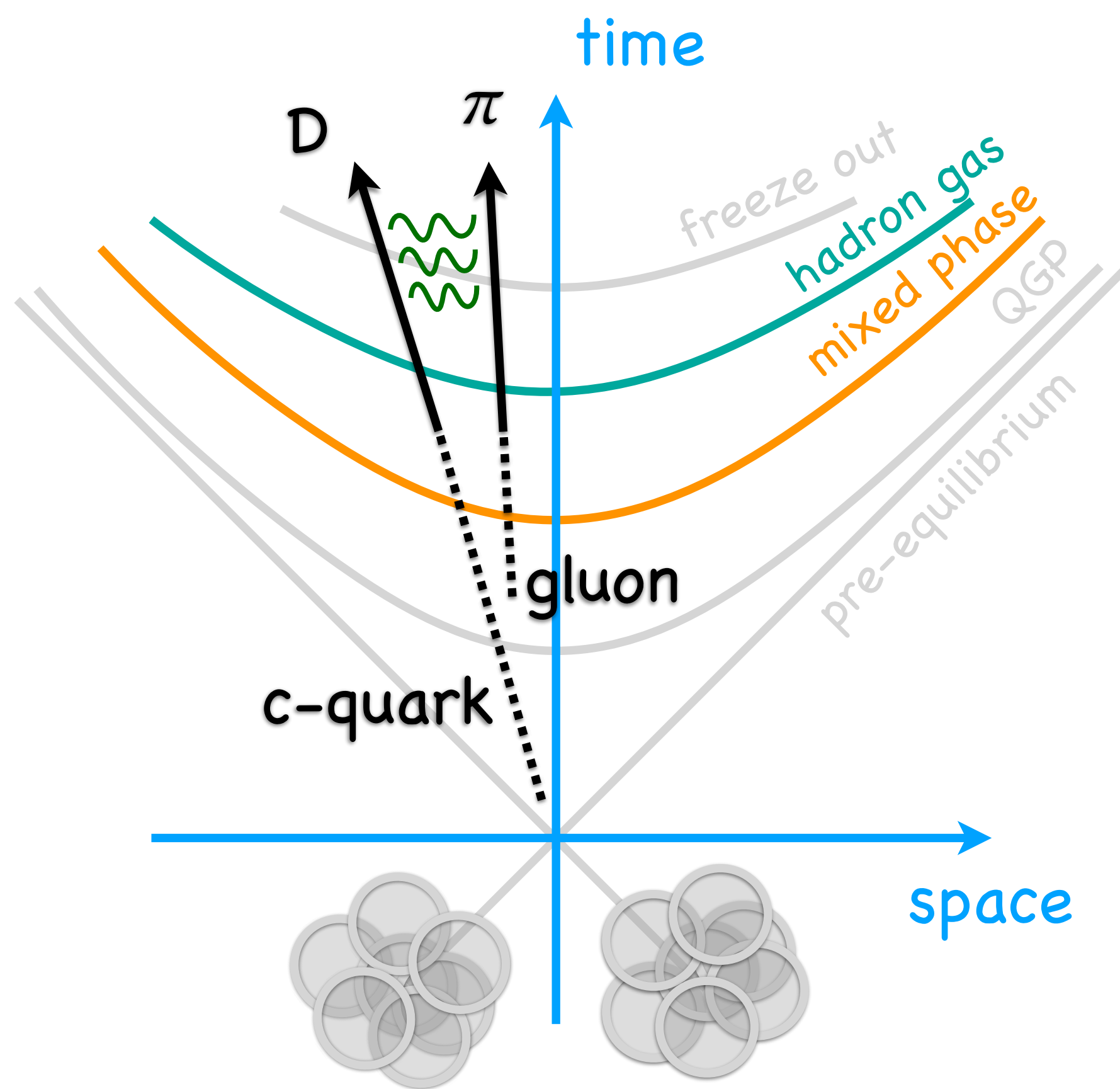
- QCD calculations on lattice predict a phase transition from the ordinary nuclear matter to a **colour-deconfined medium**, called **quark-gluon plasma** (QGP)
- Charm quarks: produced in hard scatterings before the formation of the QGP, subsequently interact with the medium constituents
 ➔ **Ideal probes of the QGP**



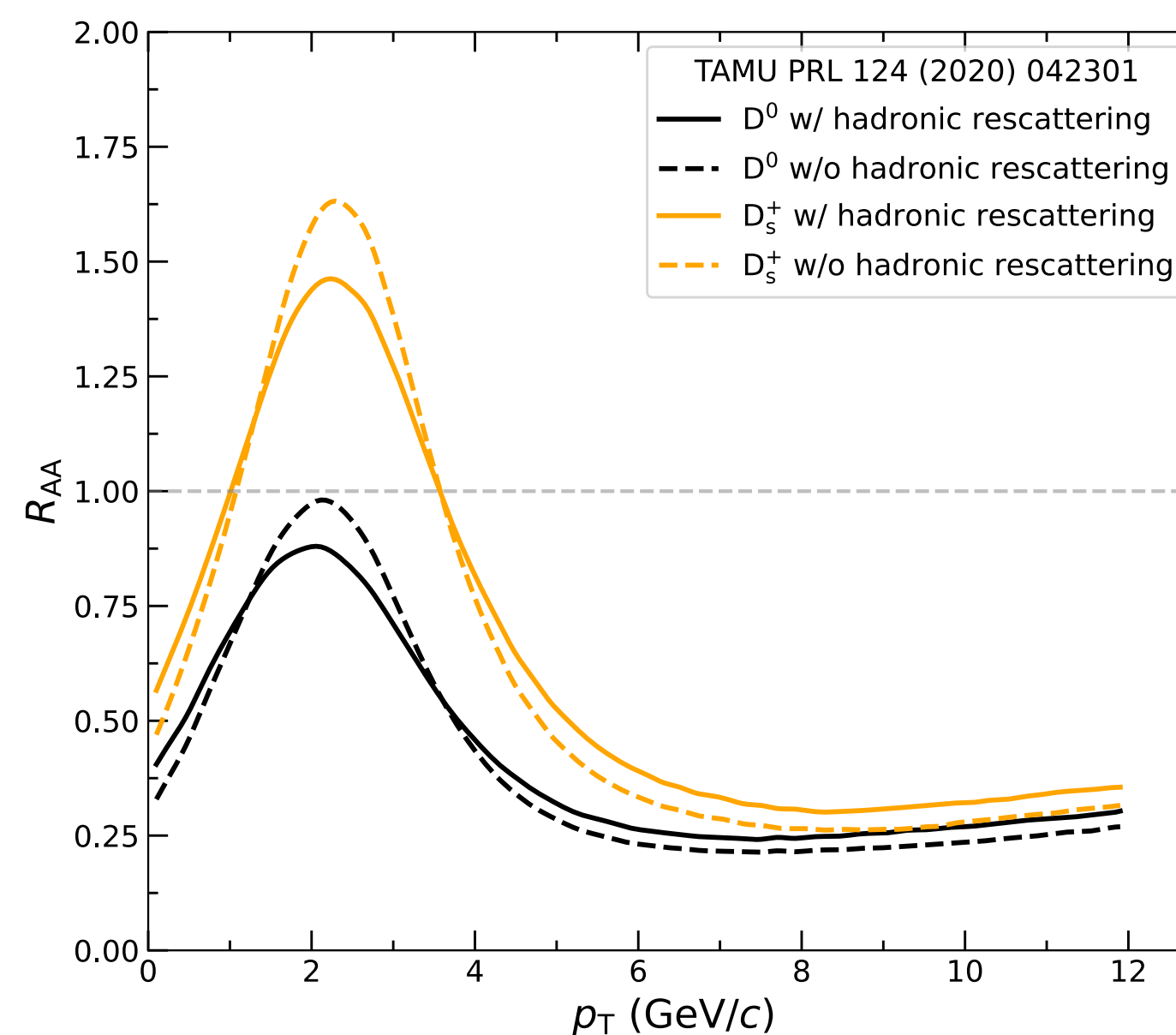
Nuclear modification factor

$$R_{AA}(p_T) = \frac{1}{\langle N_{\text{coll}} \rangle} \frac{dN_{AA}/dp_T}{dN_{pp}/dp_T}$$

Comparison with models based on **charm-quark transport** in the QGP to infer properties of the interaction between charm quarks and the medium



- QCD calculations on lattice predict a phase transition from the ordinary nuclear matter to a **colour-deconfined medium**, called **quark-gluon plasma** (QGP)
- Charm quarks: produced in hard scatterings before the formation of the QGP, subsequently interact with the medium constituents
- After the hadronisation, charm hadrons might still interact with the light hadrons produced
 - ➔ How much **hadronic rescatterings** influence our observables?



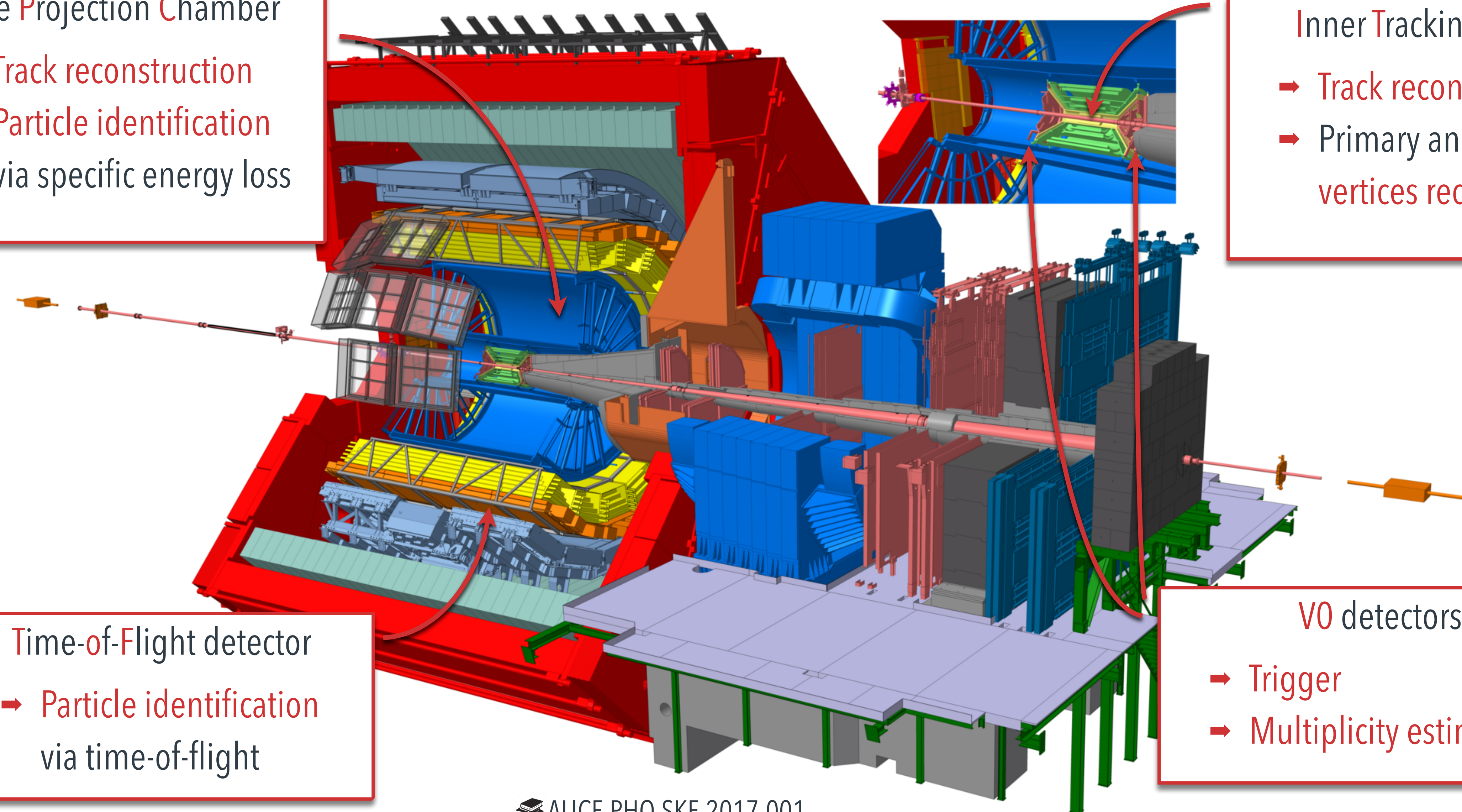
- In the TAMU model the scattering lengths used for πD and $\bar{K} D$ are:
 - ➔ $a_{\pi D}(l=3/2) = -0.10$ fm
 - ➔ $a_{\bar{K} D}(l=1) = -0.22$ fm
 - ➔ **No experimental constraints**

Time Projection Chamber

- Track reconstruction
- Particle identification via specific energy loss

Inner Tracking System

- Track reconstruction
- Primary and decay vertices reconstruction



Time-of-Flight detector

- Particle identification via time-of-flight

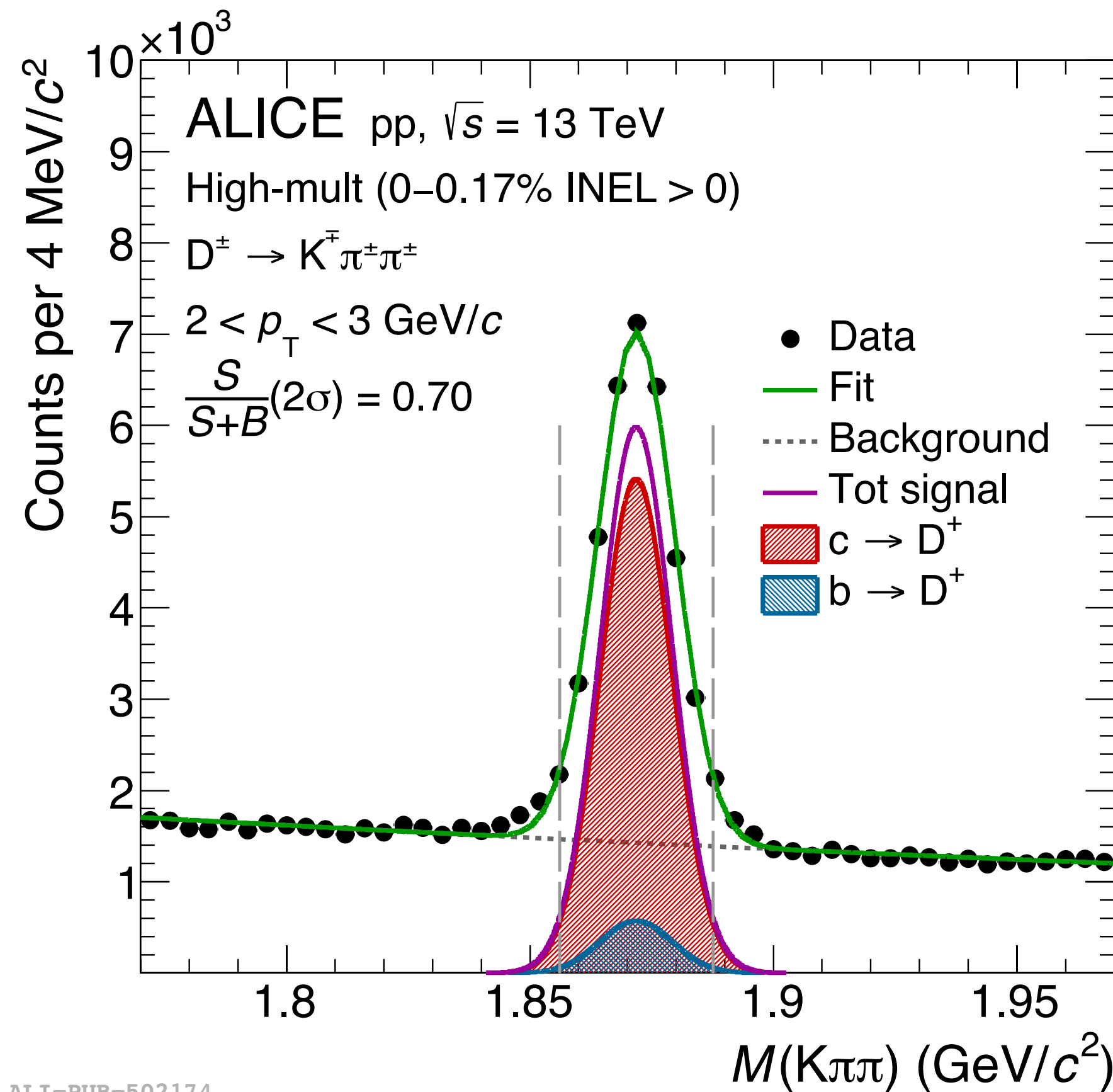
V0 detectors

- Trigger
- Multiplicity estimation

Hadron	Decay	Branching Ratio (%)
D^{*+}	$D^0(\rightarrow K^-\pi^+)\pi^+$	2.67 ± 0.02
D^+	$K^-\pi^+\pi^+$	9.38 ± 0.16

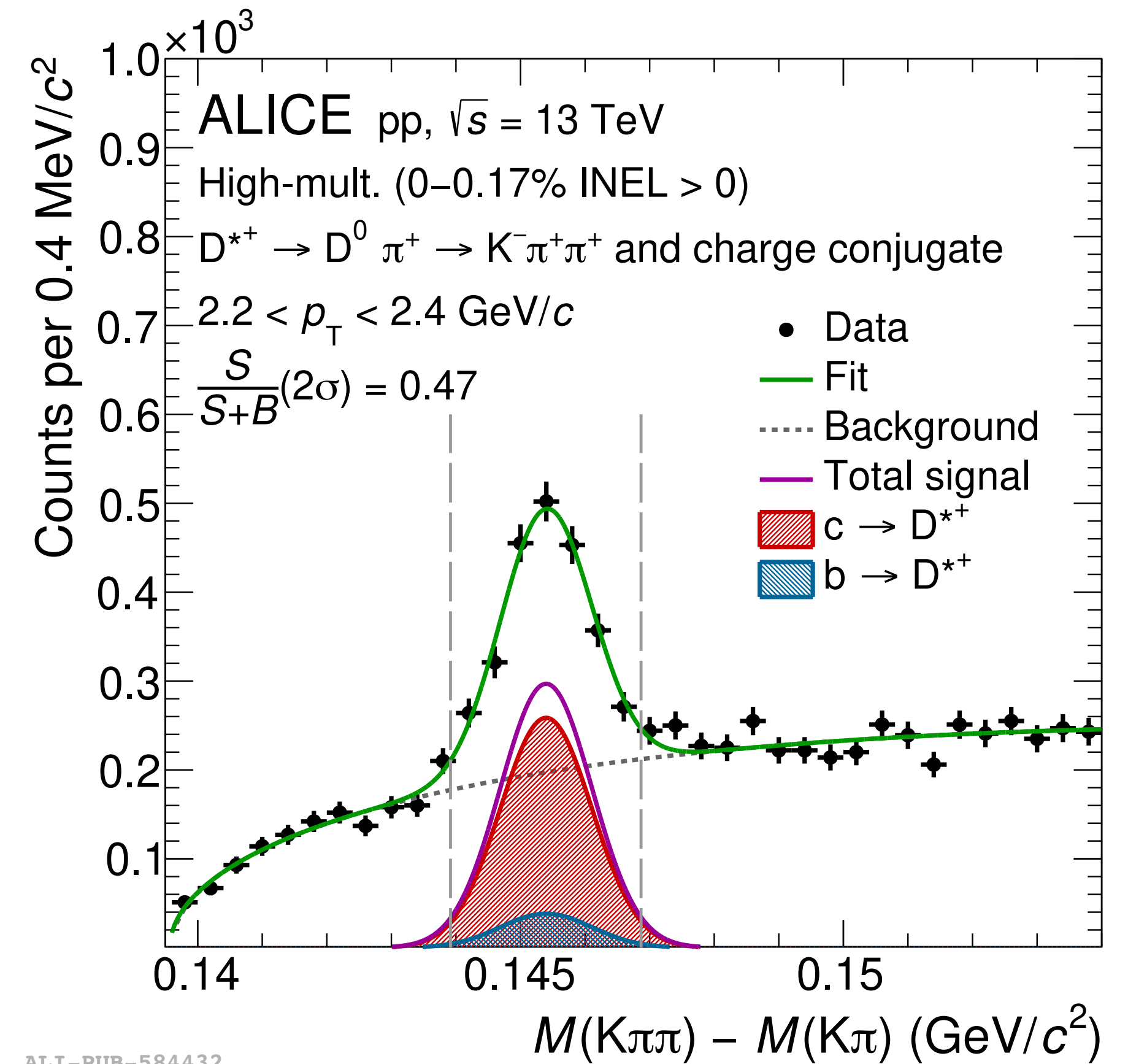
S. Navas et al. (PDG), PRD 110 (2024) 030001

- High-multiplicity data collected during LHC Run 2 ($L_{int} \approx 6 \text{ pb}^{-1}$)
- Fully reconstructed displaced decay topologies
- **Topological** and **particle-identification** (PID) selections applied to reduce combinatorial background



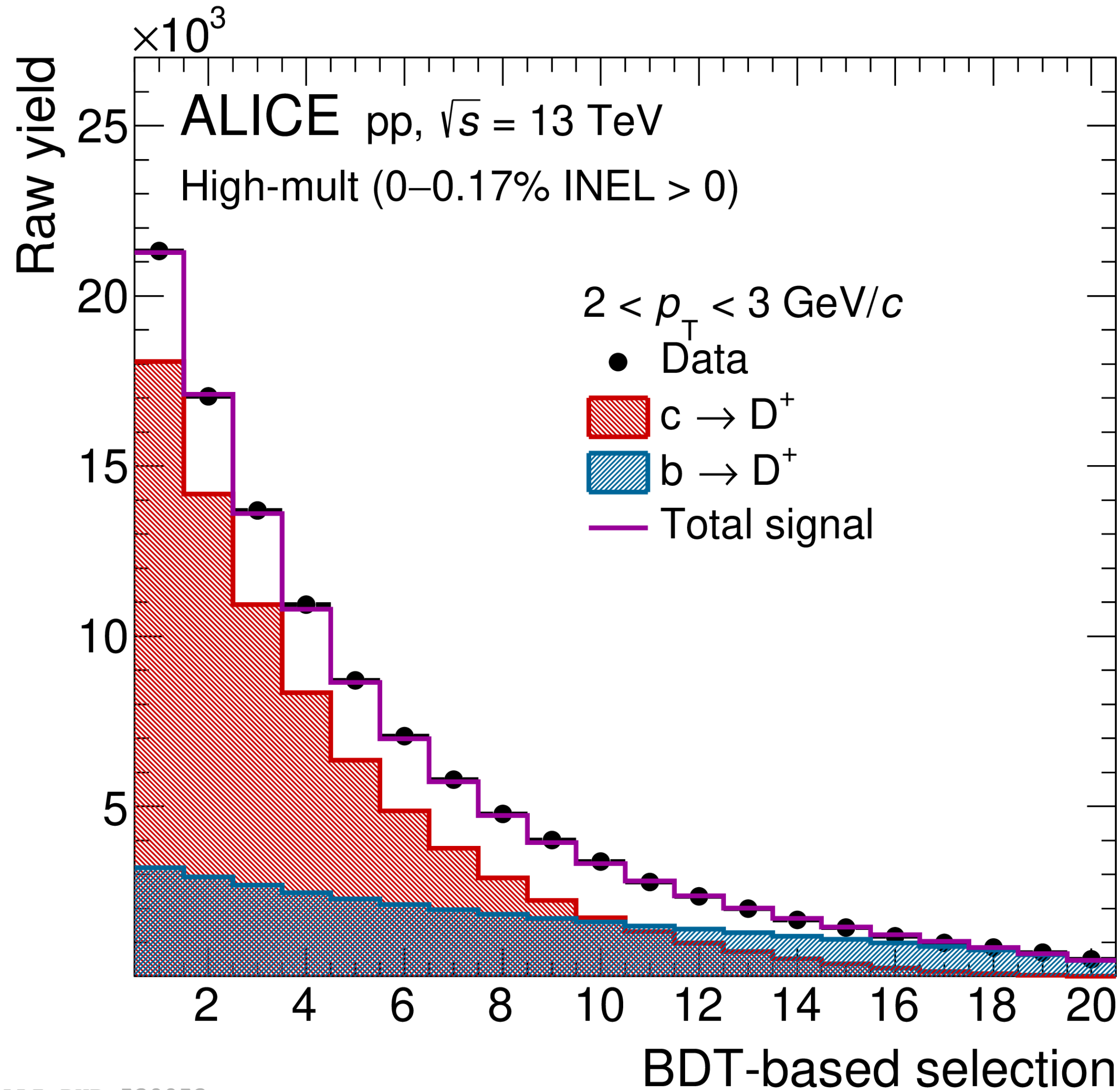
ALI-PUB-502174

ALICE, PRD 106 (2022) 052010



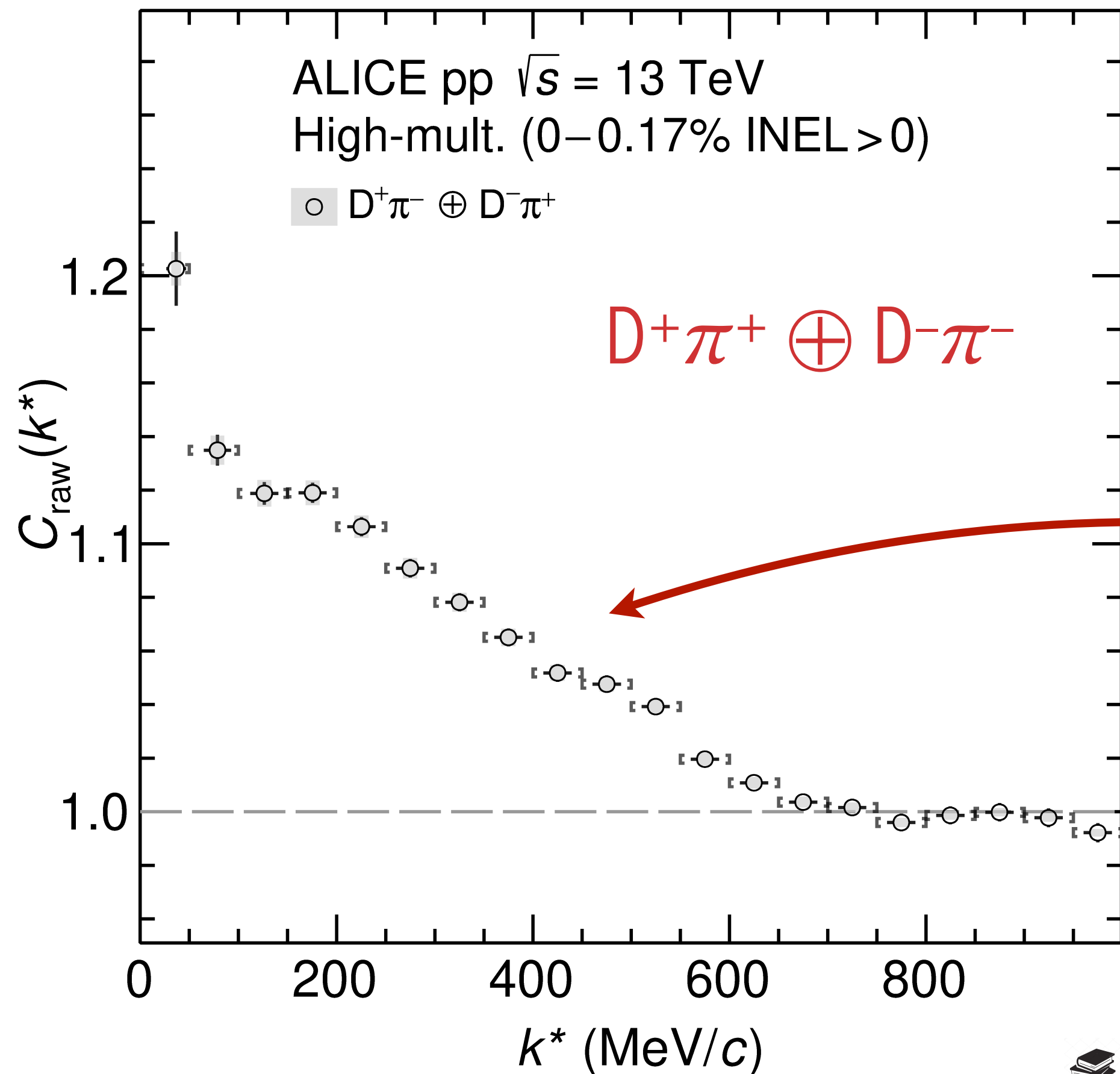
ALI-PUB-584432

ALICE, PRD 110 (2024) 032004



- Multi-class BDT classifier adopted to select D mesons and classify them as:
 - ➔ Background
 - ➔ **Prompt D mesons** (charm origin)
 - ➔ **Non-prompt D mesons** (beauty decays)
- Template fit of the raw-yield distribution obtained by sampling the BDT score rated to the probability to be non-prompt D meson
 - ➔ Provide fraction of D mesons for any given selection applied

$$C(\vec{k}^*) = \mathcal{N} \frac{N_{\text{same}}^{\text{D}\pi}(k^*)}{N_{\text{mixed}}^{\text{D}\pi}(k^*)} =$$



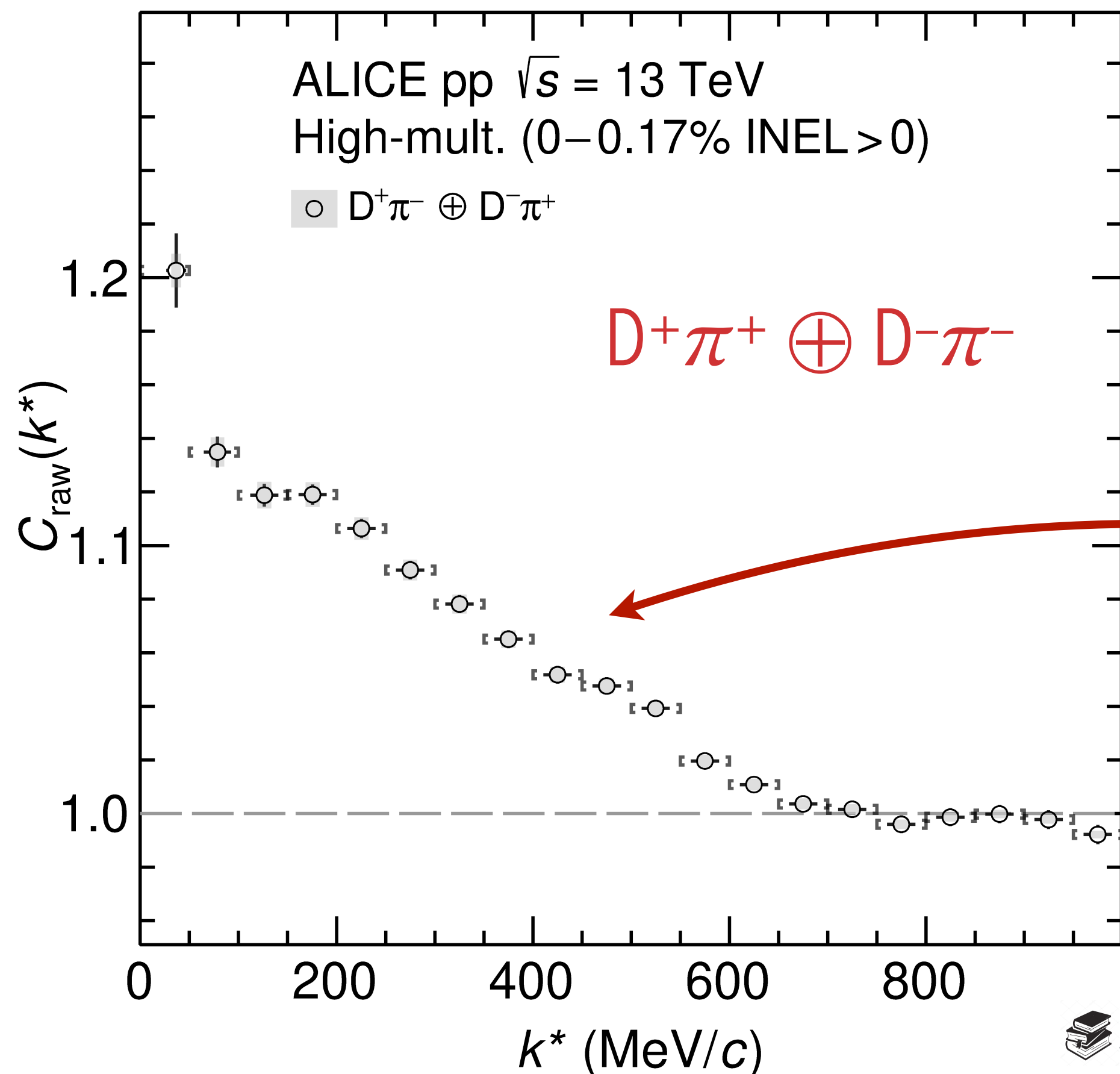
- Example: $D^\pm\pi^\mp$ candidate pairs

- ➔ D^\pm candidates selected in invariant-mass region of the signal (residual combinatorial background to be subtracted)
- ➔ Pion sample selected with PID in TPC and TOF (>99% purity)

Slow rise towards low k^* due to jet-induced momentum correlations (Parton shower)

Flat at unity for large k^* (no interaction)

$$C(\vec{k}^*) = \mathcal{N} \frac{N_{\text{same}}^{\text{D}\pi}(k^*)}{N_{\text{mixed}}^{\text{D}\pi}(k^*)} = \lambda_{\text{SB}} C_{\text{SB}}(k^*) + C_{\text{non-femto}}(k^*) \cdot [\lambda_{\text{genuine}} C_{\text{genuine}}(k^*) + \lambda_{\text{D}^+\leftarrow\text{D}^*} C_{\text{D}^+\leftarrow\text{D}^*} + \lambda_{\text{flat}}]$$



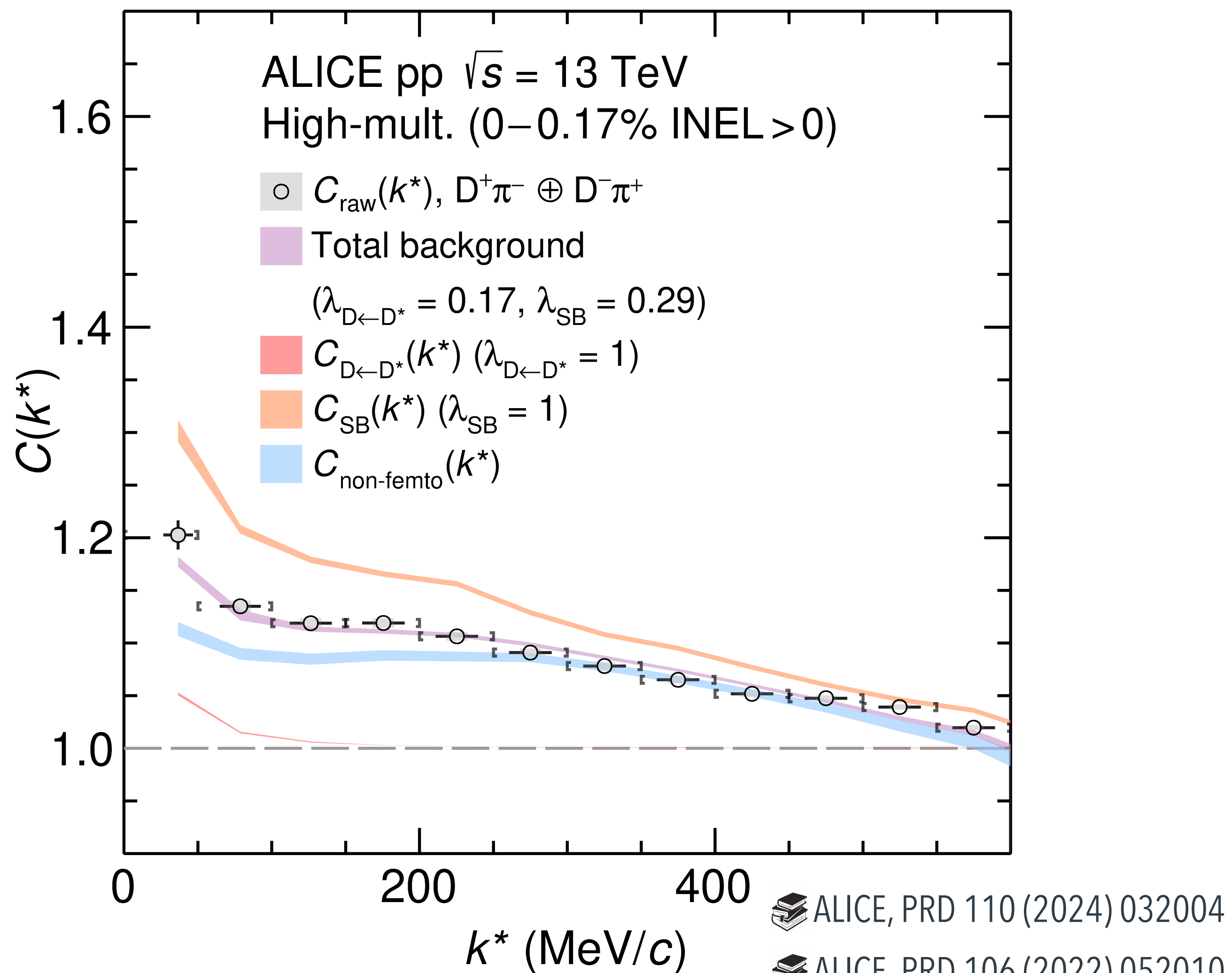
- Example: $\text{D}^\pm\pi^\mp$ candidate pairs

- ➔ D^\pm candidates selected in invariant-mass region of the signal (residual combinatorial background to be subtracted)
- ➔ Pion sample selected with PID in TPC and TOF (>99% purity)

Slow rise towards low k^* due to jet-induced momentum correlations (Parton shower)

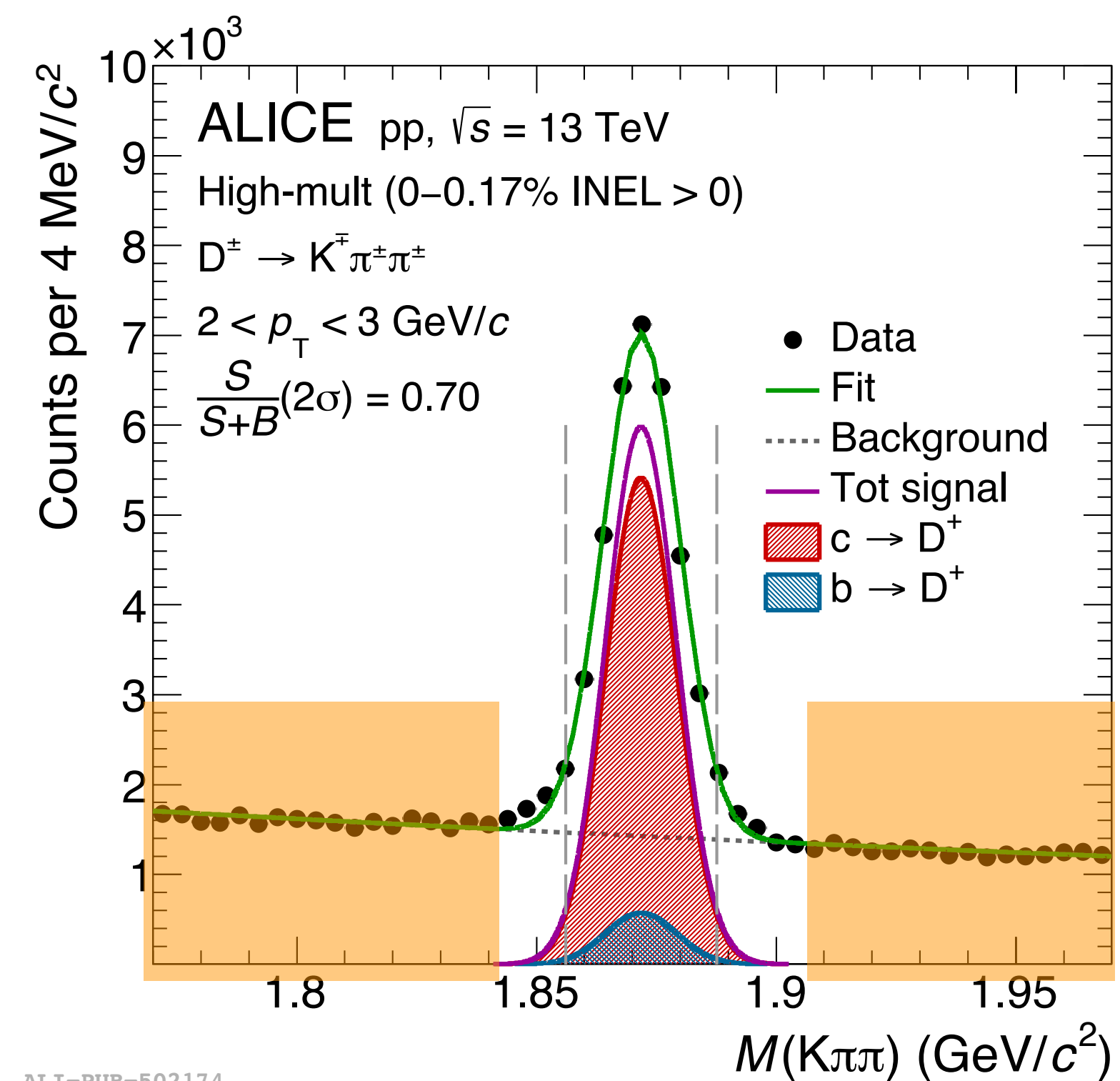
Flat at unity for large k^* (no interaction)

$$C_{\text{raw}}(\vec{k}^*) = \lambda_{\text{SB}} C_{\text{SB}}(k^*) + C_{\text{non-femto}}(k^*) \cdot [\lambda_{\text{genuine}} C_{\text{genuine}}(k^*) + \lambda_{\text{D}^+ \leftarrow \text{D}^*} C_{\text{D}^+ \leftarrow \text{D}^*} + \lambda_{\text{flat}}]$$

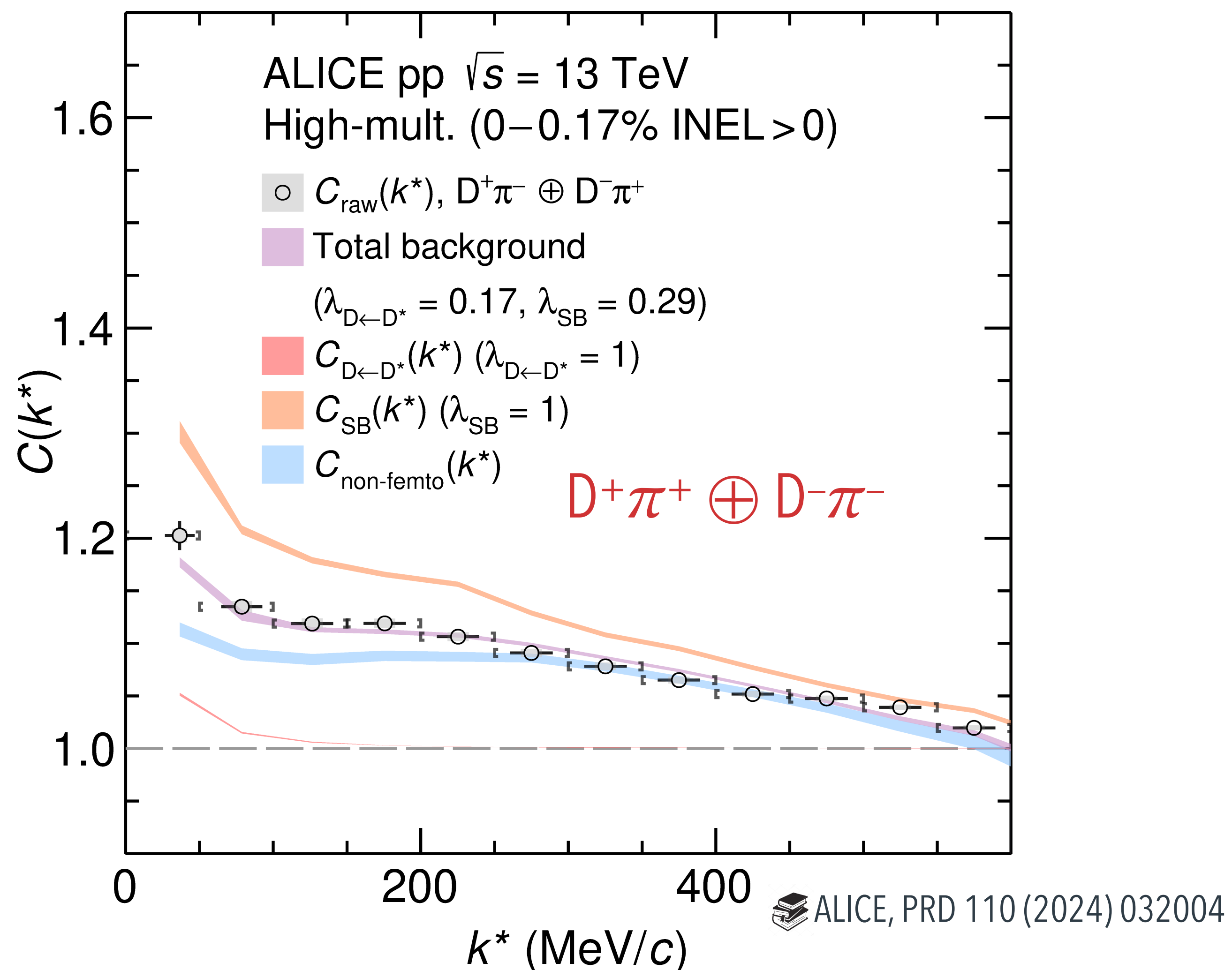


- Raw correlation function includes different sources of backgrounds

- Combinatorial background estimated from D-meson sidebands



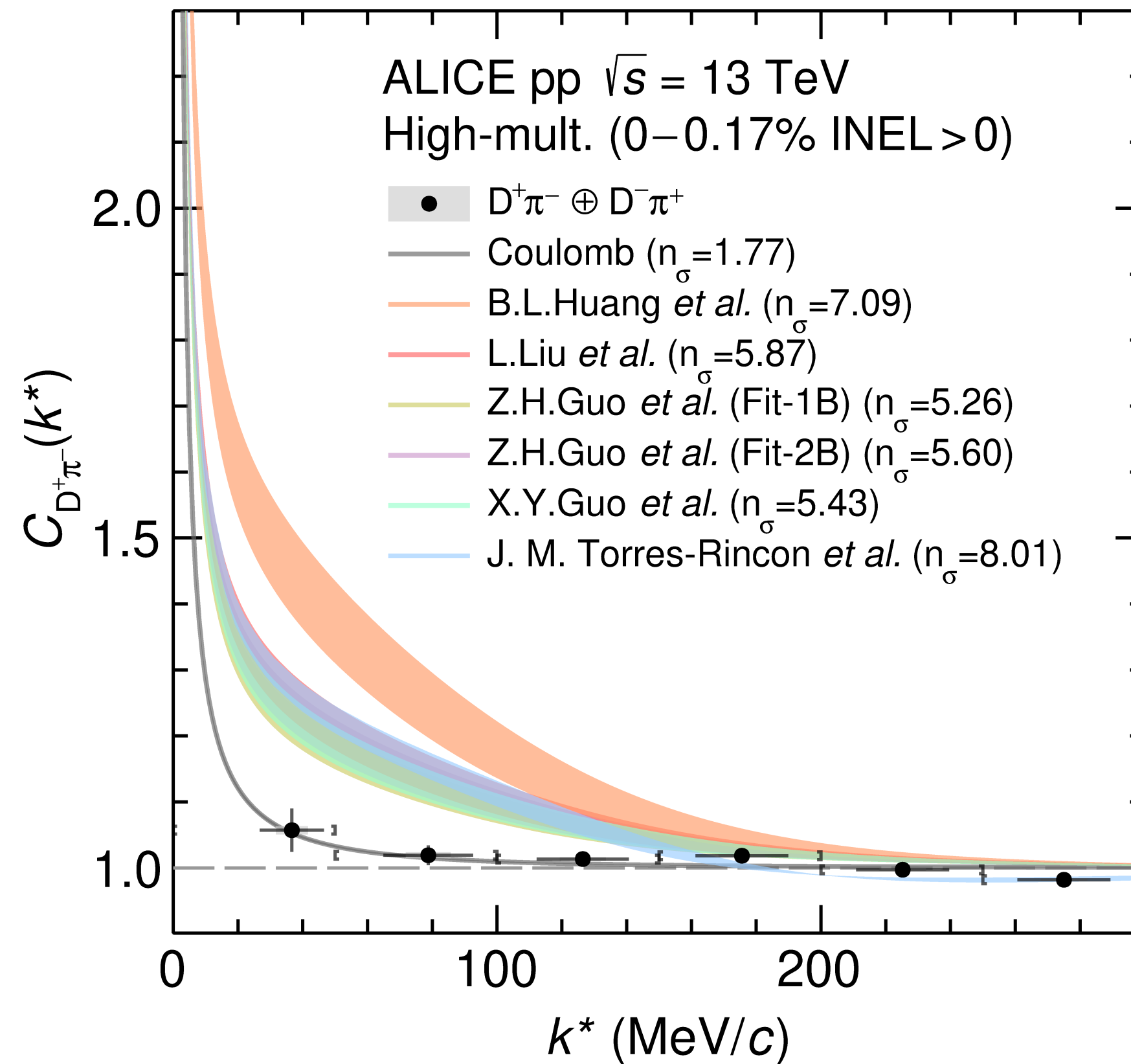
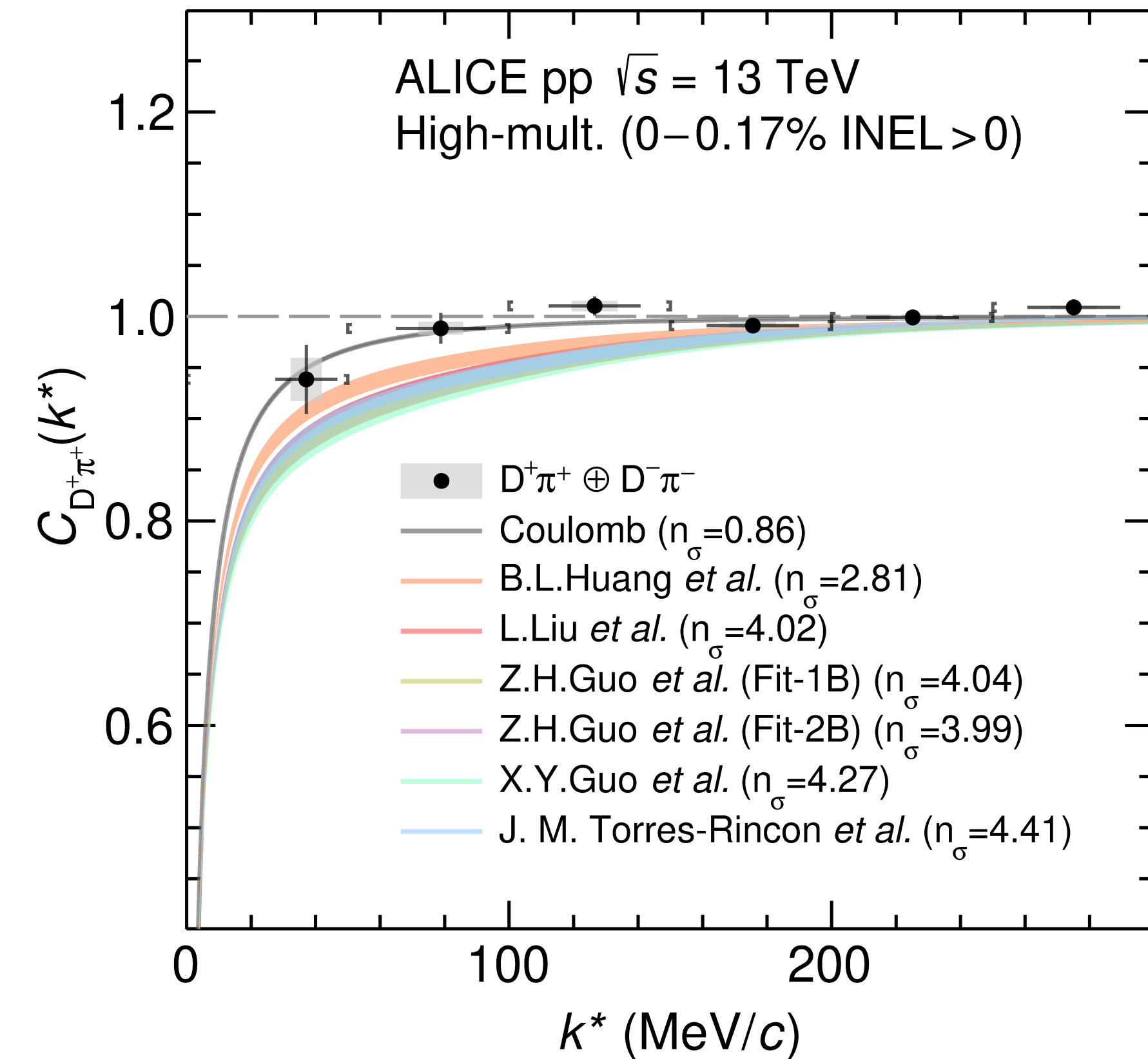
$$C_{\text{raw}}(\vec{k}^*) = \lambda_{\text{SB}} C_{\text{SB}}(k^*) + C_{\text{non-femto}}(k^*) \cdot [\lambda_{\text{genuine}} C_{\text{genuine}}(k^*) + \lambda_{D^+ \leftarrow D^*} C_{D^+ \leftarrow D^*} + \lambda_{\text{flat}}]$$



- Raw correlation function includes different sources of backgrounds
 - Combinatorial background**
estimated from D-meson sidebands
 - Jet-induced correlations (non-femto)**
estimated with PYTHIA 8
 - $D^{*\pm} \rightarrow D^\pm + X$**
obtained from $D^{*\pm}\pi^\mp$ measurement, converted to $D^\pm\pi^\mp$ momentum space with decay kinematics
- **Total background** well describes CF for large k^*

$D^+\pi^+ \oplus D^-\pi^-$

$D^+\pi^- \oplus D^-\pi^+$

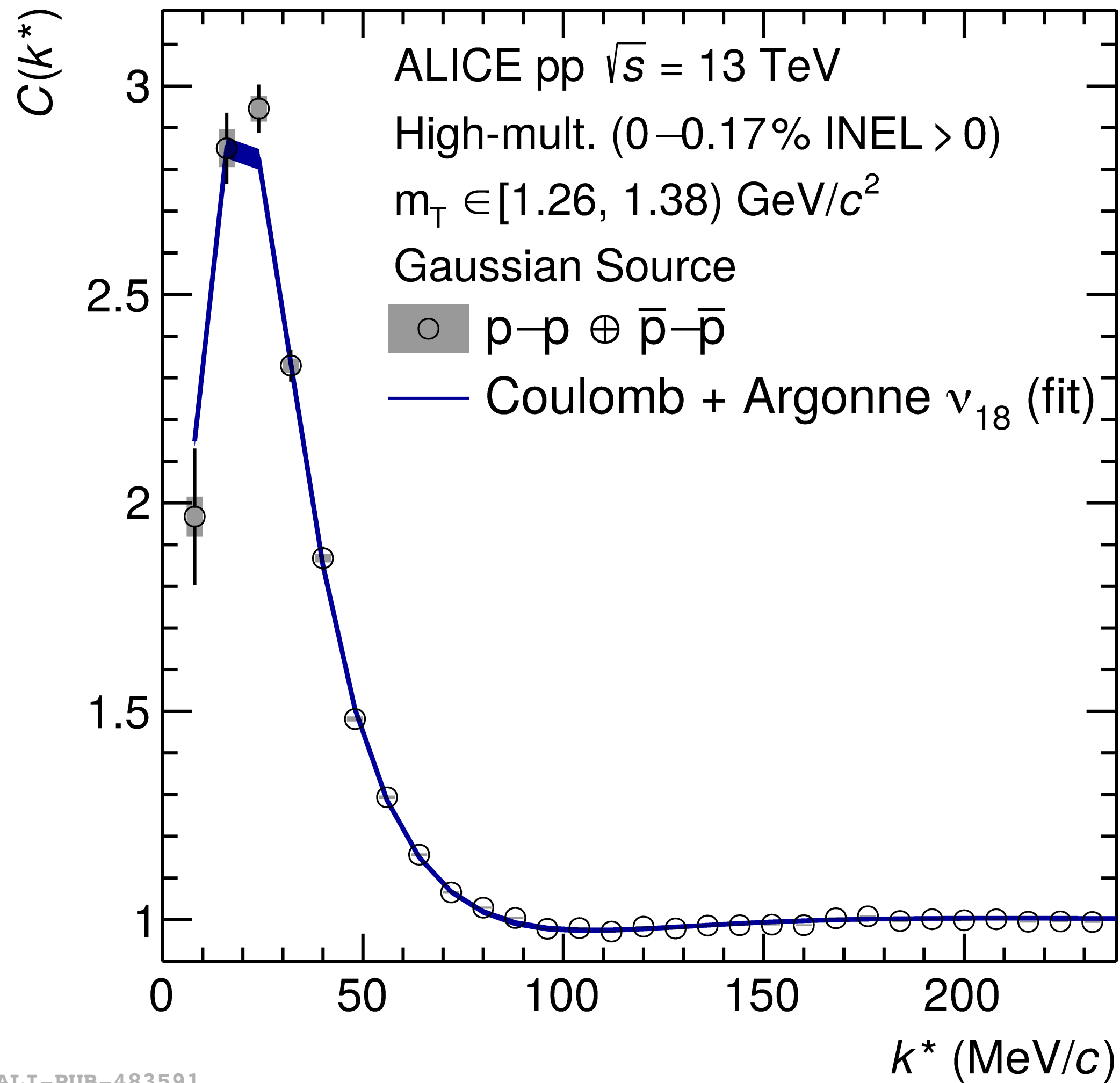


- $D^\pm\pi^\pm$
- ➔ $l = 3/2$ channel only
- $D^\pm\pi^\mp$
- ➔ $l = 3/2$ (33%), $l = 1/2$ (66%)

- 📖 L. Liu *et al.*, PRD 87 (2013) 014508
- 📖 X.Y. Guo *et al.*, PRD 98 (2018) 014510
- 📖 B.-L. Huang *et al.*, PRD 105 (2022) 036016
- 📖 Z.-H. Guo *et al.* EPJC 79 (2019) 13
- 📖 J.M. Torres-Rincon *et al.*, PRD 108 (2023) 096008

- Both same-sign and opposite sign correlation functions **compatible with Coulomb-only hypothesis**
- ➔ Strong interaction "weaker" than the one predicted by theoretical predictions

Phys. Lett. B 811 (2020) 135849

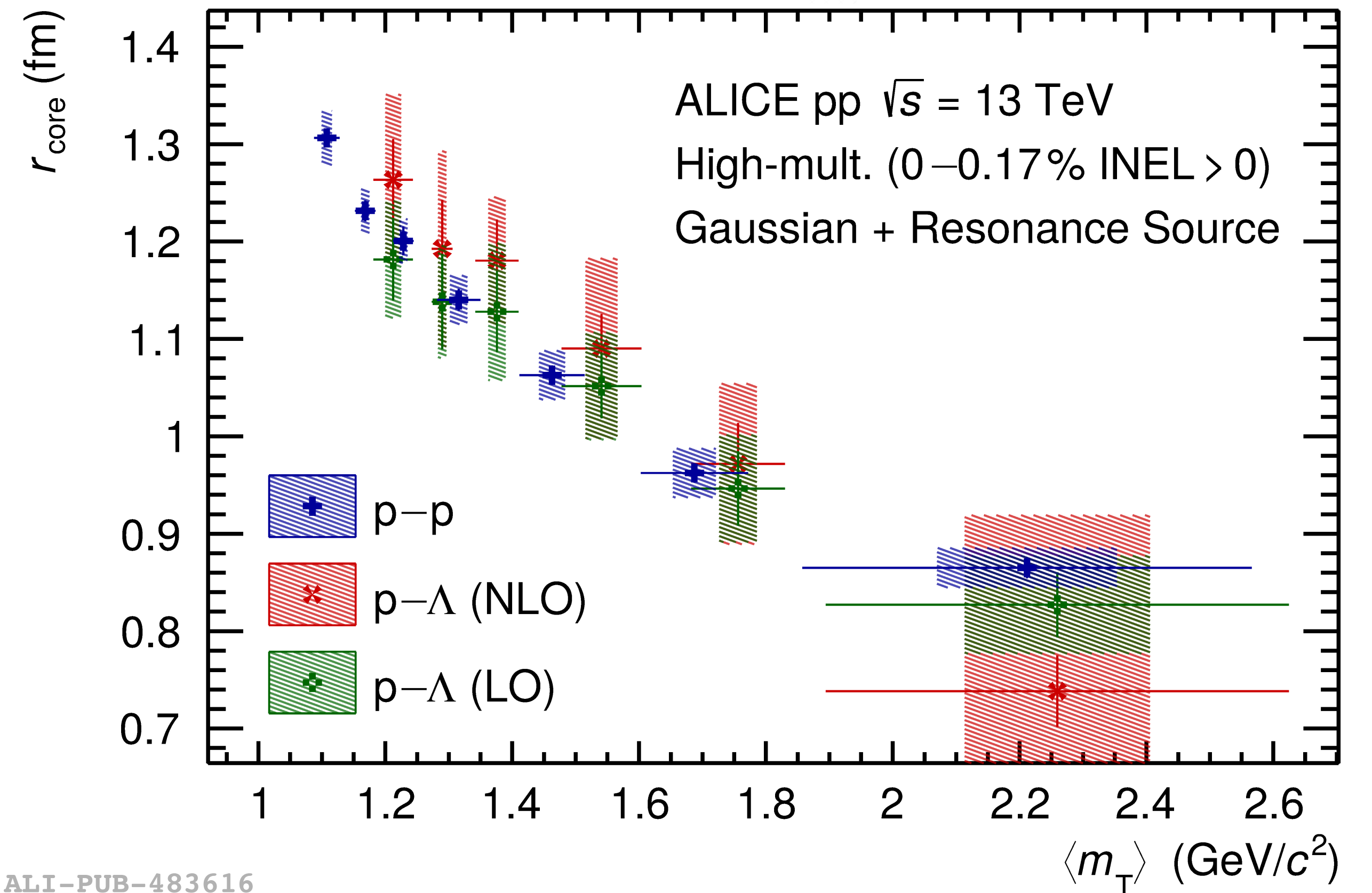


ALI-PUB-483591

- Model the source considering the core radius corresponding to the average m_T and adding resonances

- Fit correlation functions of $p\text{-}p$ and $p\text{-}\Lambda$ pairs
 - ➔ Interaction precisely described
 - ➔ Gaussian source with radius as free parameter

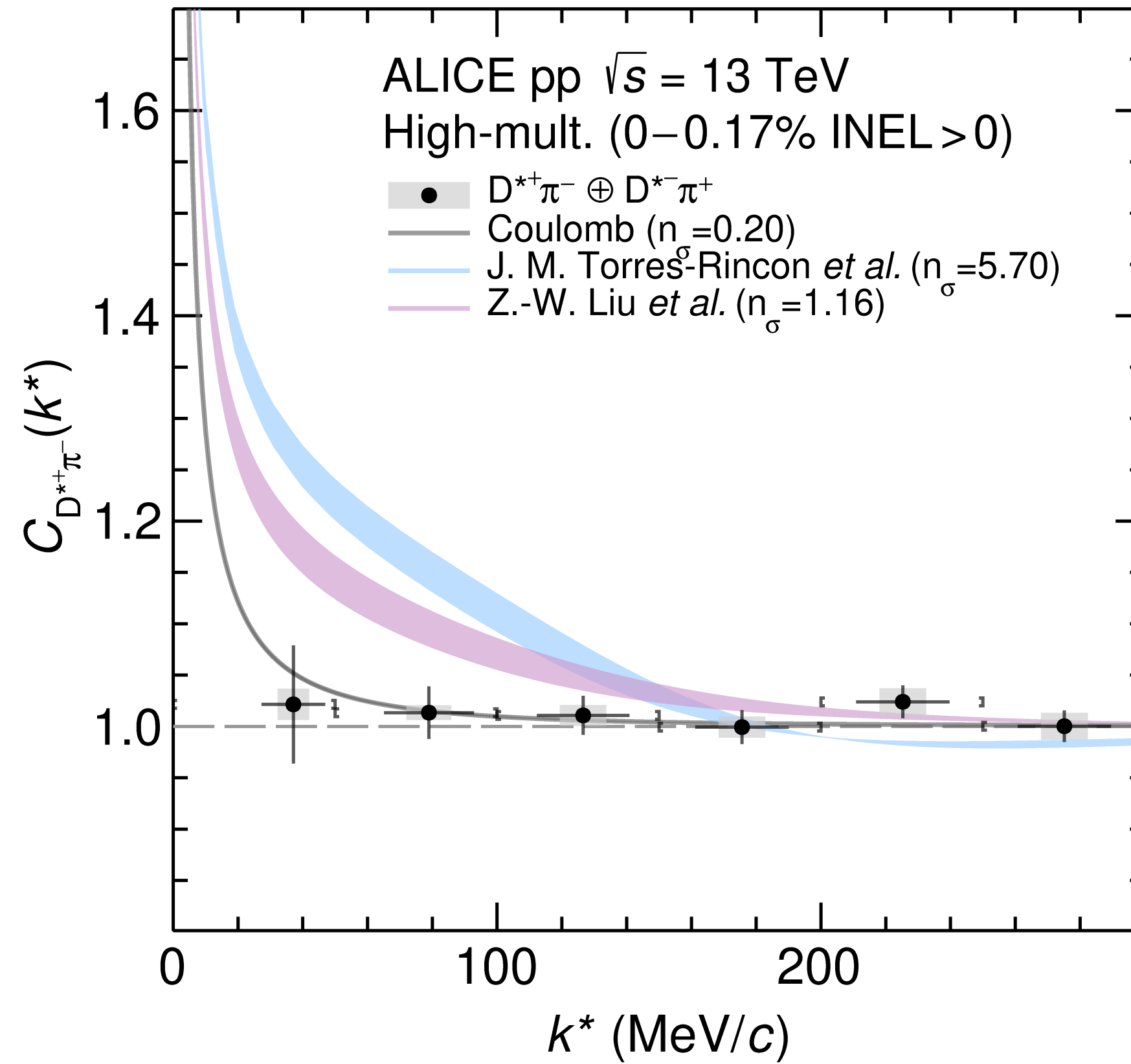
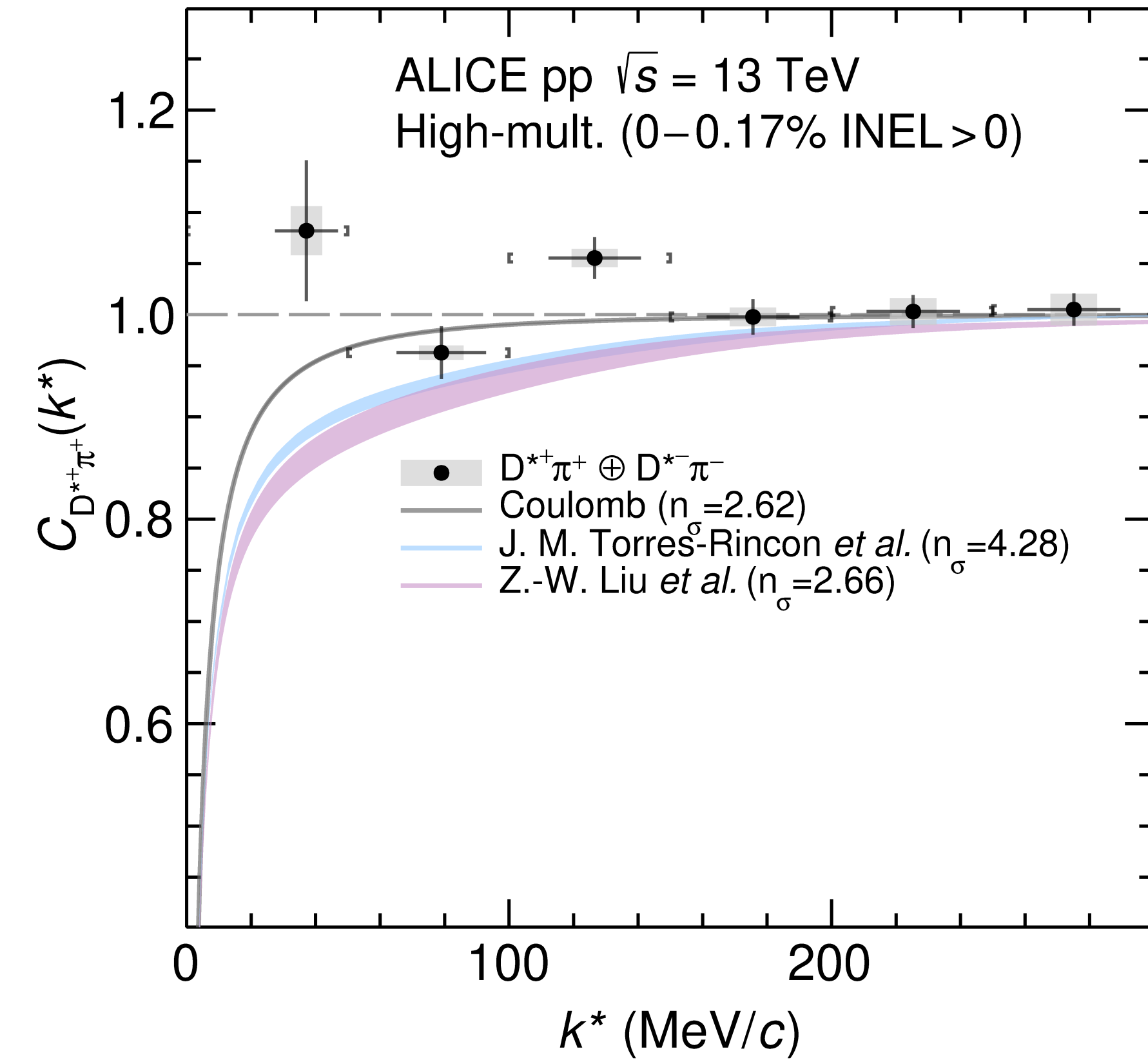
Phys. Lett. B 811 (2020) 135849



ALI-PUB-483616

$D^{*+}\pi^+ \oplus D^{*-}\pi^-$

$D^{*+}\pi^- \oplus D^{*-}\pi^+$



- $D^{*\pm}\pi^\mp$
- ➔ $l = 3/2$ channel only
- $D^{*\pm}\pi^\pm$
- ➔ $l = 3/2$ (33%), $l = 1/2$ (66%)

L. Liu *et al.*, Phys. Rev. D87 (2013) 014508

J.M. Torres-Rincon *et al.*, PRD 108 (2023) 096008

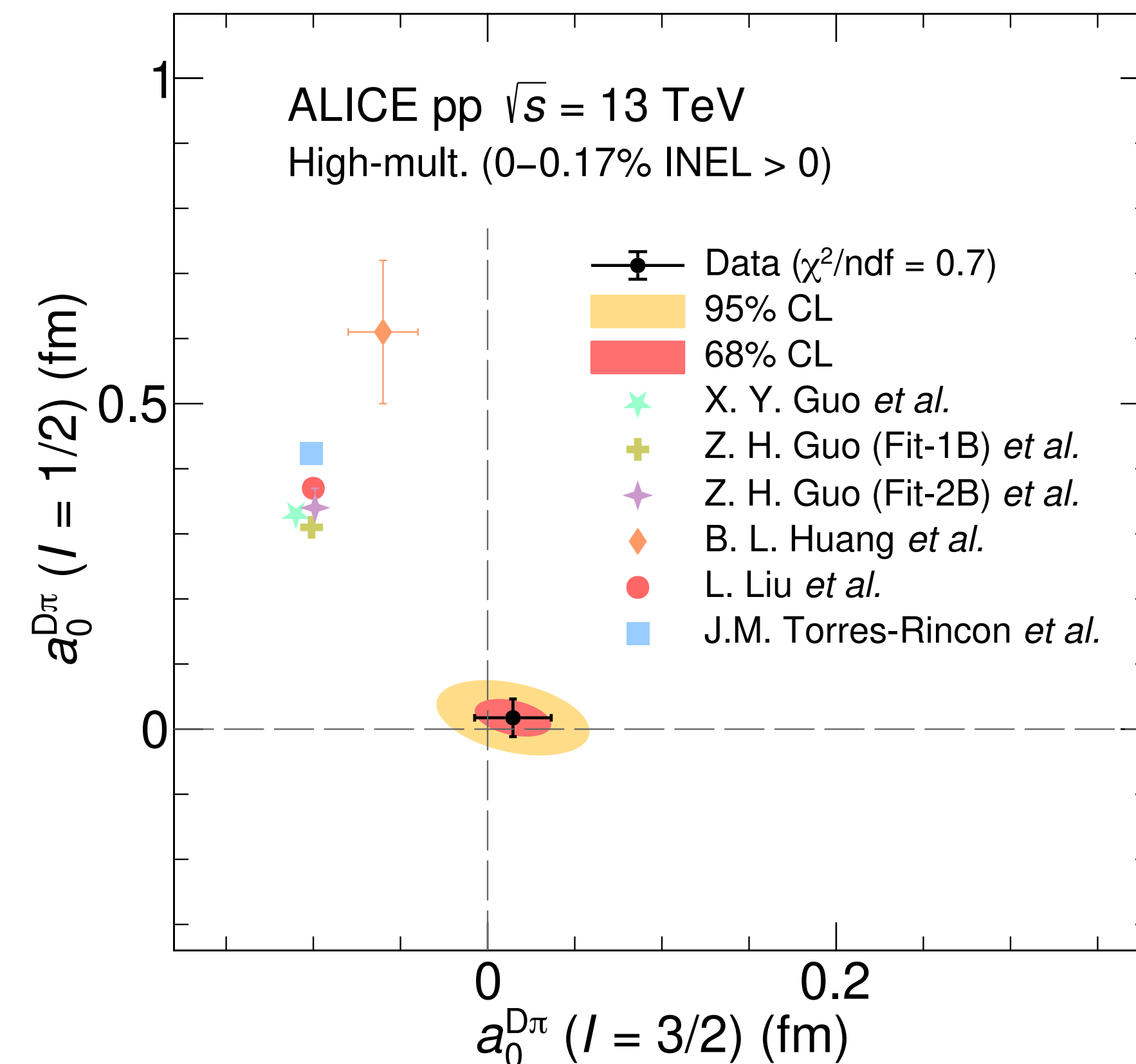
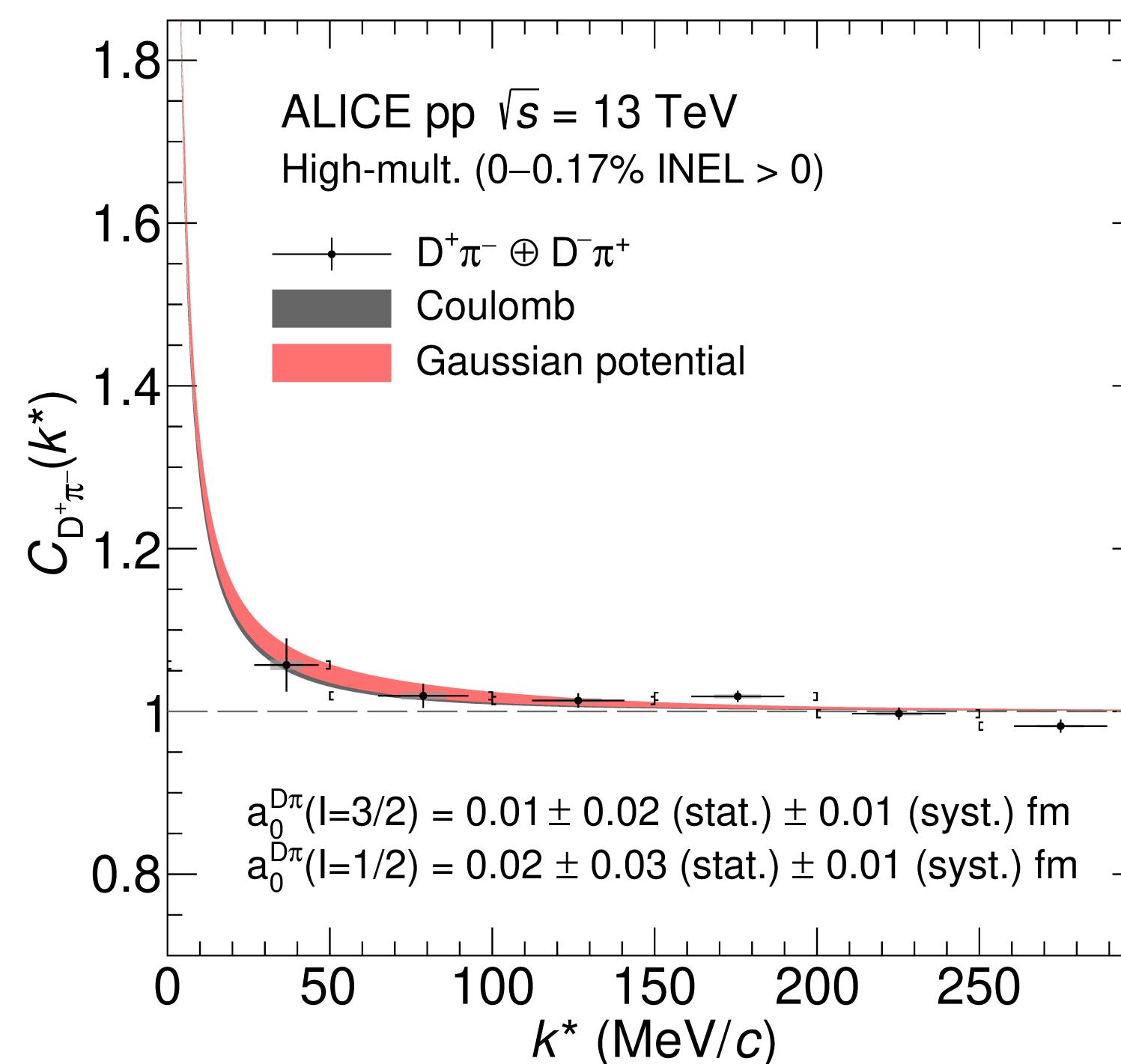
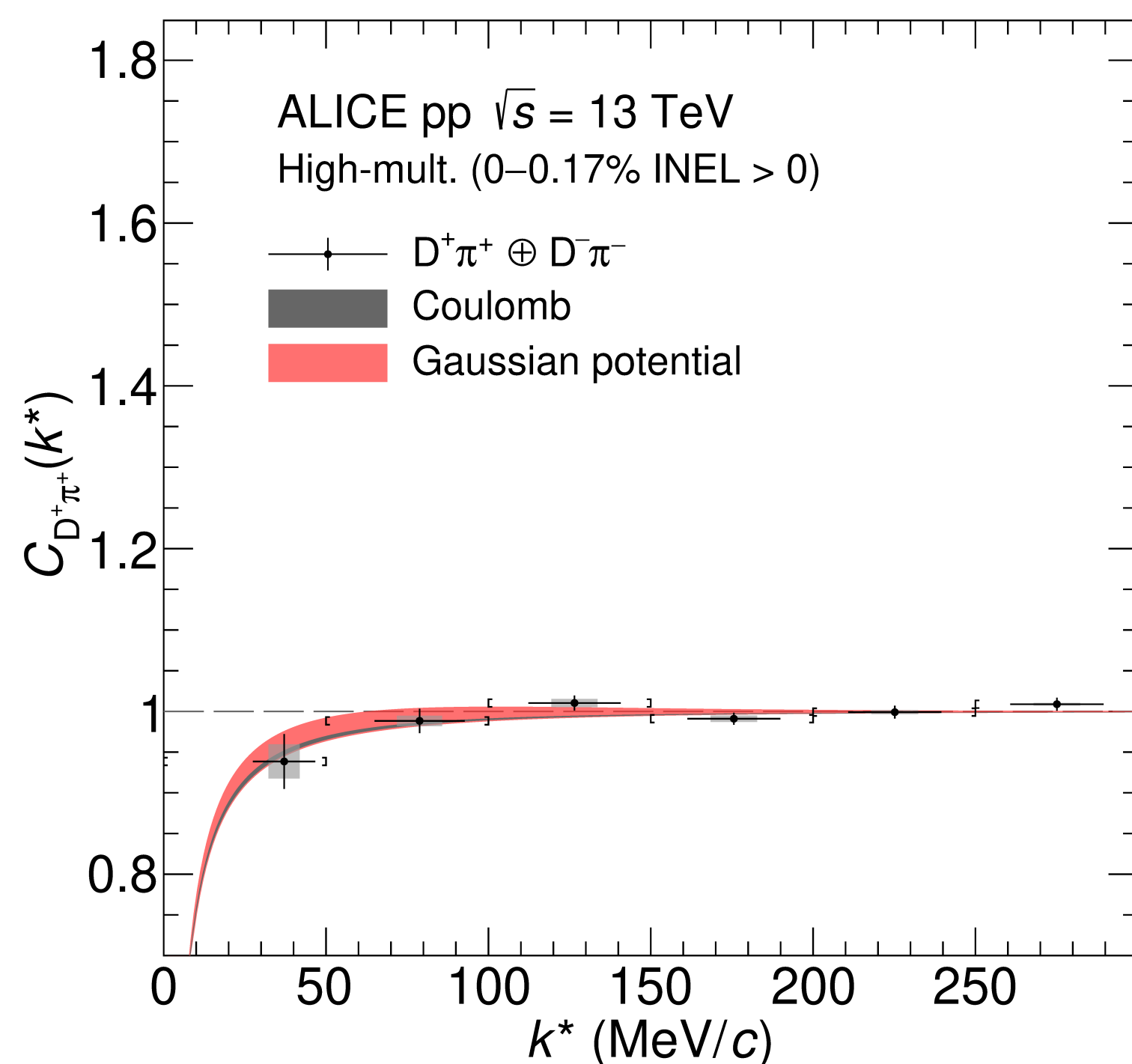
● Similar results for the $D^{*\pm}\pi^\mp$

➔ Expected due to heavy-quark spin symmetry

- **Scattering lengths extracted from data** via a χ^2 minimisation procedure
 - ➔ Model prediction computed varying the scattering lengths using **Gaussian-potential** approximation (meson exchange)

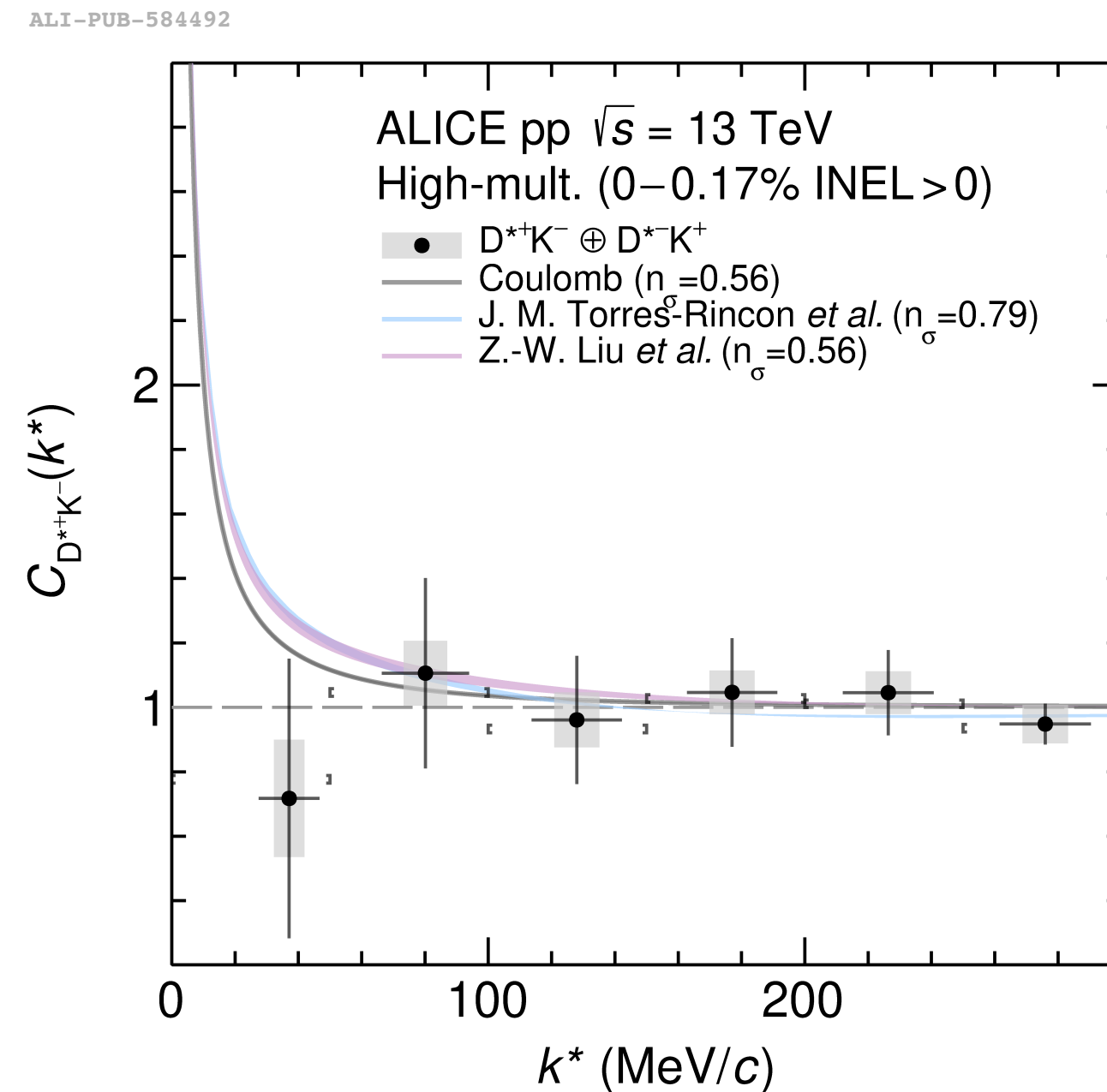
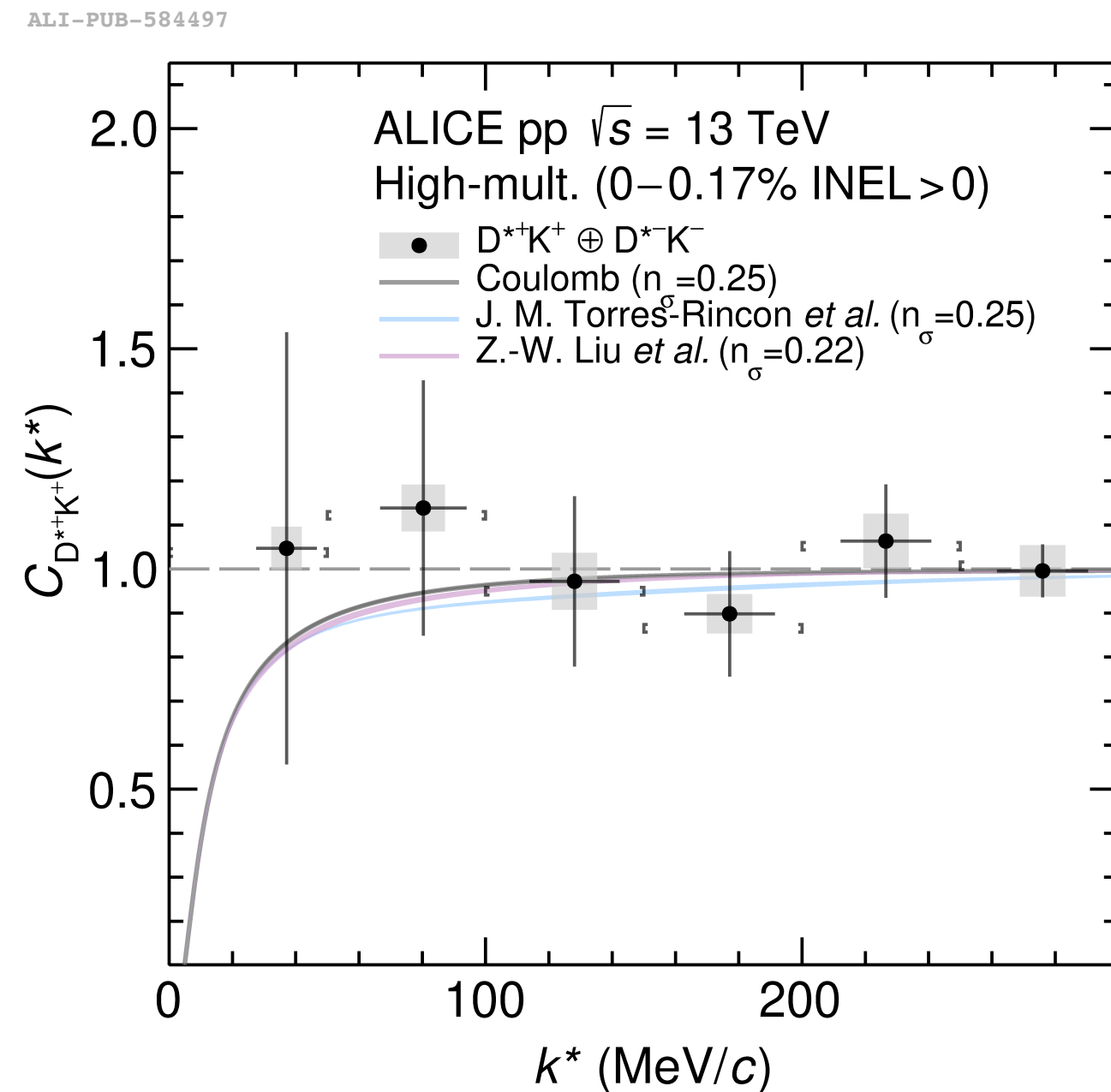
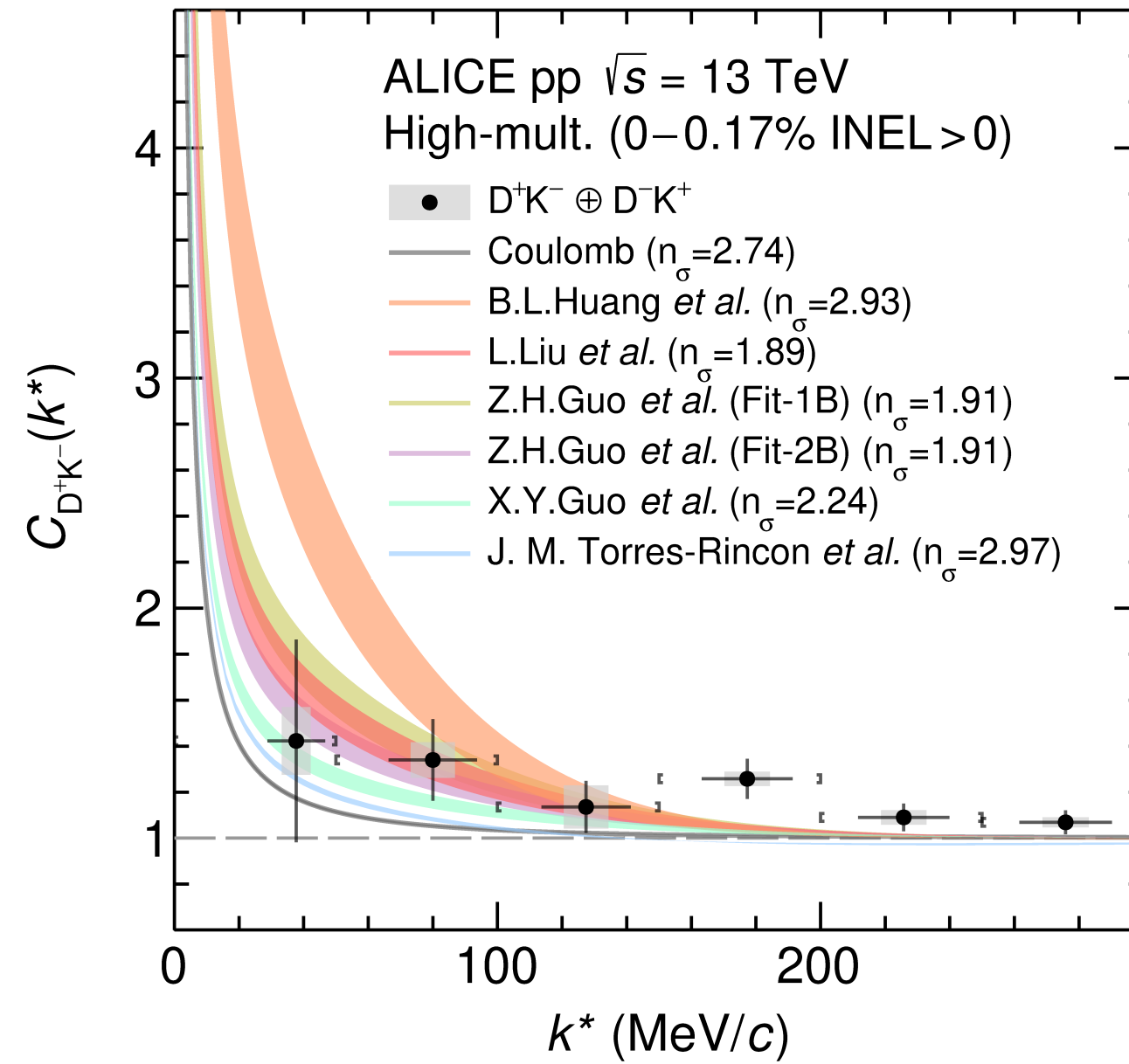
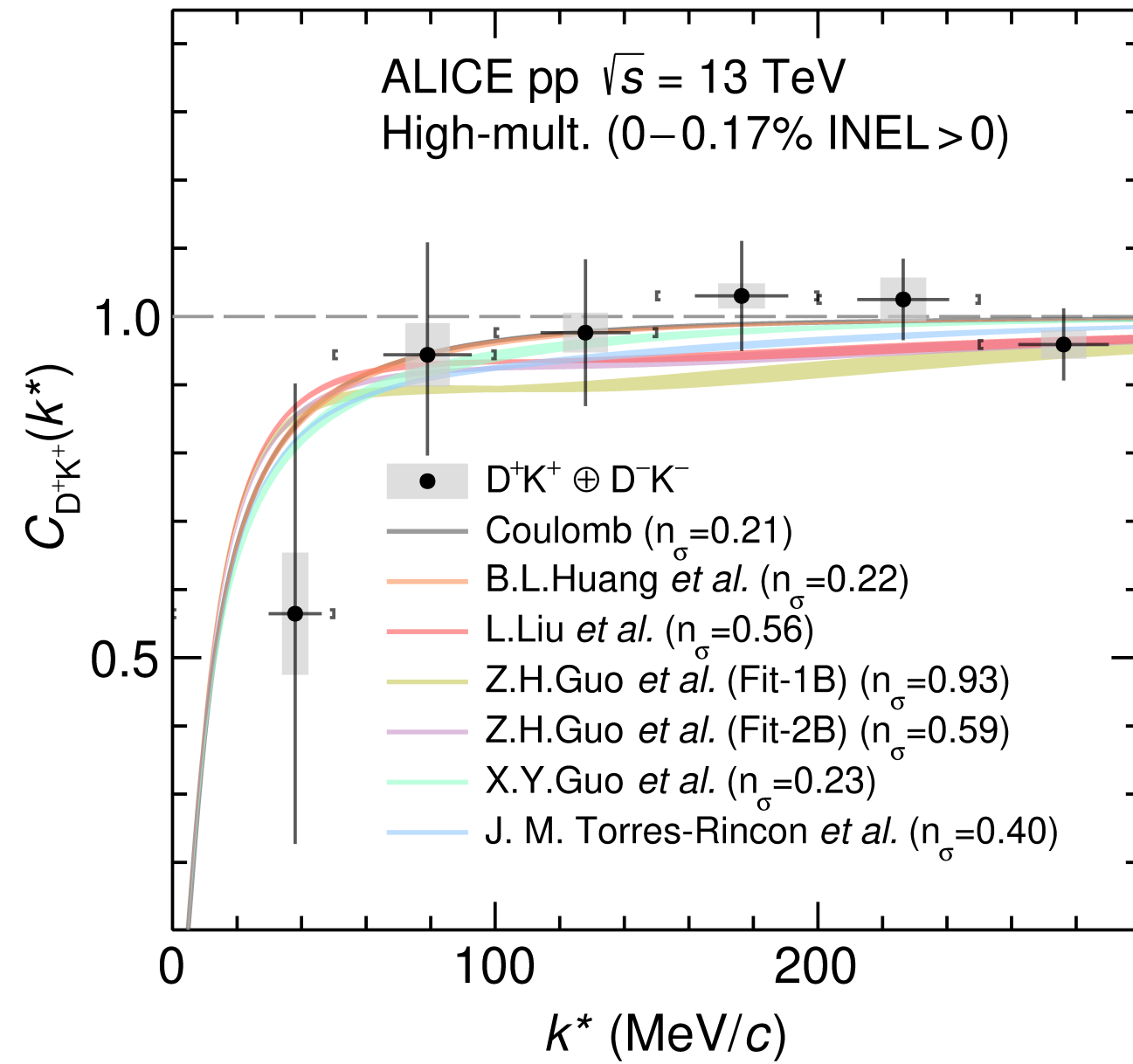
$$V(r) = V_0 \exp(-m_\rho^2 r^2)$$

Y. Kamyia et al, EPJA 58 (2022) 131



ALI-PUB-584542

- Experimental scattering lengths for both isospin channels compatible with zero
 - ➔ **>5 σ disagreement with models in $l=1/2$**

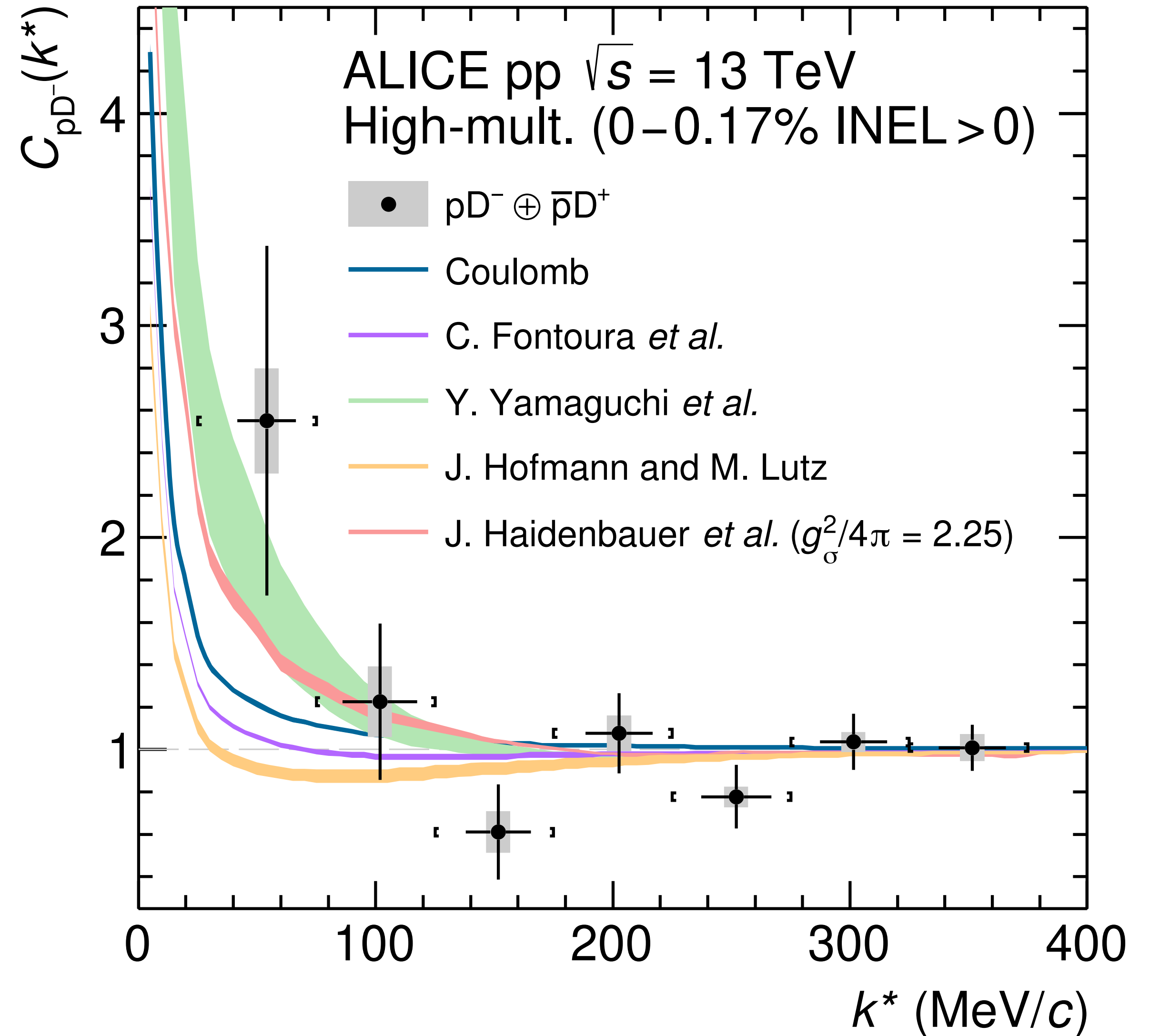


- $D^{(*)}\pm K^\pm$
→ $l = 1$ channel only
- $D^{(*)}\pm K^\mp$
→ $l = 0$ (50%), $l = 1$ (50%)
- Experimental data compatible with both Coulomb interaction and Coulomb + strong interaction

→ **Higher precision needed to draw conclusions**

- 📖 L. Liu *et al.*, PRD 87 (2013) 014508
- 📖 X.-Y. Guo *et al.*, PRD 98 (2018) 014510
- 📖 B.-L. Huang *et al.*, PRD 105 (2022) 036016
- 📖 Z.-H. Guo *et al.* EPJC 79 (2019) 13
- 📖 J.M. Torres-Rincon *et al.*, PRD 108 (2023) 096008

- pD^-
 - ➔ Most of the models predict repulsive interaction
 - ➔ Possible bound state formation (Yamaguchi et al)
- Data compatible with Coulomb only interaction, but comparison slightly improved when also attractive strong interaction is considered
 - ➔ **Higher precision needed to draw conclusions**



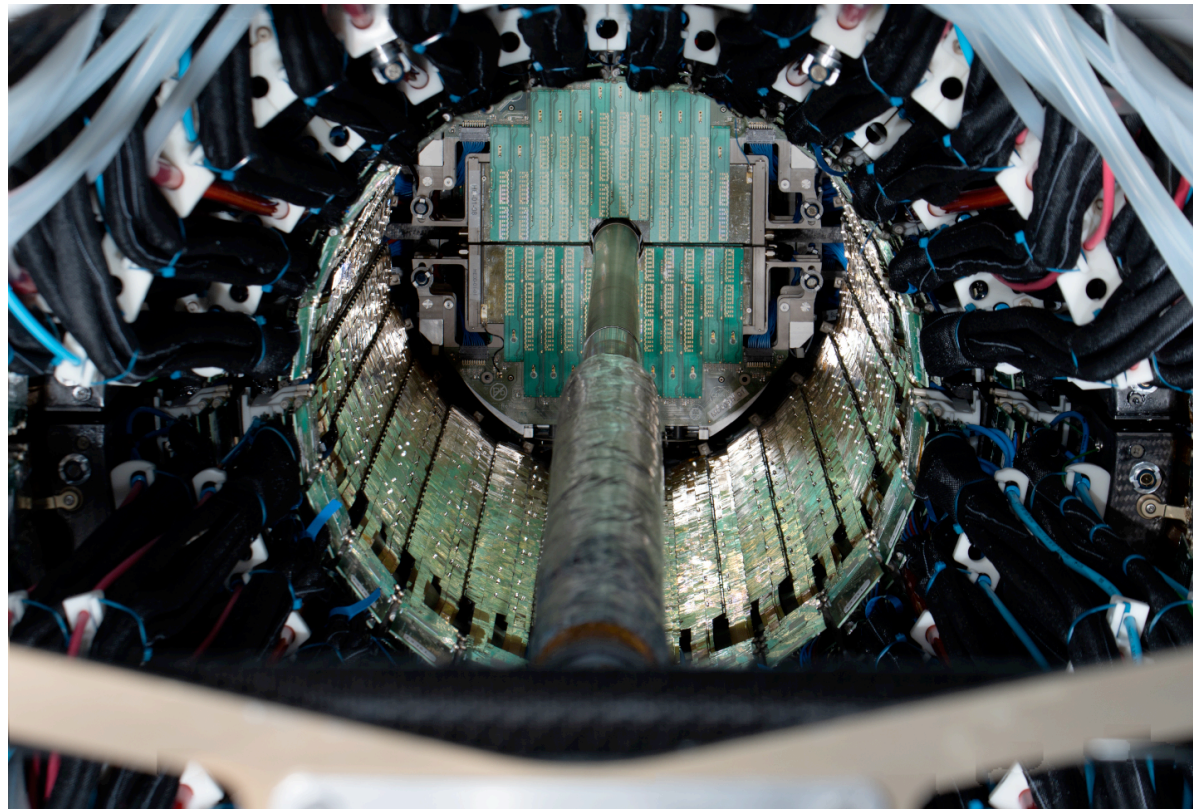
J. Haidenbauer et al, Eur. Phys. J. A33 (2007) 107–117

J. Hofmann and M. Lutz, Nucl. Phys. A 763 (2005) 90–139

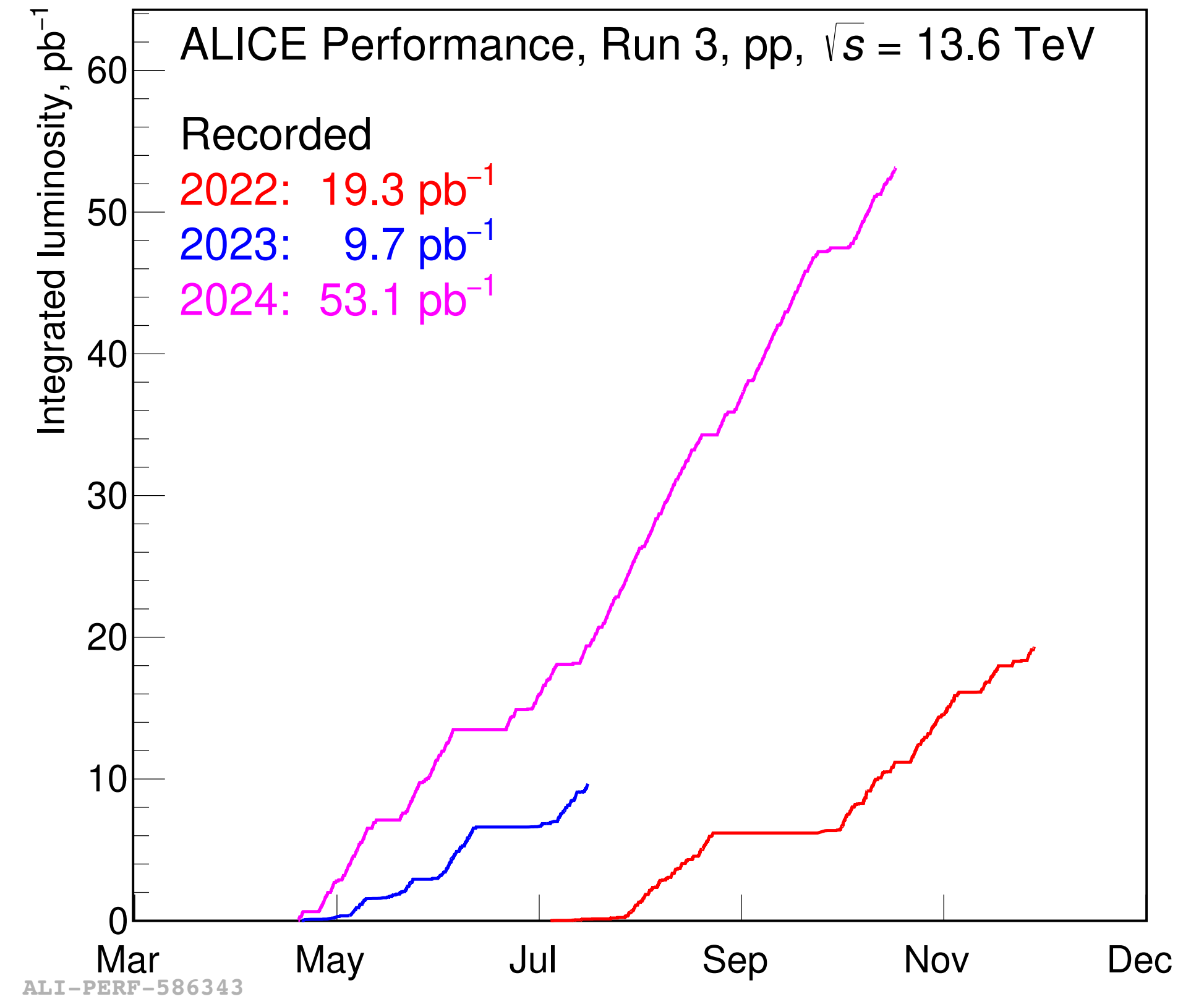
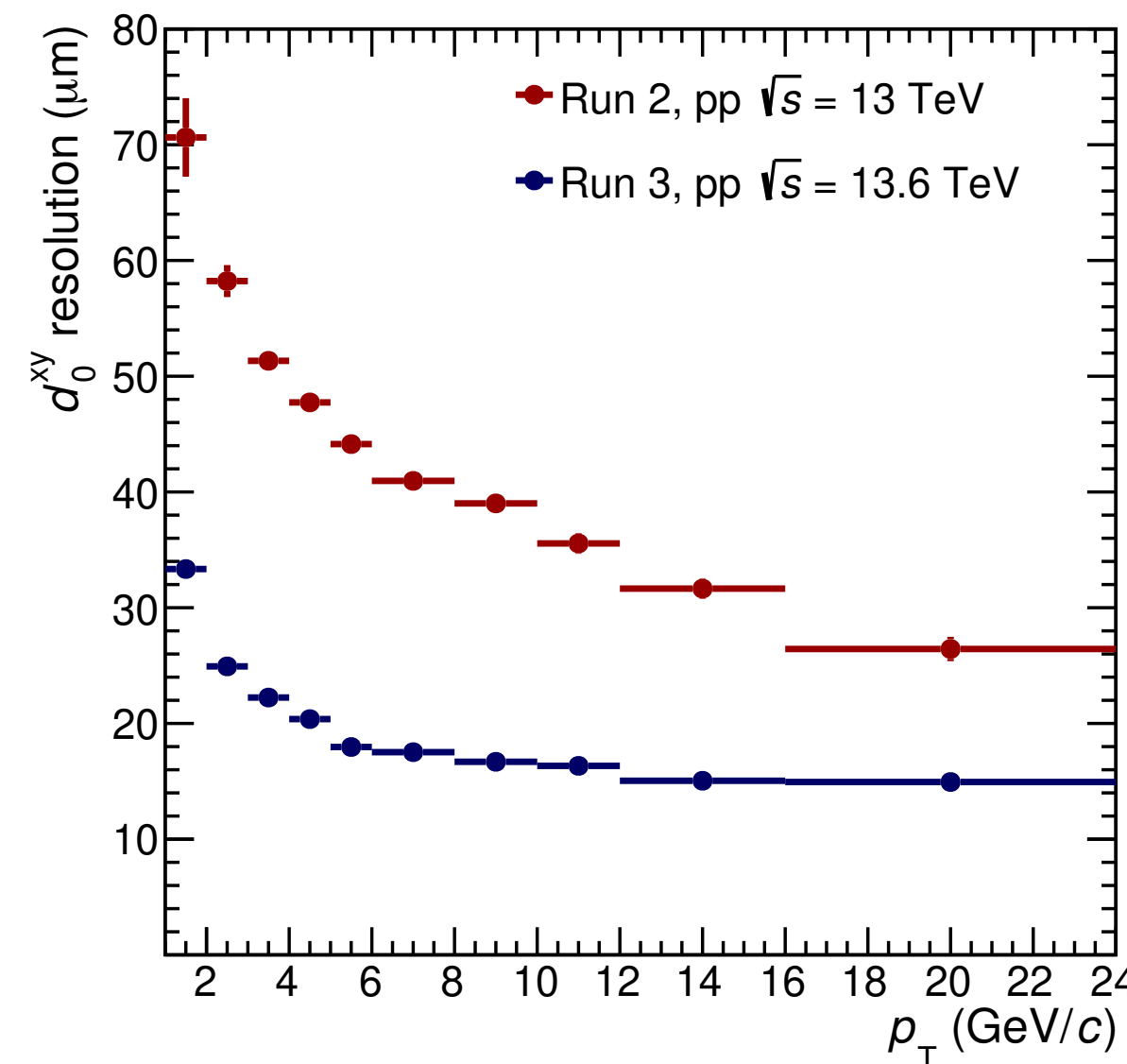
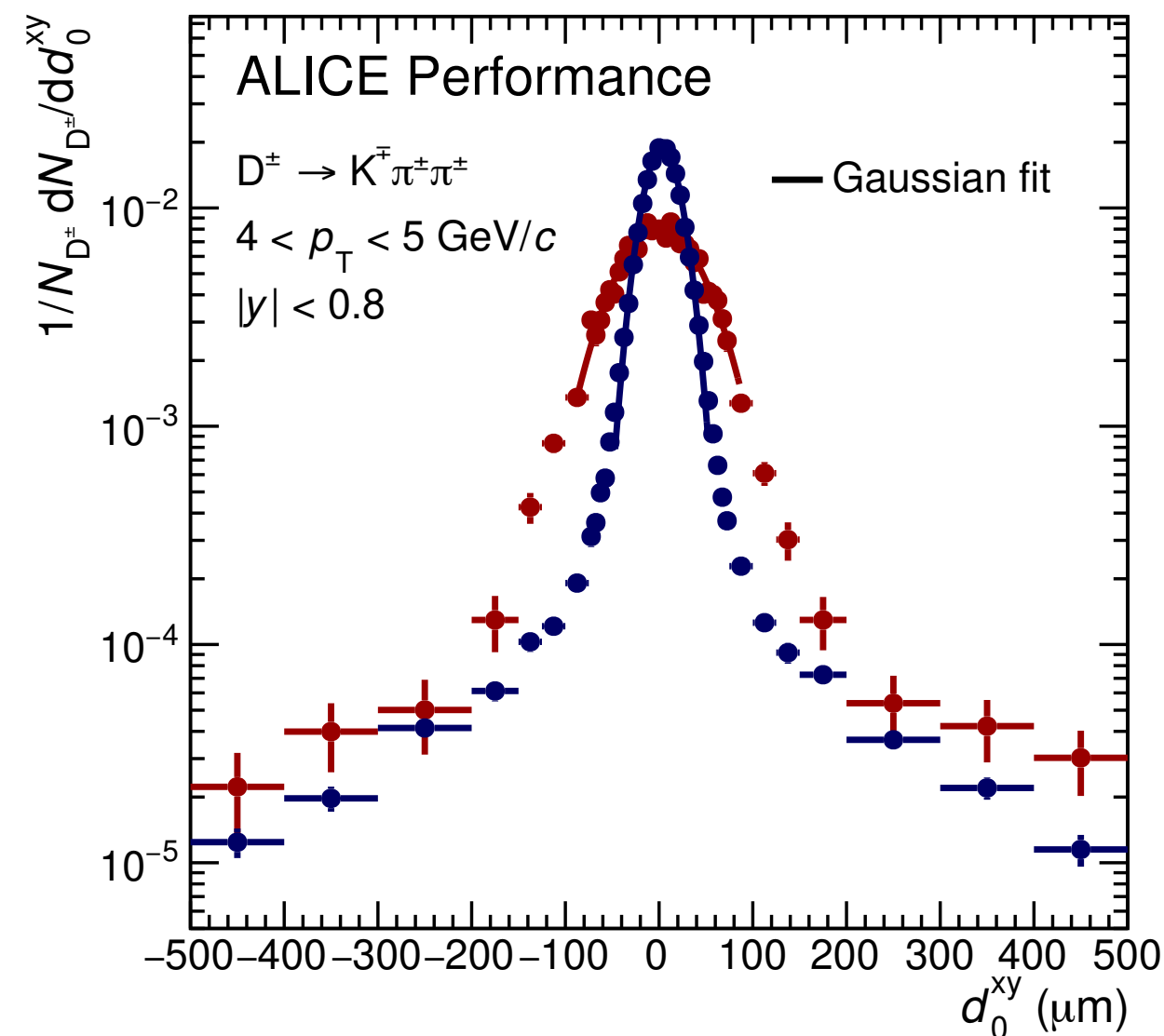
Fontoura et al, Phys. Rev. C 87 (2013) 025206

Yamaguchi et al, Phys. Rev. D84 (2011) 014032

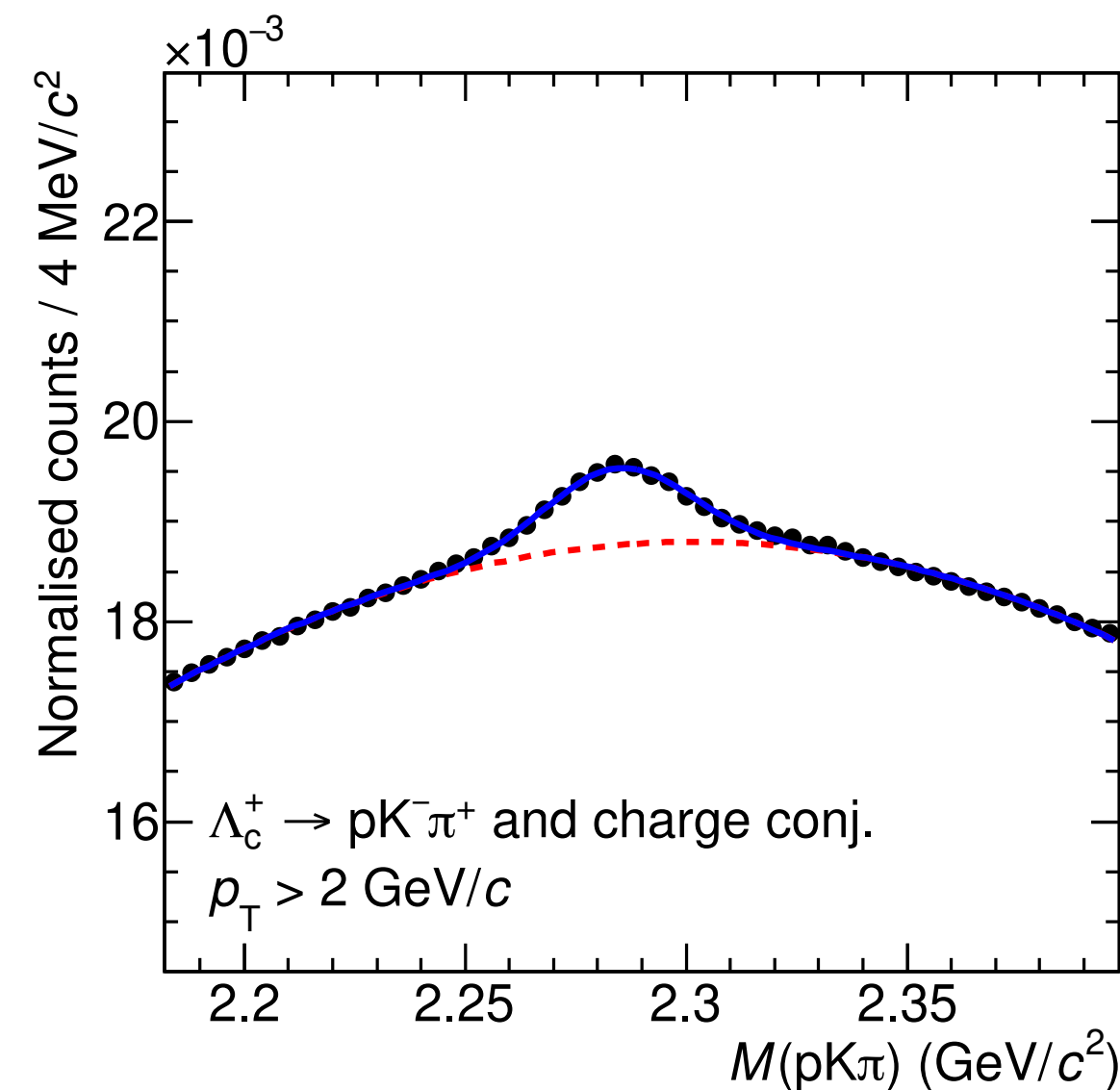
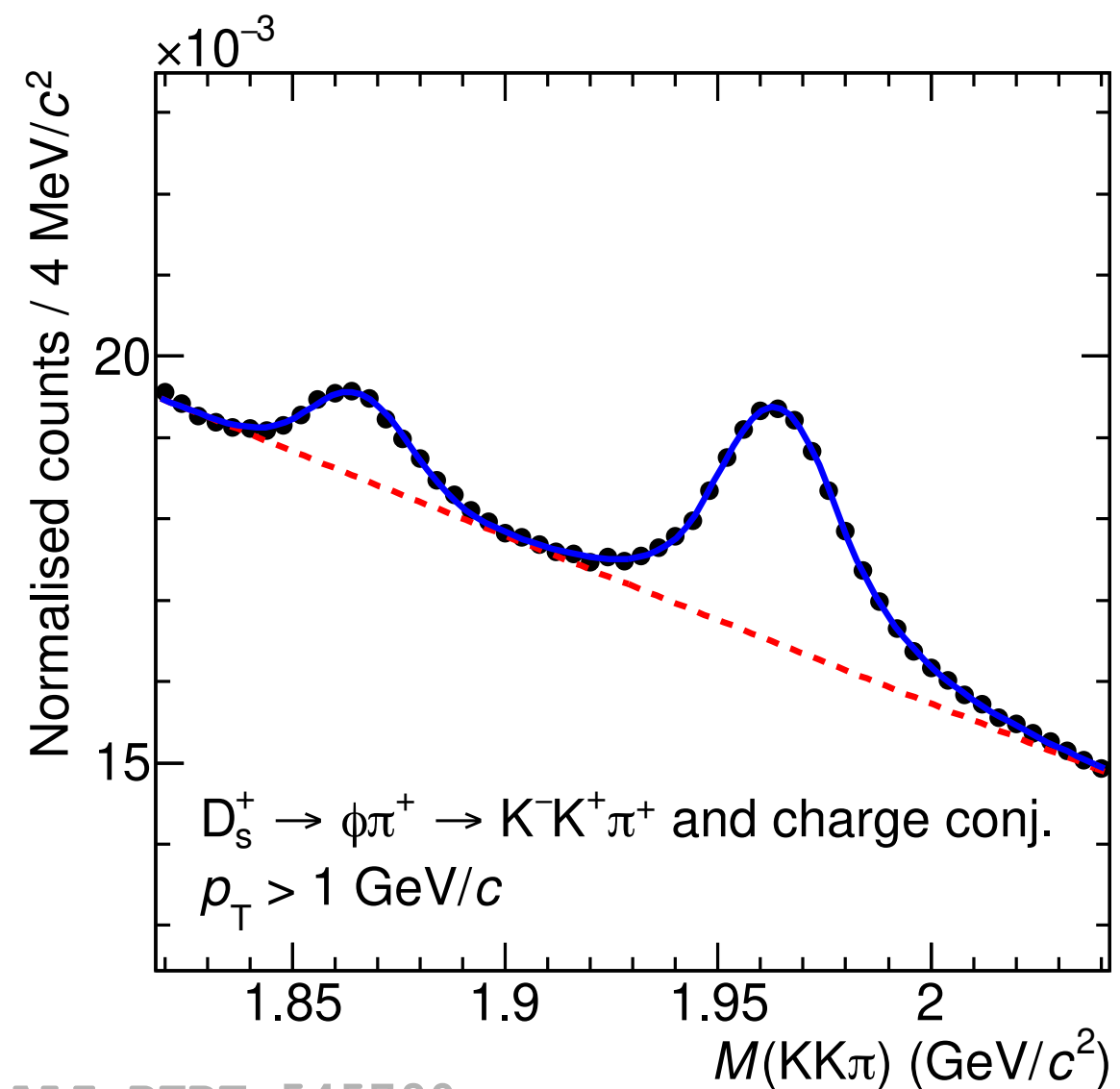
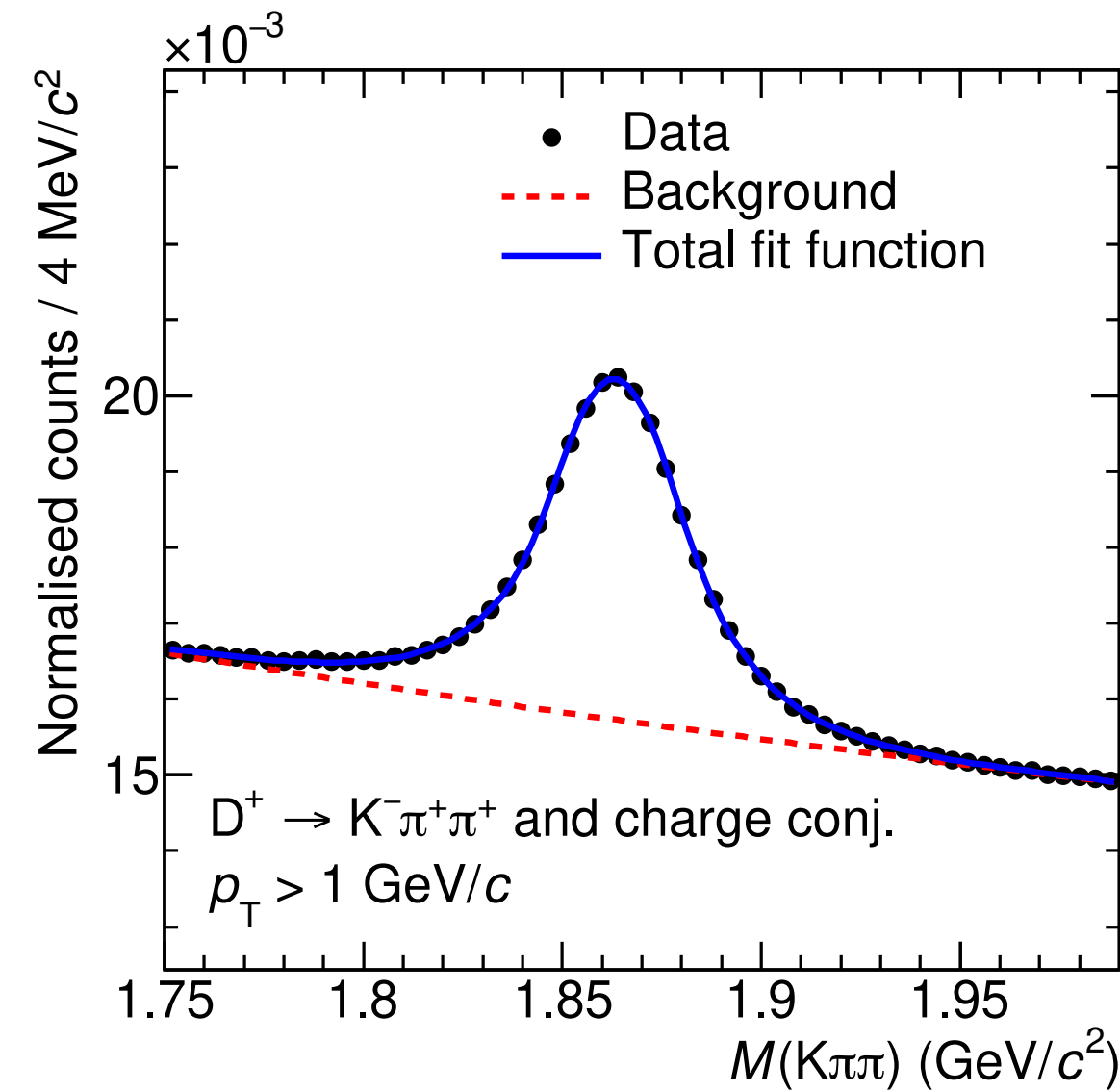
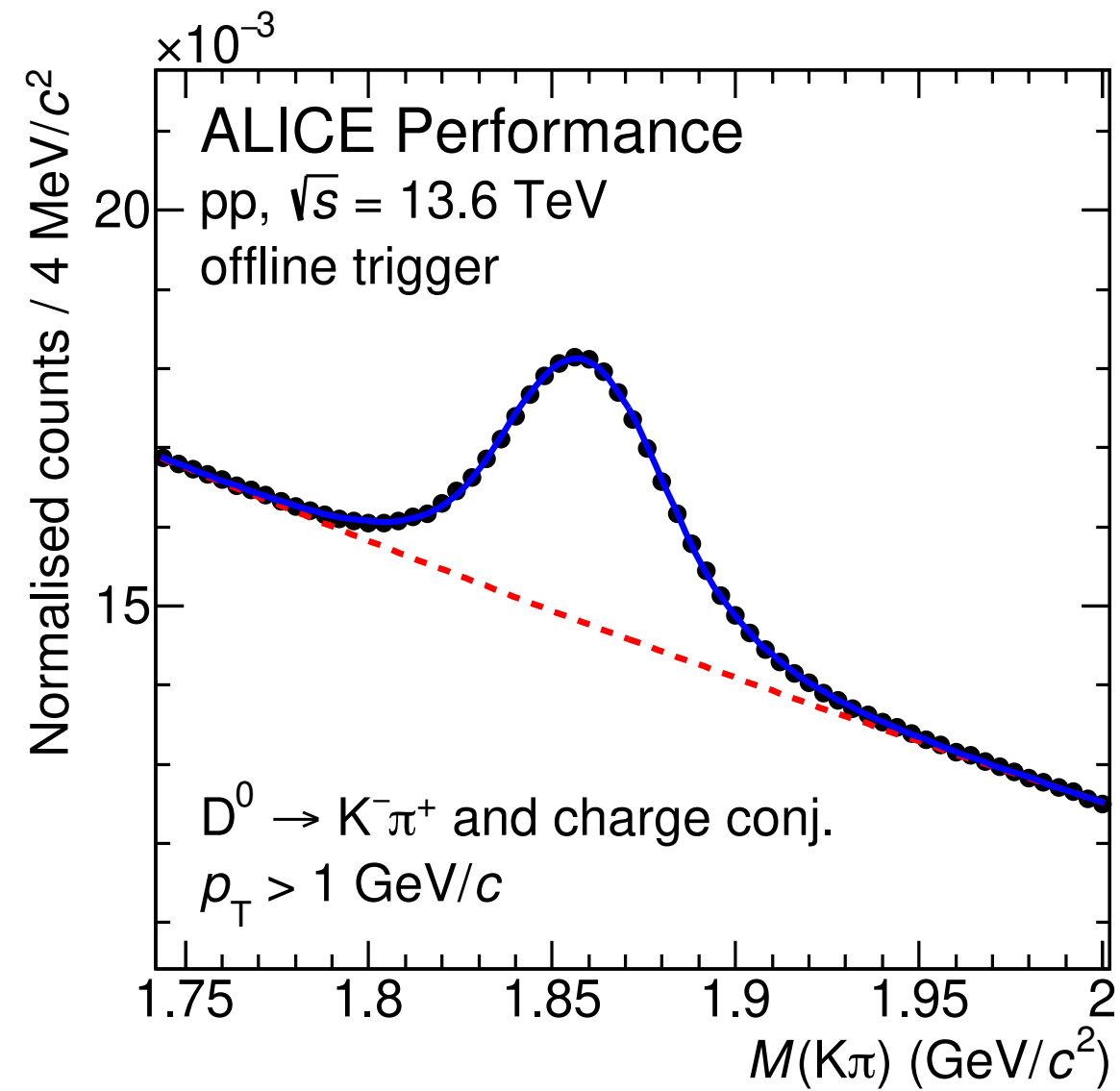
- The ALICE detector was substantially upgraded during the Long Shutdown 2
 - ➔ **New silicon inner tracker** (7 layers of monolithic active pixel sensors)



- ➔ Factor 2x-5x better impact-parameter resolution than Run 2 detector

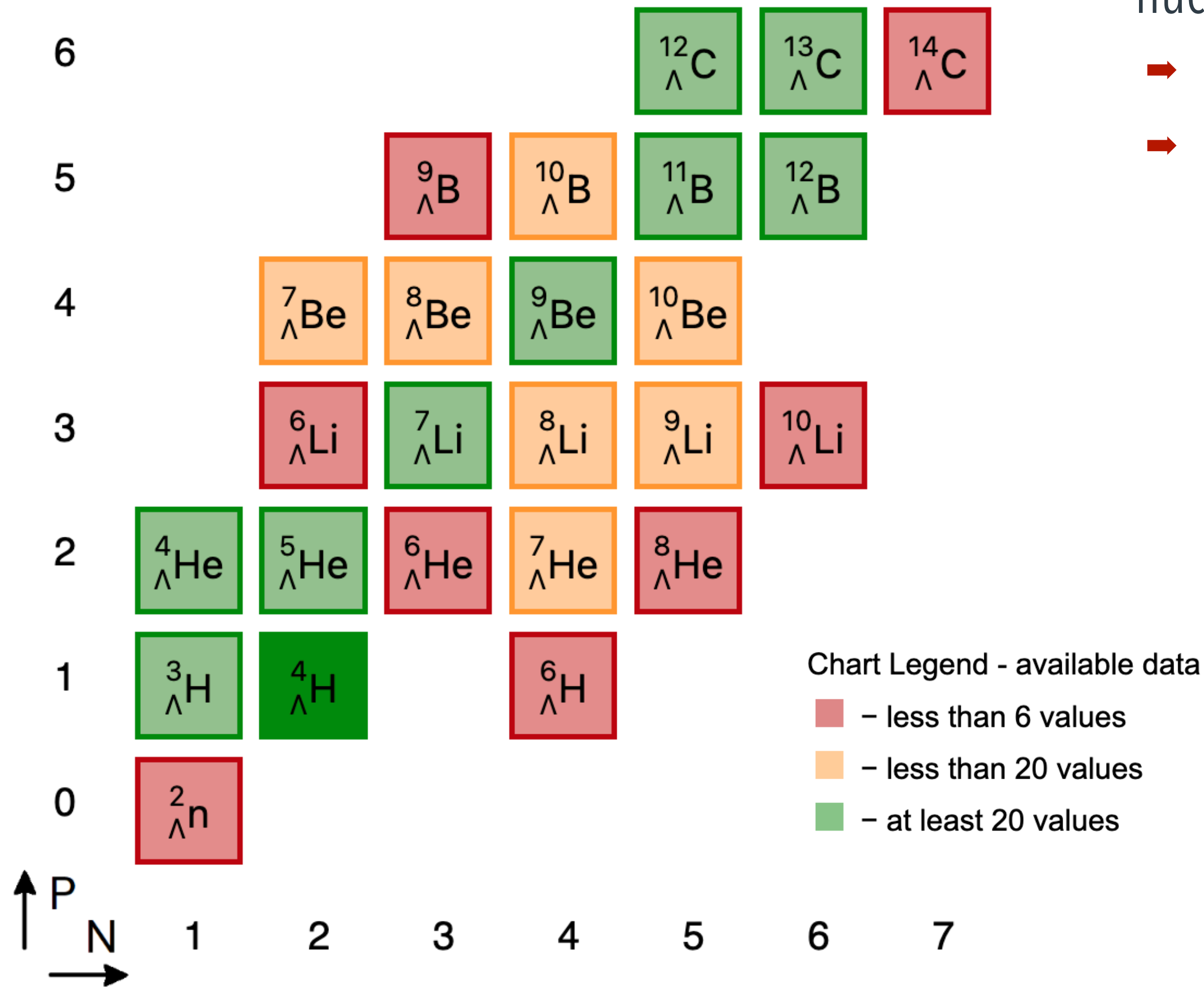


- **Continuous readout:**
 - ➔ Readout rate increased by a factor x500 (x50) in proton-proton (Pb-Pb) collisions

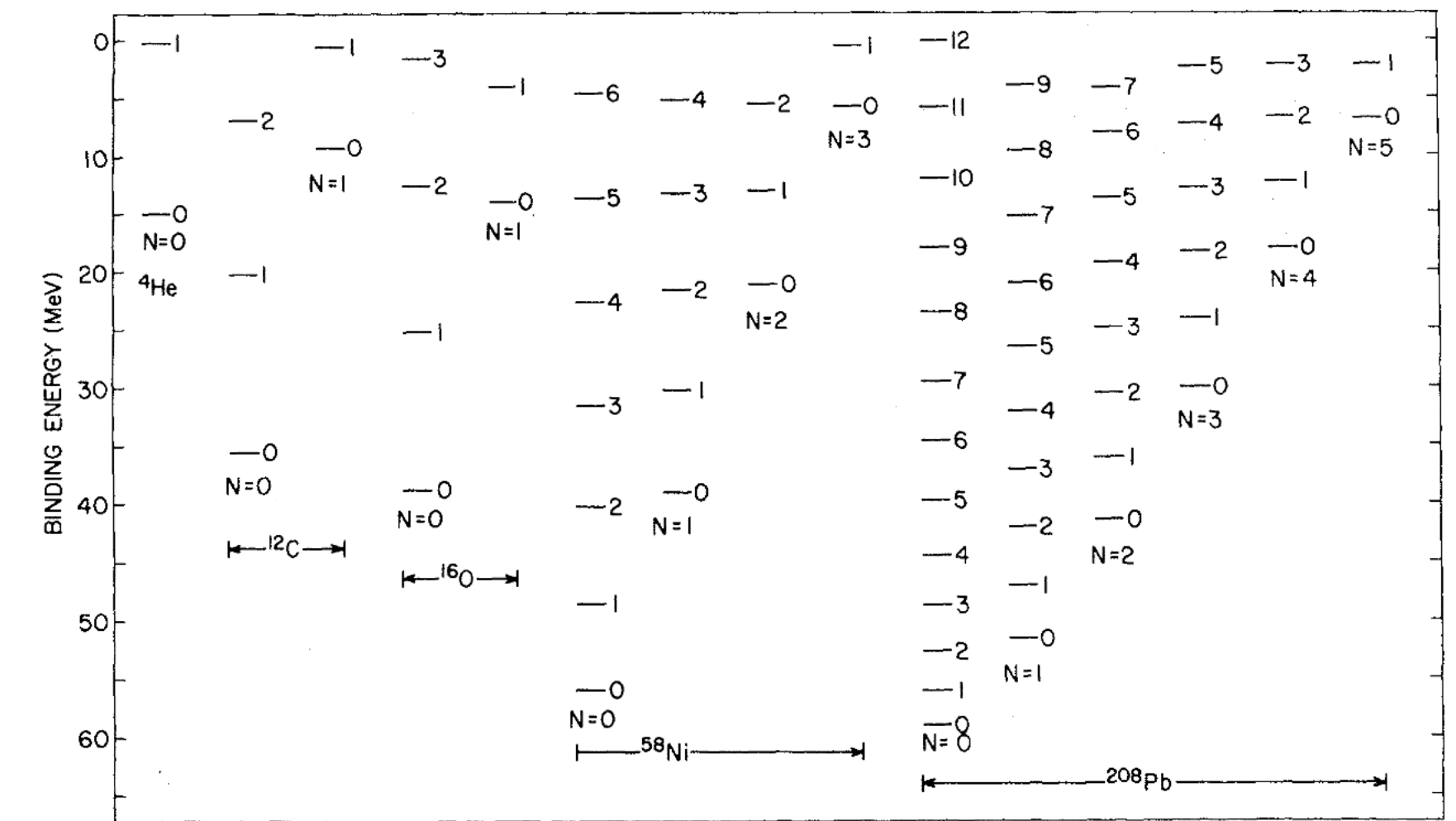


- Dedicated **software triggers** for specific measurements
 - ➔ Including a trigger on events with a Λ_c^+ -baryon candidate and a proton candidate having small k^*
- Performance plots from the quality control of the software triggers for a partial dataset of 2022 data

Hypernuclei database

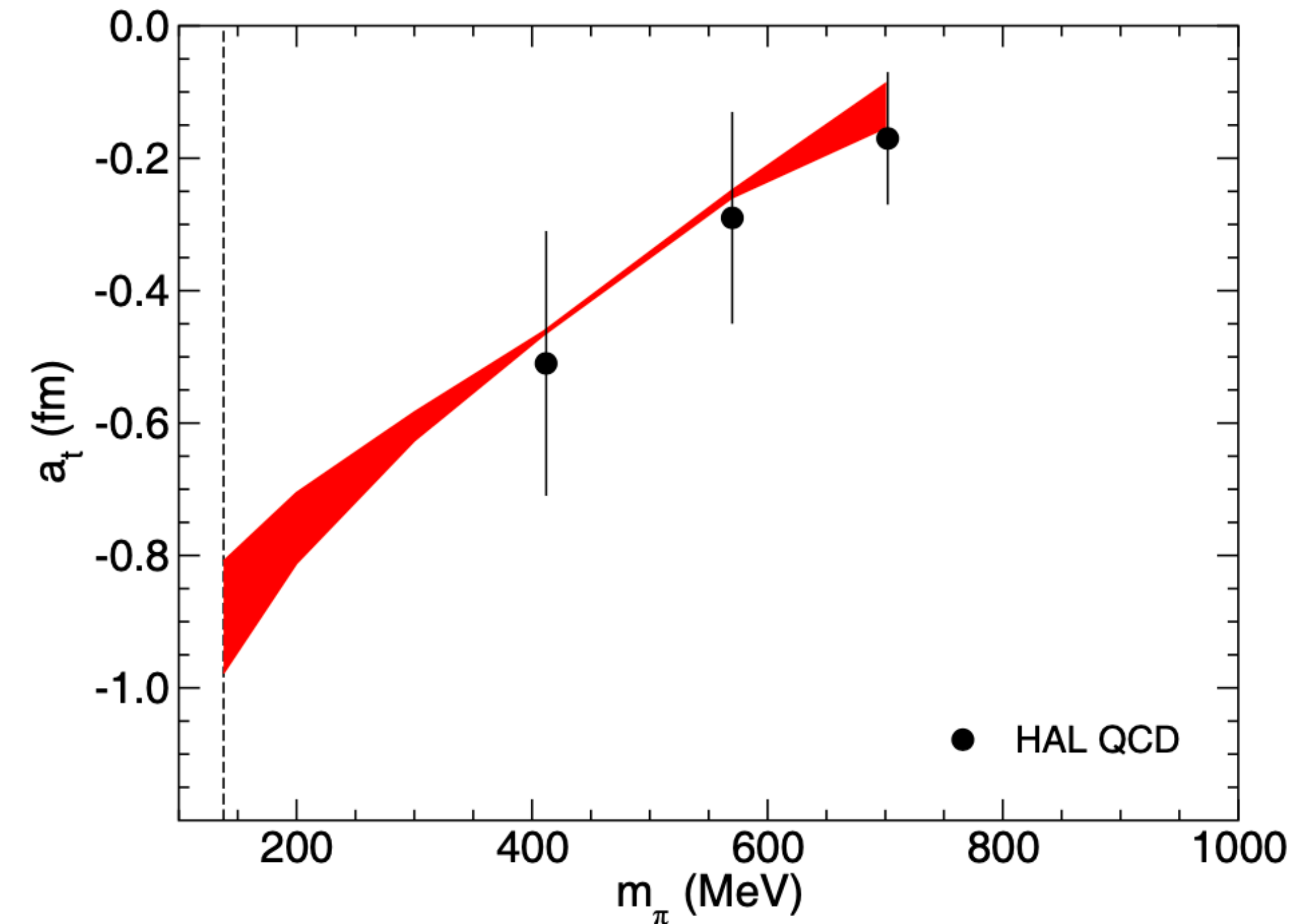
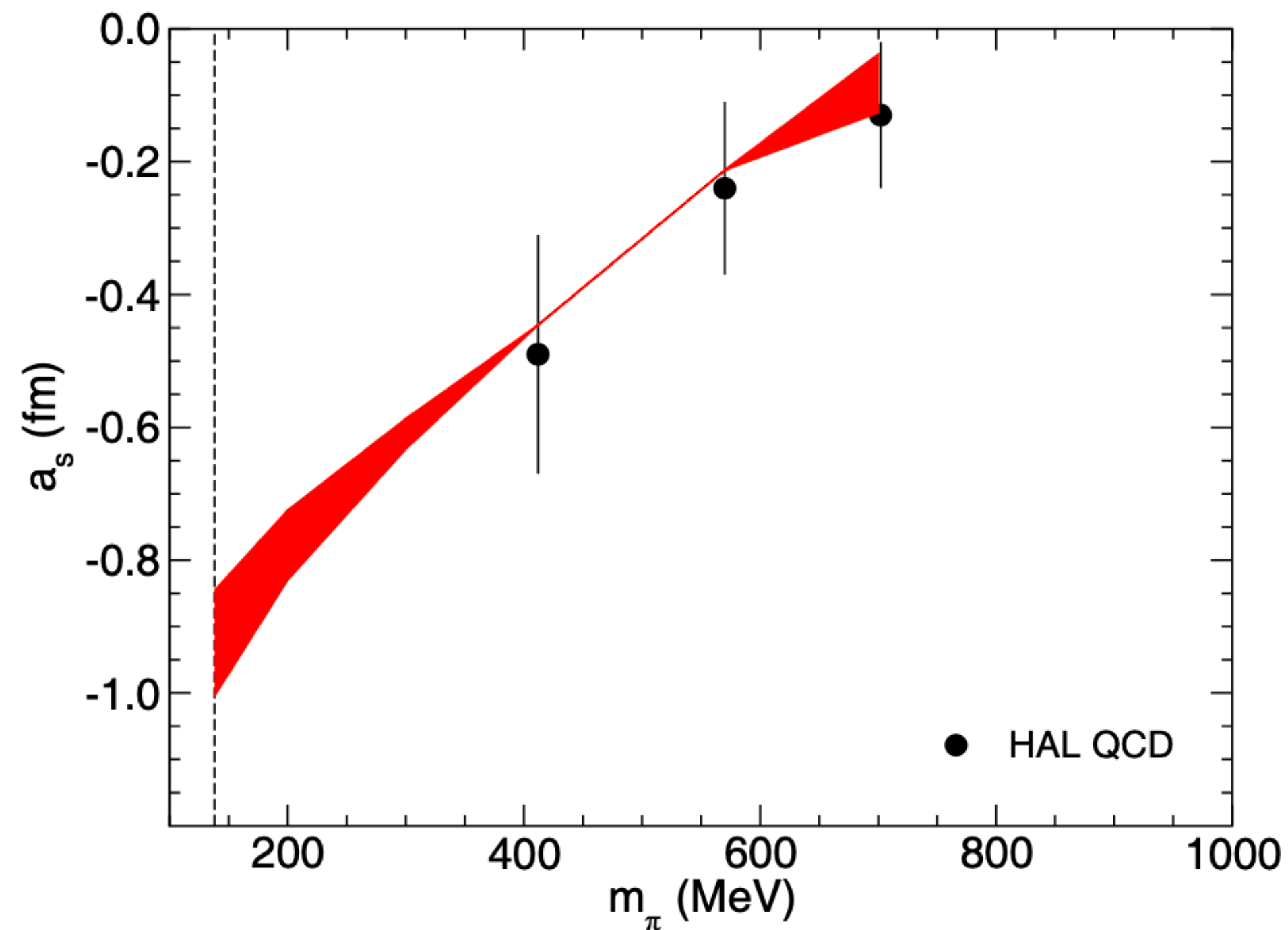


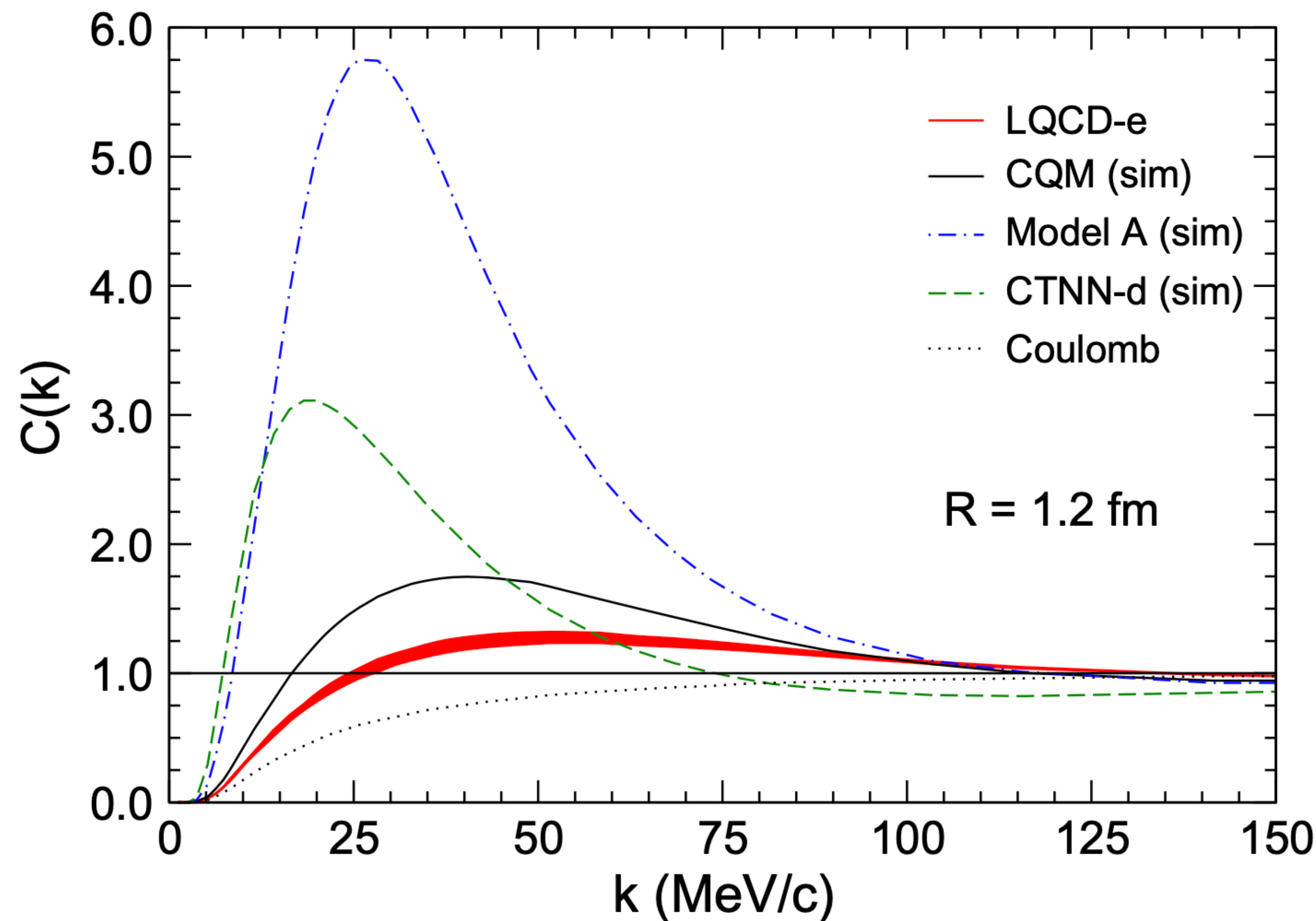
- **Hypernuclei**: bound states of strange baryons (hyperons) and ordinary nucleons
 - Several observations starting from 1950s
 - **Extend the nuclear chart** to a third dimension, the strangeness one
 - ▶ What about **charm**?



Charm hypernuclear spectrum already computed in 1977

- The lightest possible charmed hypernucleus (c-deuteron) can exist only if the strong **interaction between a charm-baryon and a nucleus is attractive**
- Lattice QCD calculations (HAL QCD) available at unphysical quark masses
 - ➔ Extrapolated to physical quark masses with unitarized chiral perturbation theory





- Quantitatively different predictions from different models

➔ LQCD-e (same as slide 25)

📖 J. Haidenbauer et al, EPJA (2018) 54: 199

➔ CQM: interaction derived within the constituent-quark model

📖 H. Garcilazo et al, EPJC 79 (2019) 598

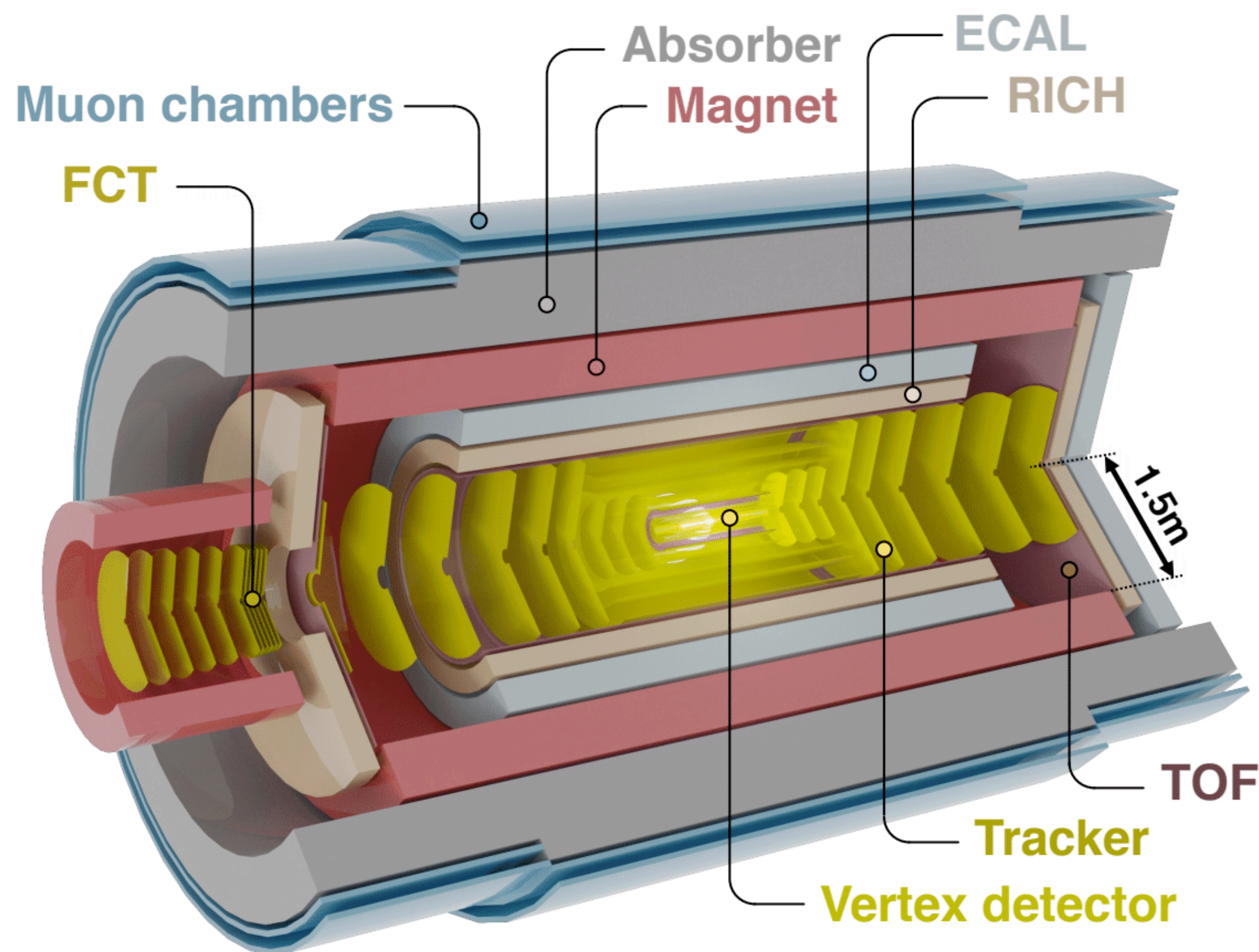
➔ CTNN-d and Model A: extension of the meson-exchange hyperon-nucleon potential

- ▶ Formation of bound states with binding energies of the order of that of the deuteron (CTNN-d) in both S-waves

📖 I. Vidana et al, PRC 99 (2019) 045208

📖 S. Maeda et al, PTEP 2016 (2016) 023D02

- Proposed upgrade for LHC Run 5 and 6

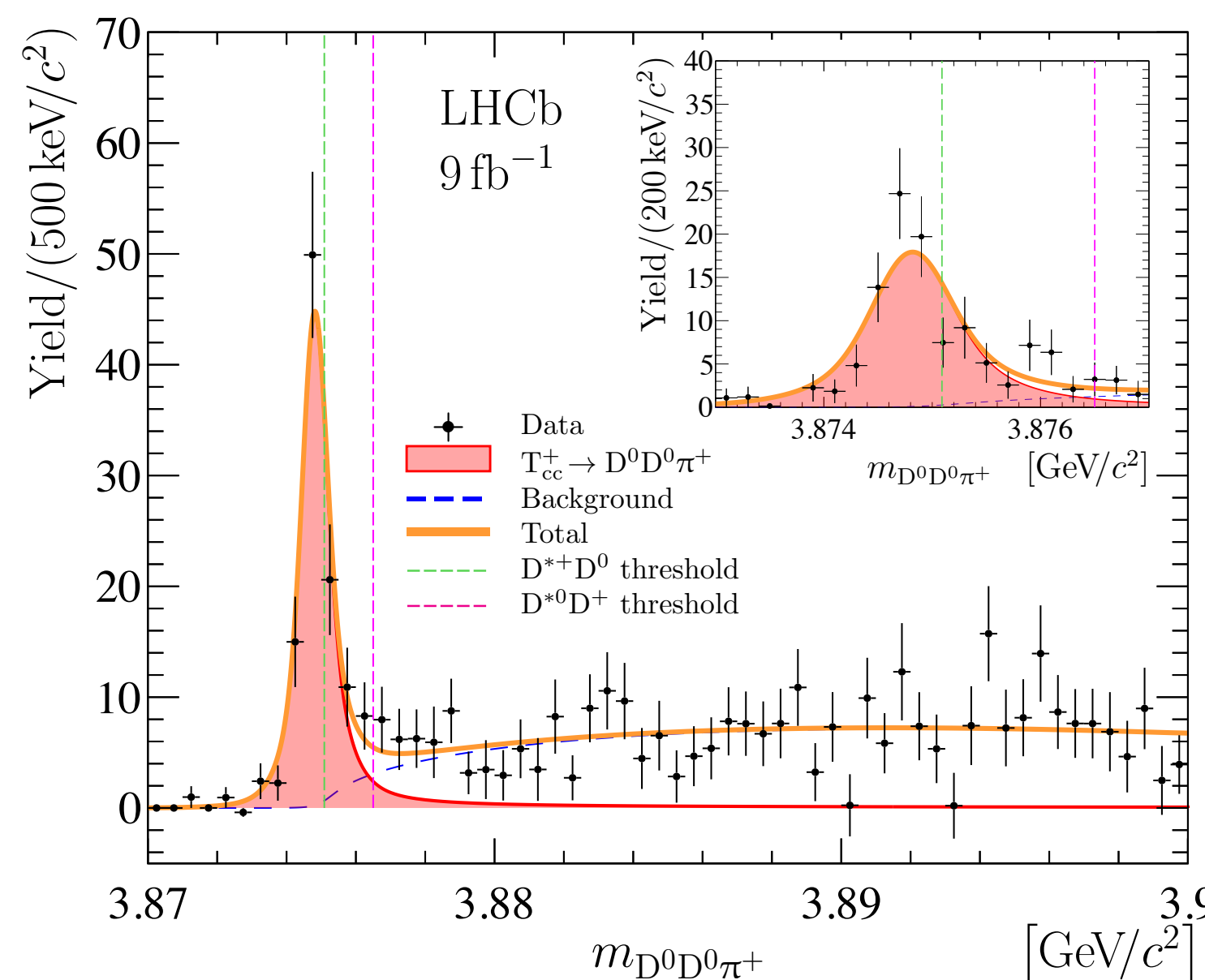
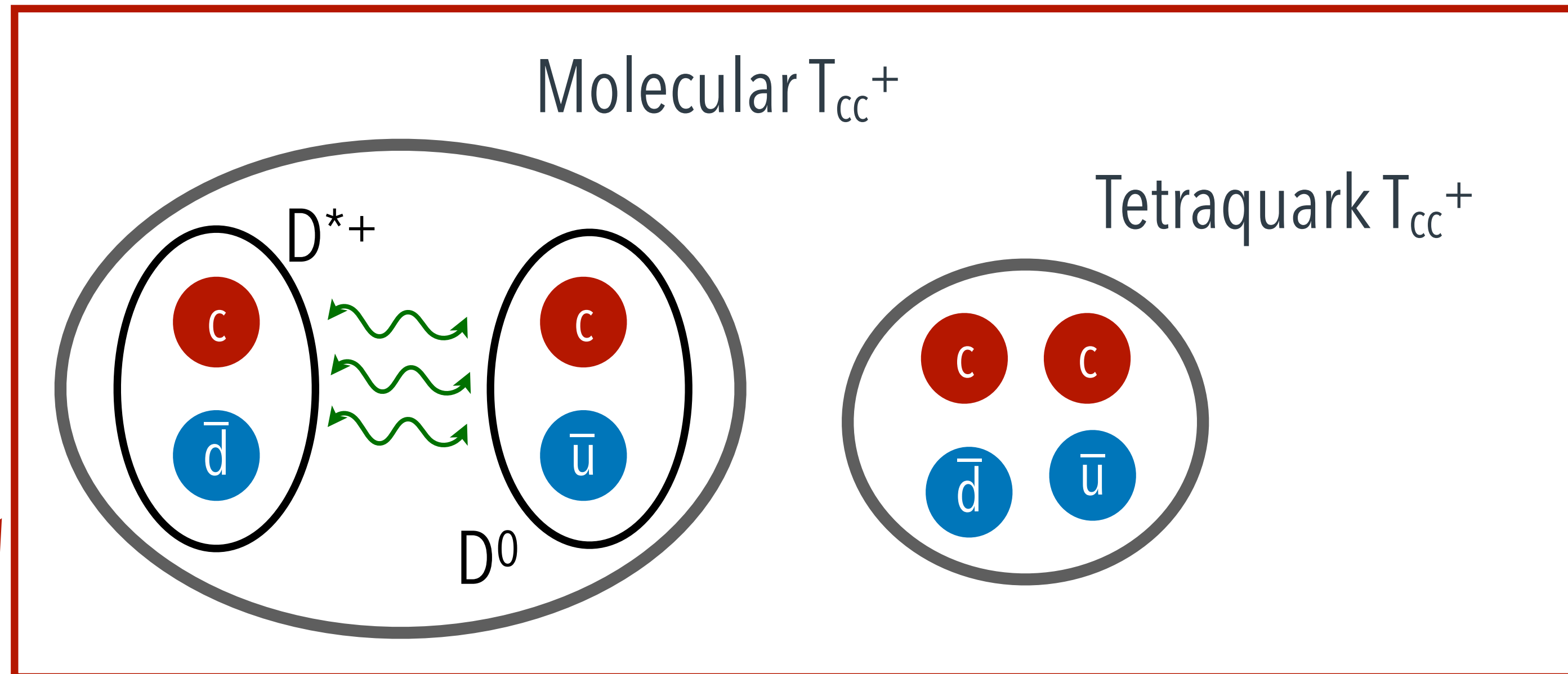


- Original proposal
 - Large acceptance ($|\eta| < 4$)
 - All silicon tracker with $\sigma_p/p \approx 1\%$
 - First tracking layer at 5 mm from primary vertex
 - $\sim 10\%$ X_0 overall material budget (0.1% X_0 for the first layer)
 - Impact parameter resolution $10\ \mu\text{m}$ for tracks with $p = 200\ \text{MeV}/c$
 - Excellent hadron and lepton PID
 - Silicon-based TOF and RICH
 - Muon chambers with absorber
 - x5 more AA luminosity than Run 3&4

- Possible descoping under discussion

● Charm molecules?

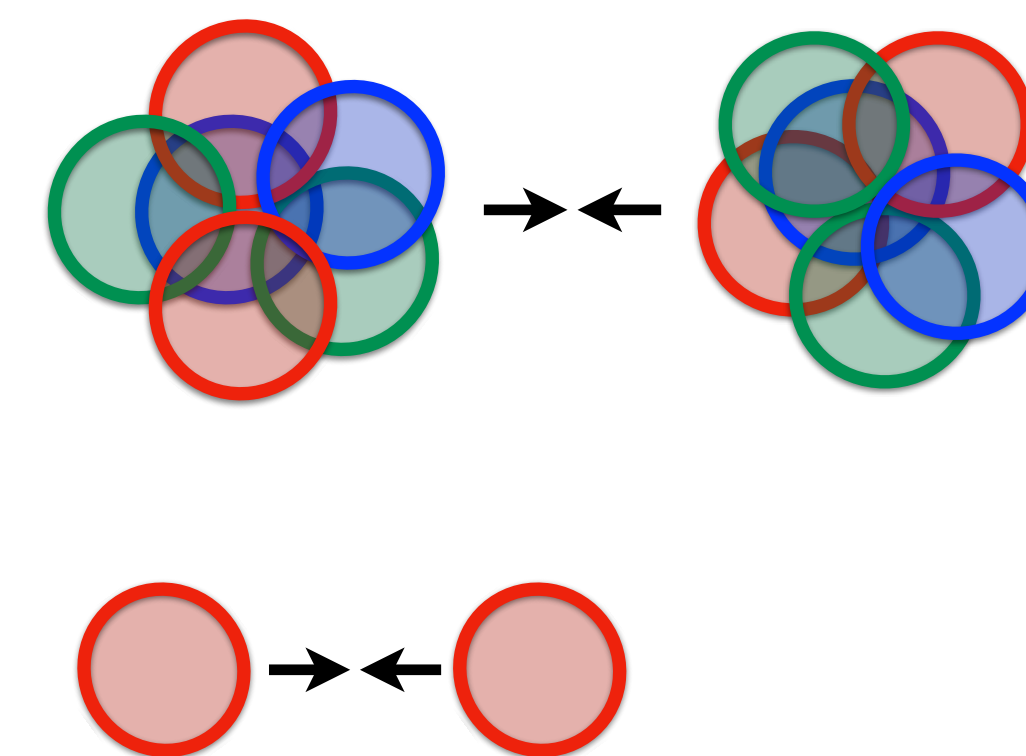
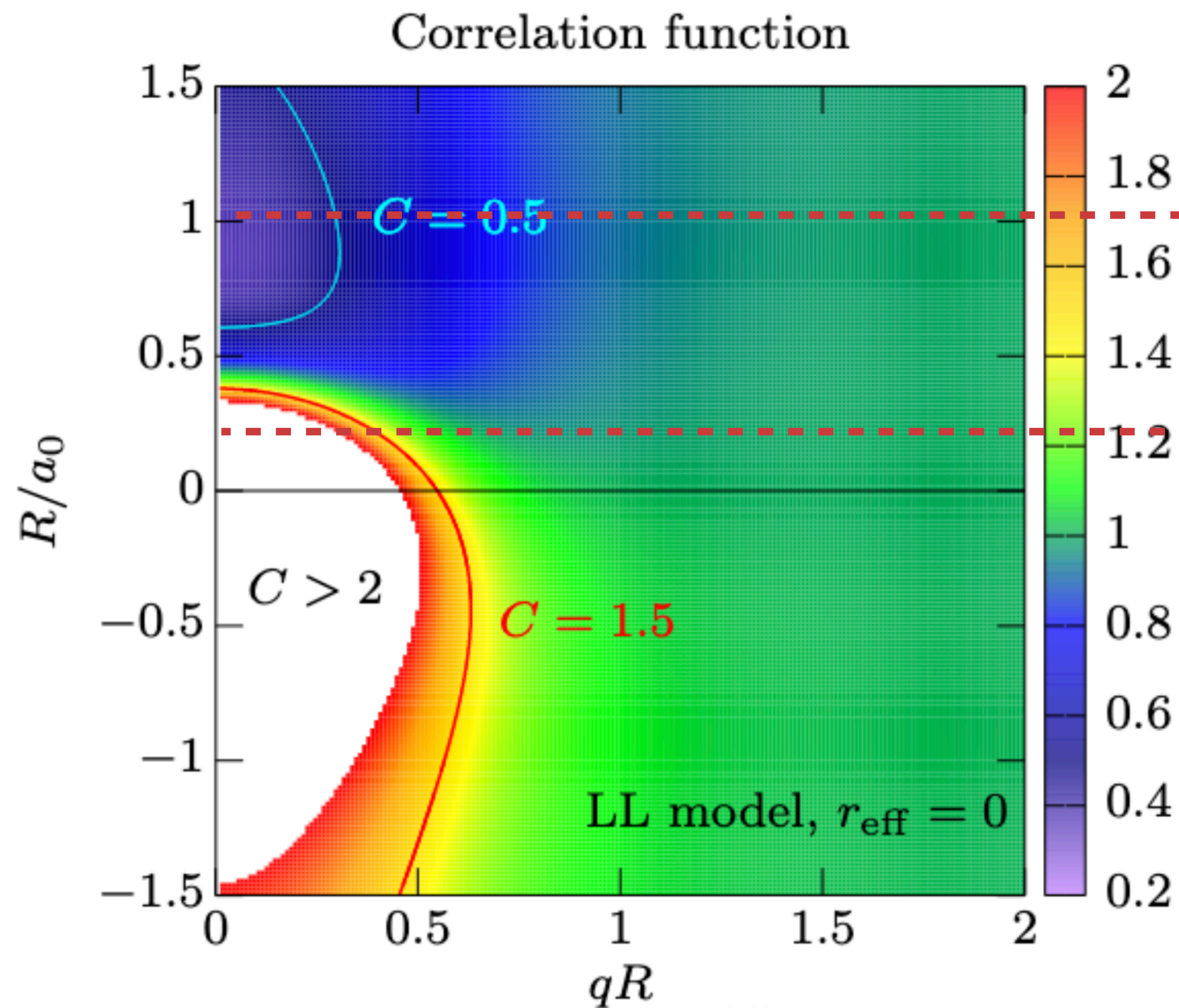
System	$I (J^{P(C)})$	Candidate
np	$0 (1^+)$	deuteron
ND	$0 (1/2^-)$	$\Lambda_c(2765)$
ND*	$0 (3/2^-)$	$\Lambda_c(2940)$
ND	$0 (1/2^-)$	$\Sigma_c(2800)$
$D^*\bar{D}$	$0 (1^{++})$	X(3872)
D^*D	$0 (1^+)$	T_{cc}
$D_1\bar{D}$	$0 (1^{--})$	Y(4260)
$D_1\bar{D}^*$	$0 (1^{--})$	Y(4360)
$\Sigma\bar{D}$	$1/2 (1/2^-)$	$P_c(4312)$
$\Sigma\bar{D}^*$	$1/2 (1/2^-)$	$P_c(4457)$
$\Sigma\bar{D}^*$	$1/2 (3/2^-)$	$P_c(4440)$



- Just below DD^* threshold
- ➔ ideal candidate to be a molecular state

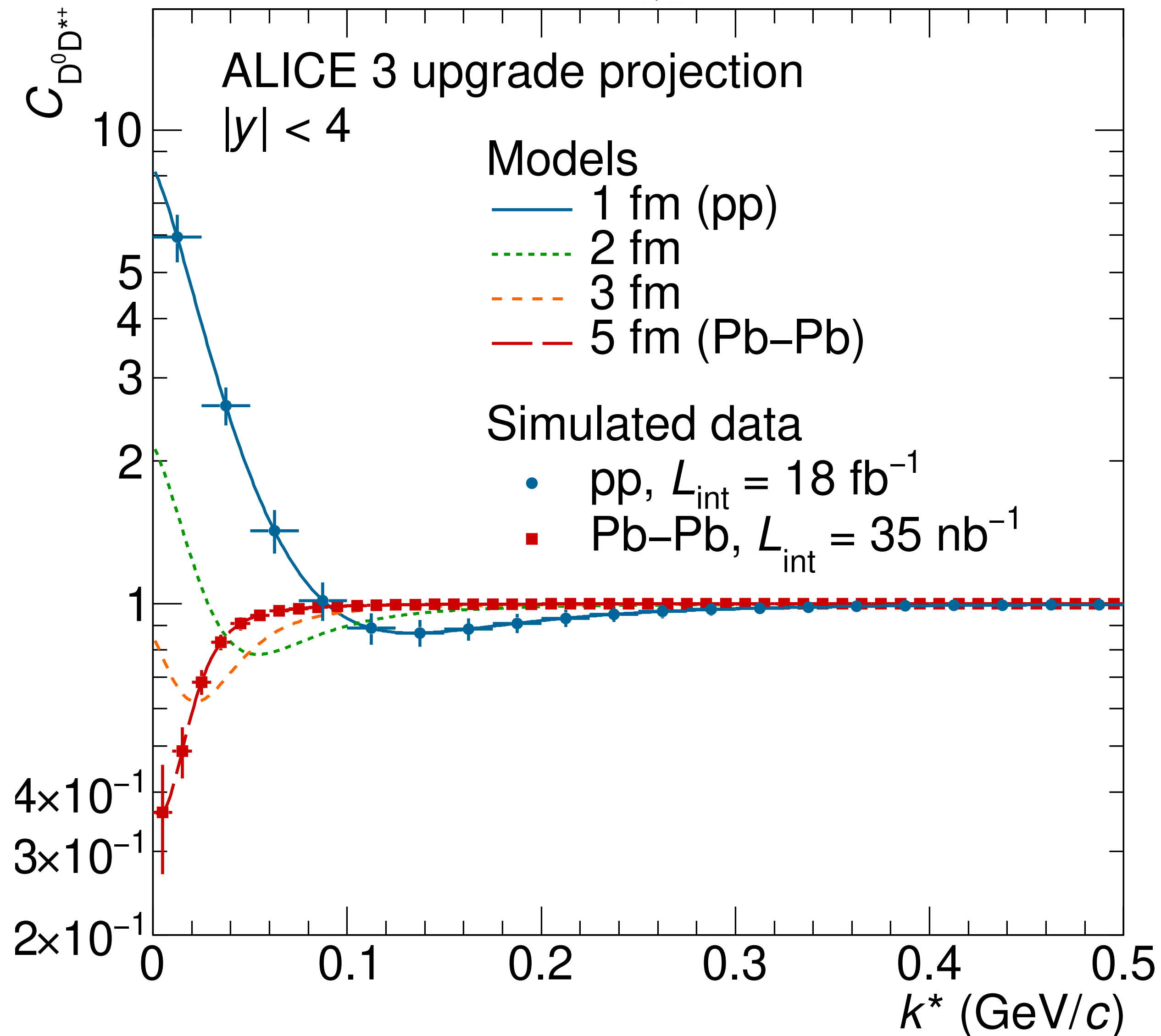
Fang-Zheng Peng et al, Phys. Rev. D 105, 034028 (2022)

LHCb, Nature Physics 18 (2022) 751-754



- Interplay between system size and scattering length
- ➔ size-dependent modification of the correlation function in presence of a bound state

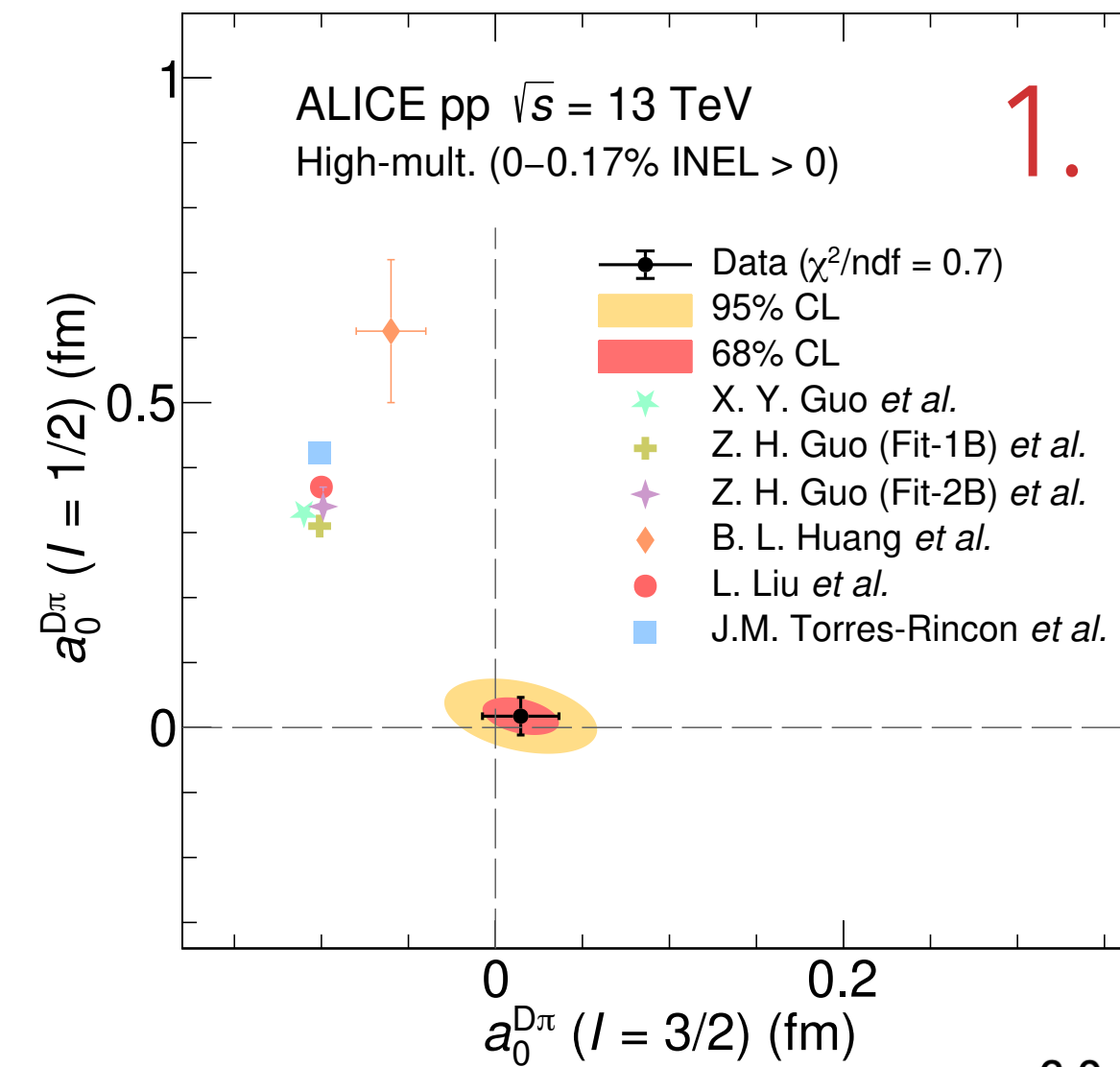
ALICE3 LOI: CERN-LHCC-2022-009



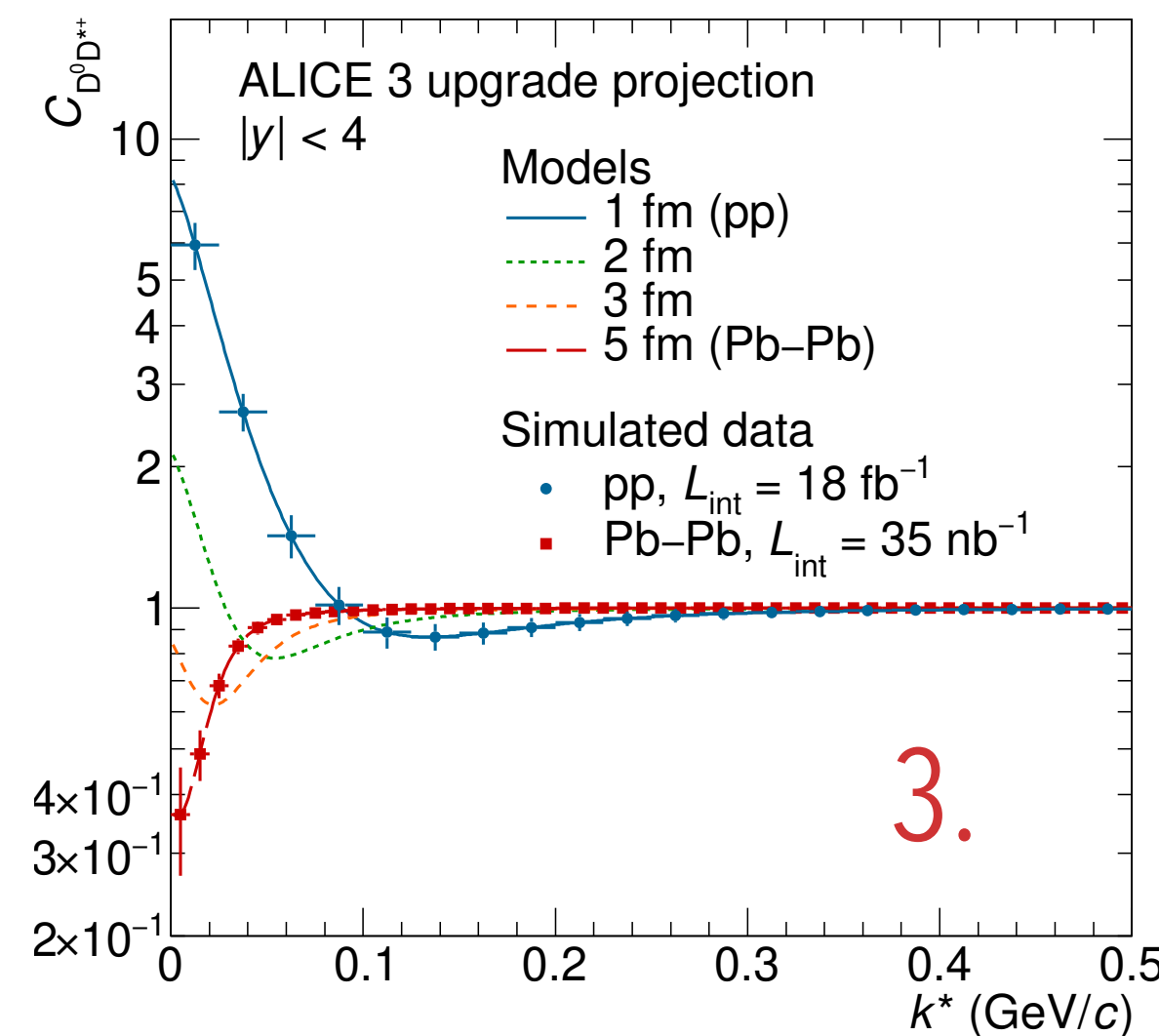
- ALICE 3: large acceptance, high luminosity, excellent spatial resolution
 - ➔ Run 5: ideal laboratory for the measurement of charm-hadron momentum correlations in different colliding systems
- Interplay between system size and scattering length
 - ➔ size-dependent modification of the correlation function in presence of a bound state

Yuki Kamyia et al, arXiv:2203.13814

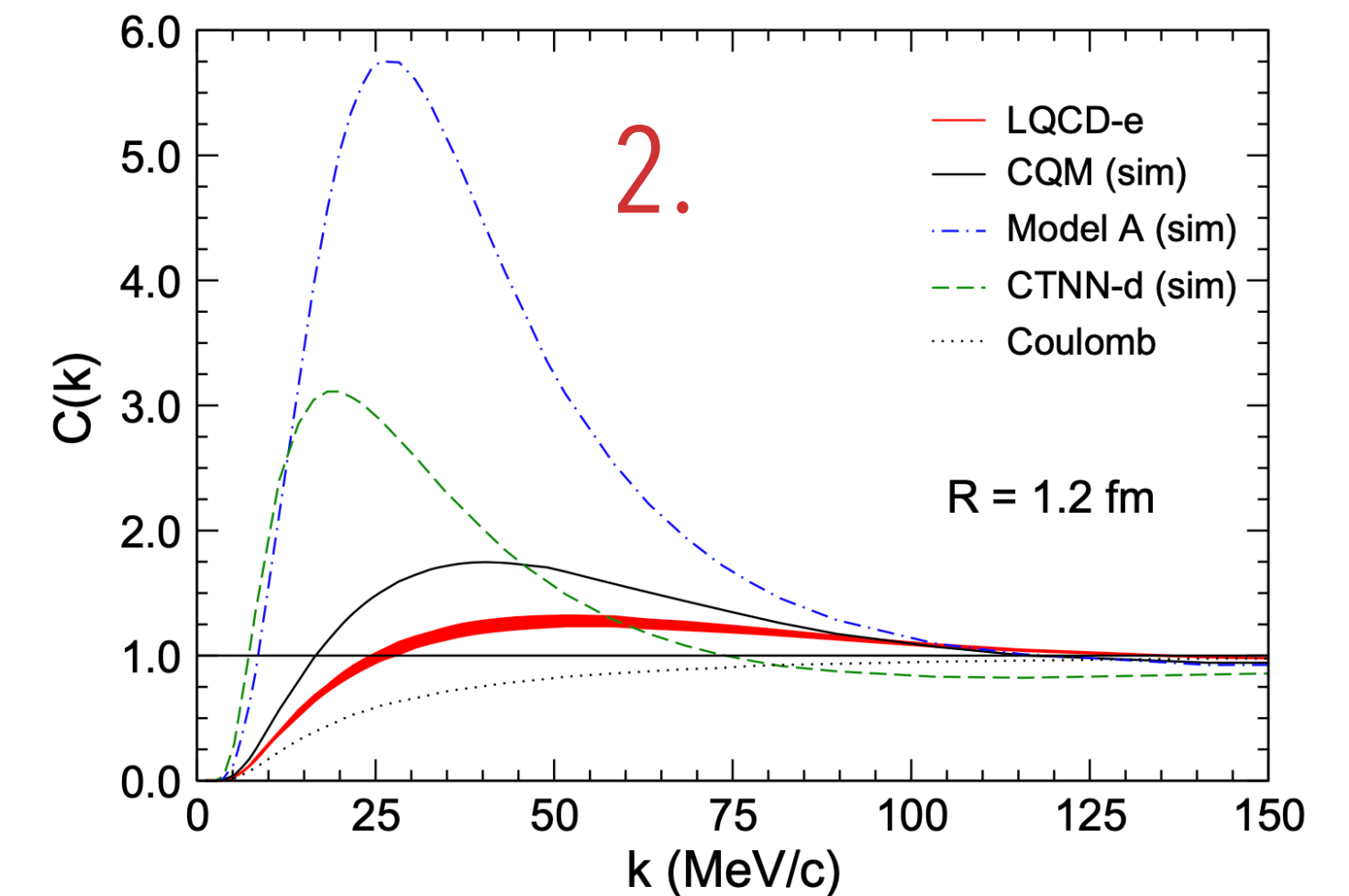
- First measurements of femtoscopy with charm mesons** performed with ALICE using data collected in Run 2
 - ➔ Typically "weaker" strong interaction measured compared to theoretical predictions
- Expected significant improvements** thanks to the ALICE upgrades installed for **Run 3** (improved pointing resolution and readout capabilities)
 - ➔ Measure interactions between charm baryons and nucleons
- Proposed** wide acceptance, ultralight silicon-based experiment for **Run 5 (ALICE 3)**
 - ➔ Measure interactions between pairs of charm hadrons to investigate nature of exotic states



ALI-PUB-584542



ALI-SIMUL-502575



The image features a central white circle with a dark grey outline, representing the sun. From the top and bottom edges of this circle, numerous thin, red lines radiate outwards, creating a sunburst effect. The background is a dark grey color. A horizontal white band passes through the center of the sun, containing the text.

ADDITIONAL SLIDES

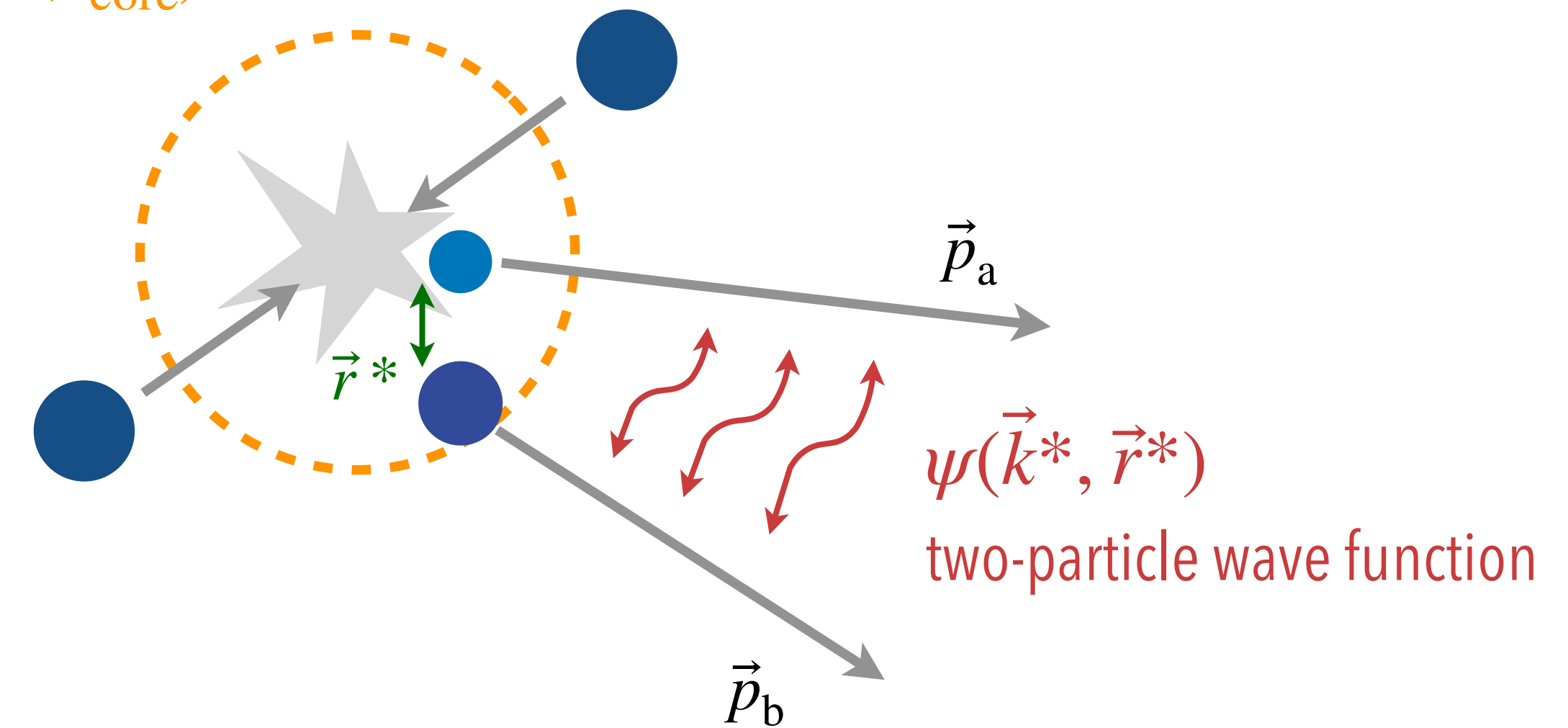
$$C(\vec{k}^*) = \int S(\vec{r}^*) |\psi(\vec{k}^*, \vec{r}^*)|^2 d^3 r^*$$

→ **Emitting source**: hypersurface at kinematic freezeout of final-state particles

- Described with a Gaussian core

$$G(r^*, r_{\text{core}}(m_T)) = \frac{1}{(4\pi r_{\text{core}}^2(m_T))^{3/2}} \cdot \exp\left(-\frac{r^{*2}}{4r_{\text{core}}^2(m_T)}\right)$$

$G(\vec{r}^*, r_{\text{core}})$ Gaussian core



$$C(\vec{k}^*) = \int S(\vec{r}^*) |\psi(\vec{k}^*, \vec{r}^*)|^2 d^3 r^*$$

$S(\vec{r}^*)$ source function

$G(\vec{r}^*, r_{\text{core}})$ Gaussian core

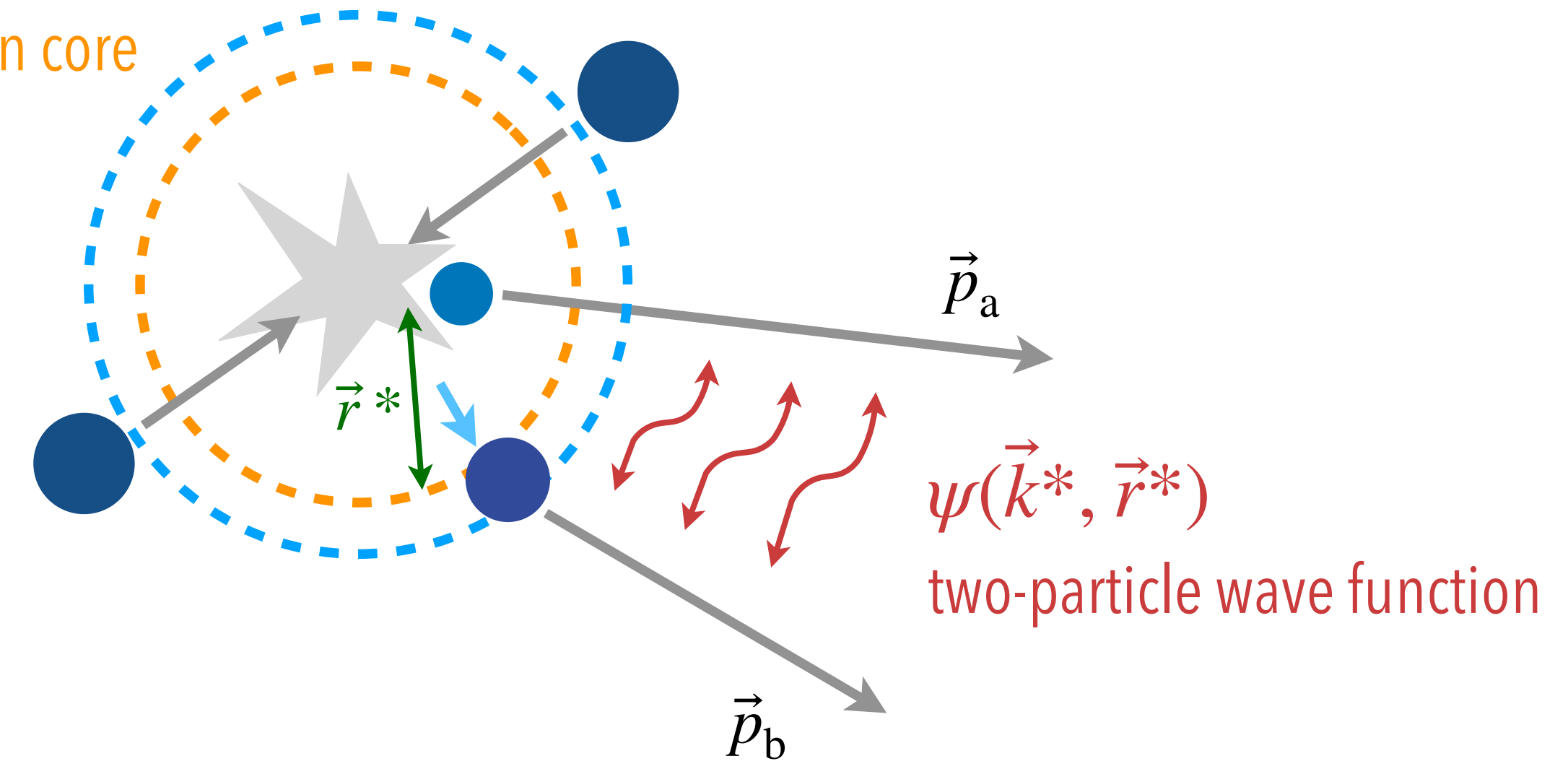
→ **Emitting source**: hypersurface at kinematic freezeout of final-state particles

- Described with a Gaussian core

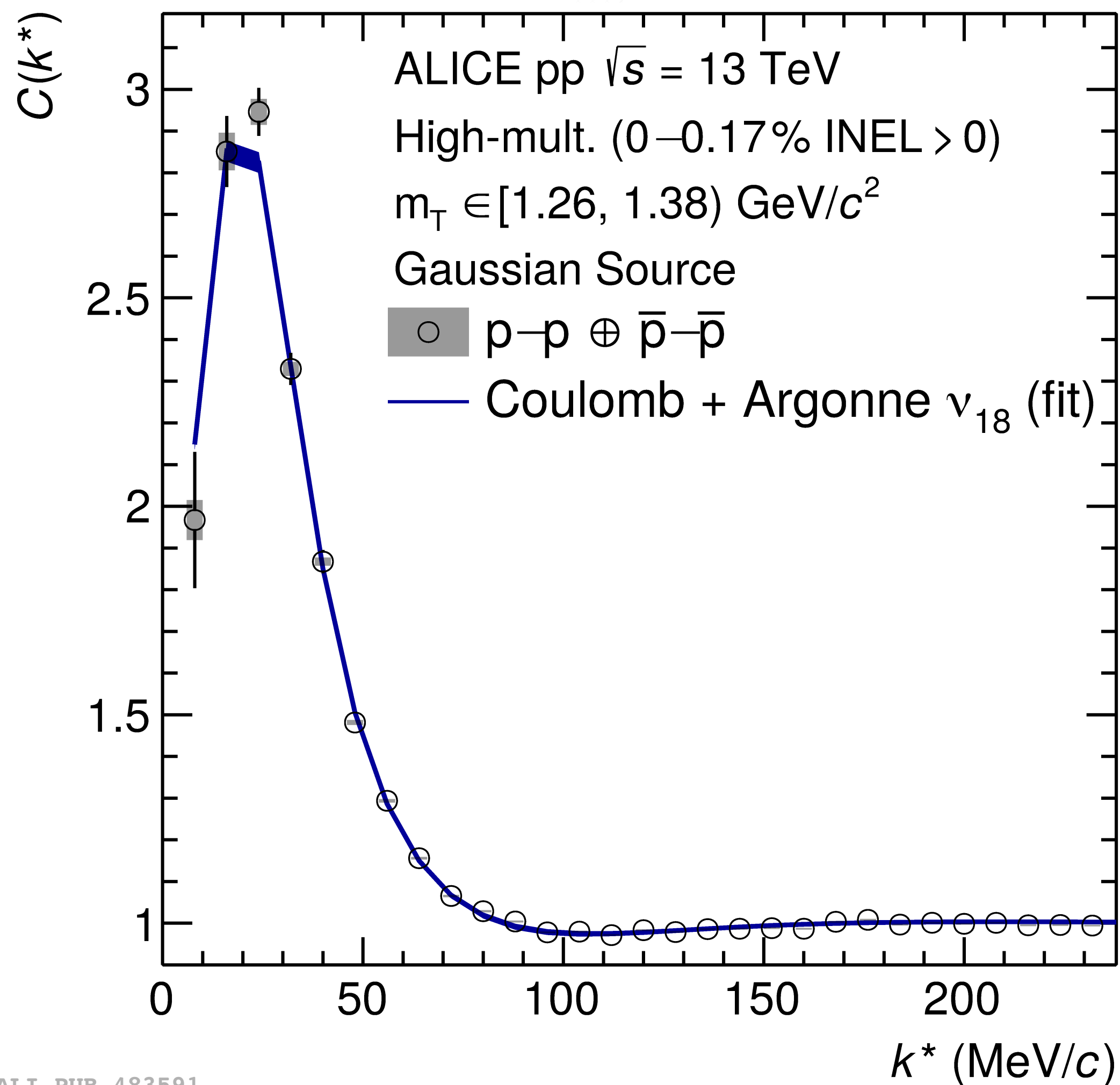
$$G(r^*, r_{\text{core}}(m_T)) = \frac{1}{(4\pi r_{\text{core}}^2(m_T))^{3/2}} \cdot \exp\left(-\frac{r^{*2}}{4r_{\text{core}}^2(m_T)}\right)$$

- Short-lived strongly decaying resonances effectively enlarge it

$$E(r^*, M_{\text{res}}, \tau_{\text{res}}, p_{\text{res}}) = \frac{1}{s} \exp\left(-\frac{r^*}{s}\right) \quad \text{with} \quad s = \beta\gamma\tau_{\text{res}} = \frac{p_{\text{res}}}{M_{\text{res}}}\tau_{\text{res}}$$



Phys. Lett. B 811 (2020) 135849

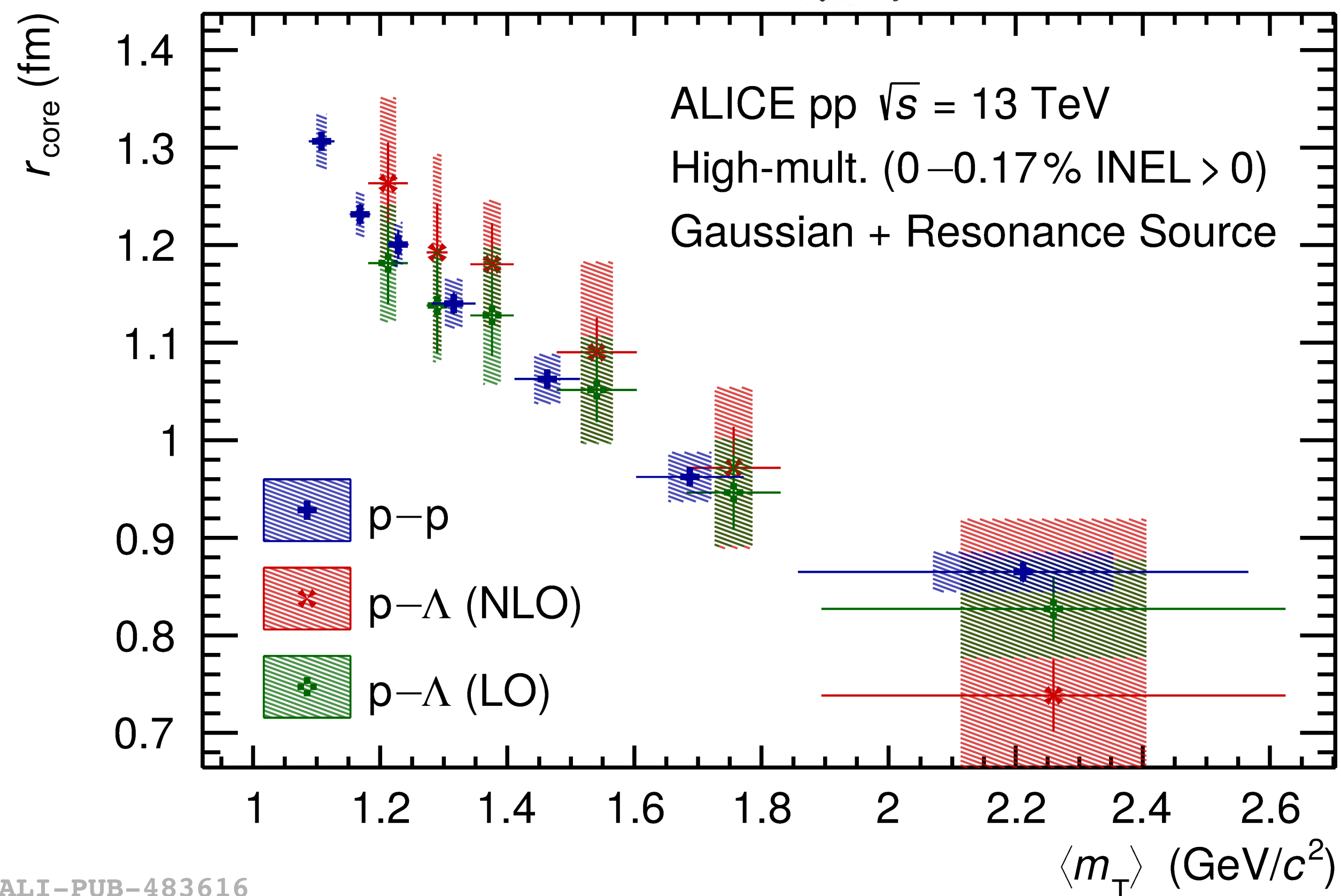


ALI-PUB-483591

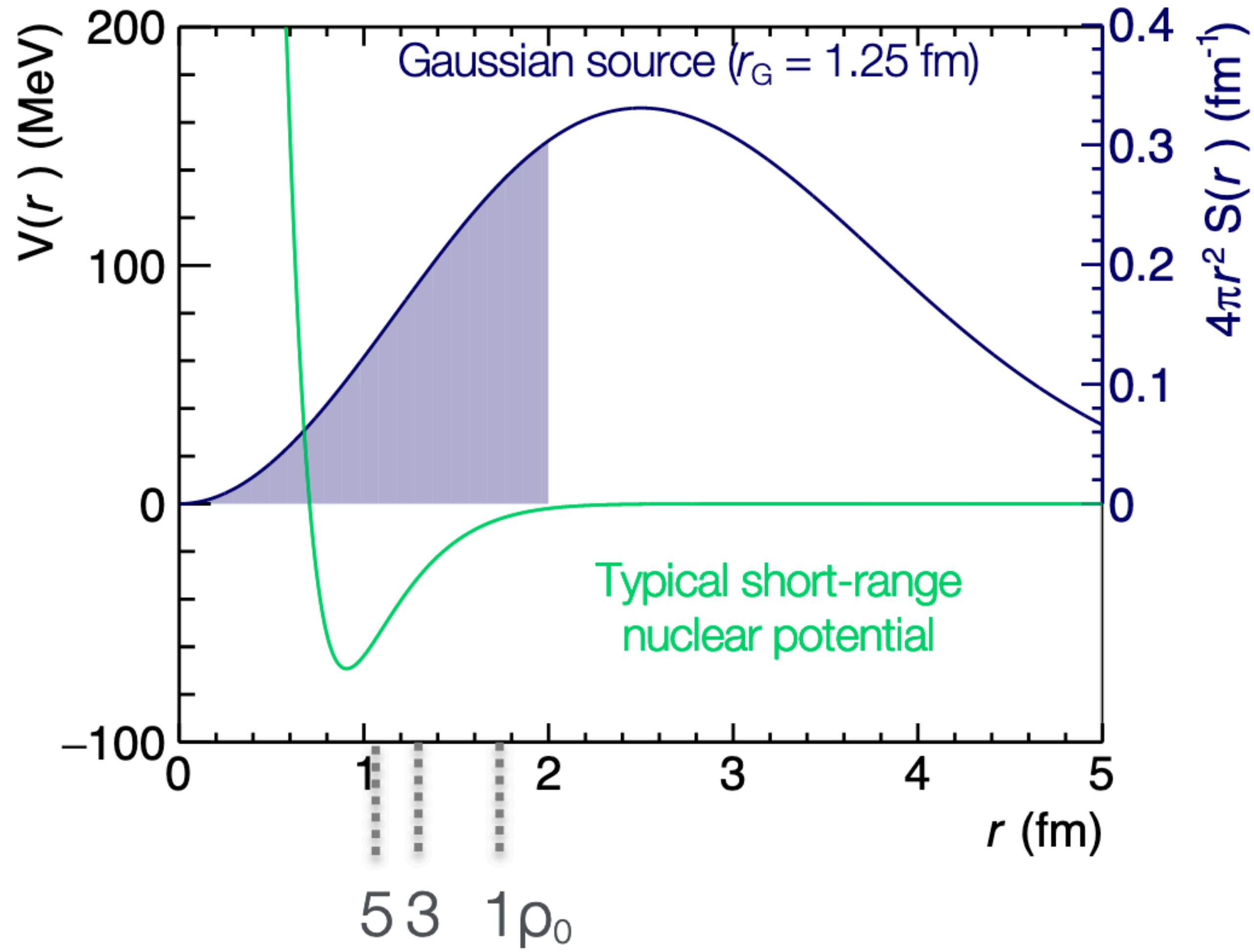
- Source size ~ 1 fm makes the high-multiplicity pp system suitable for the study of hadron–hadron interactions

- Fit correlation functions of p–p and p– Λ pairs
 - ➔ Interaction precisely described
 - ➔ Gaussian source with radius as free parameter

Phys. Lett. B 811 (2020) 135849

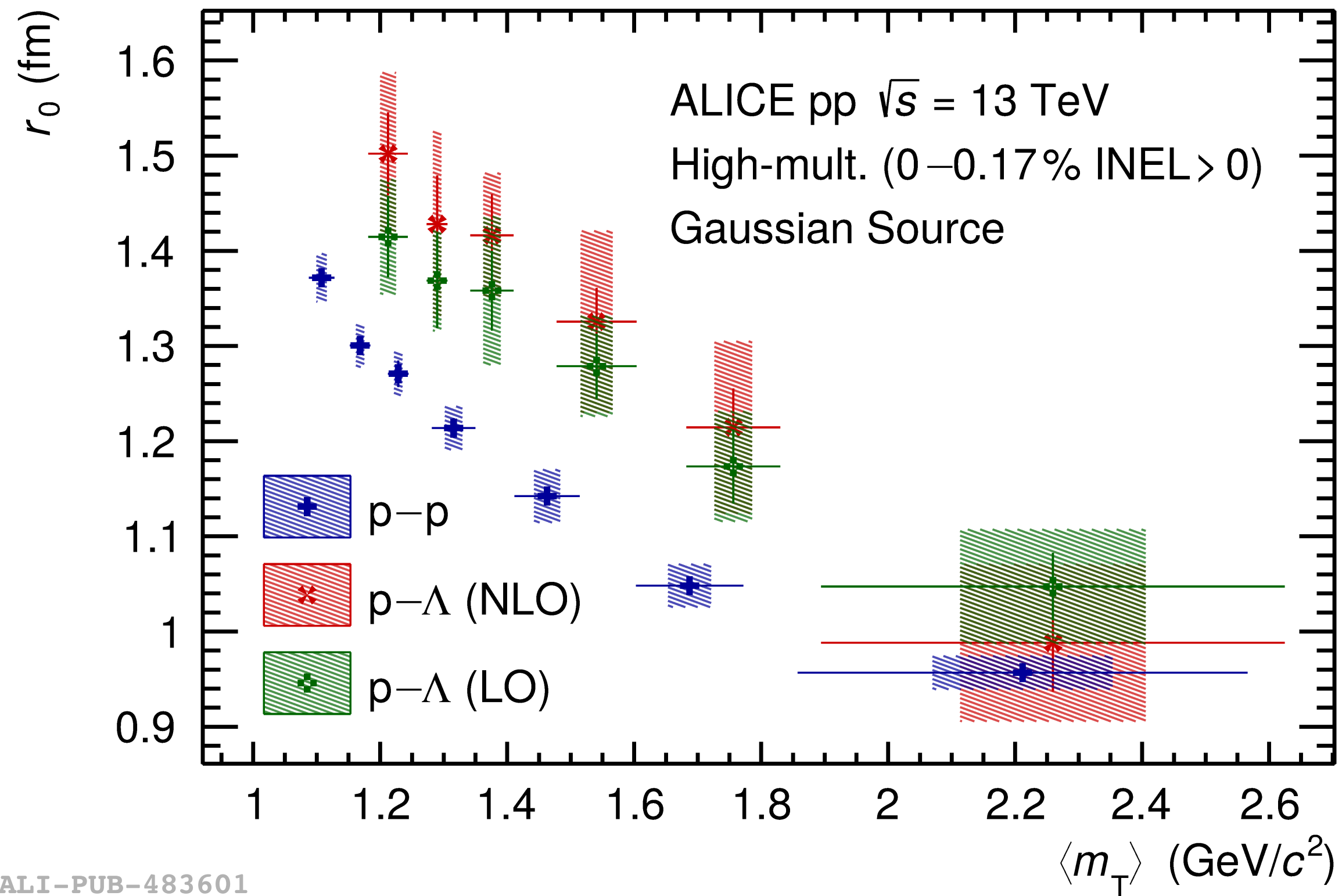


ALI-PUB-483616



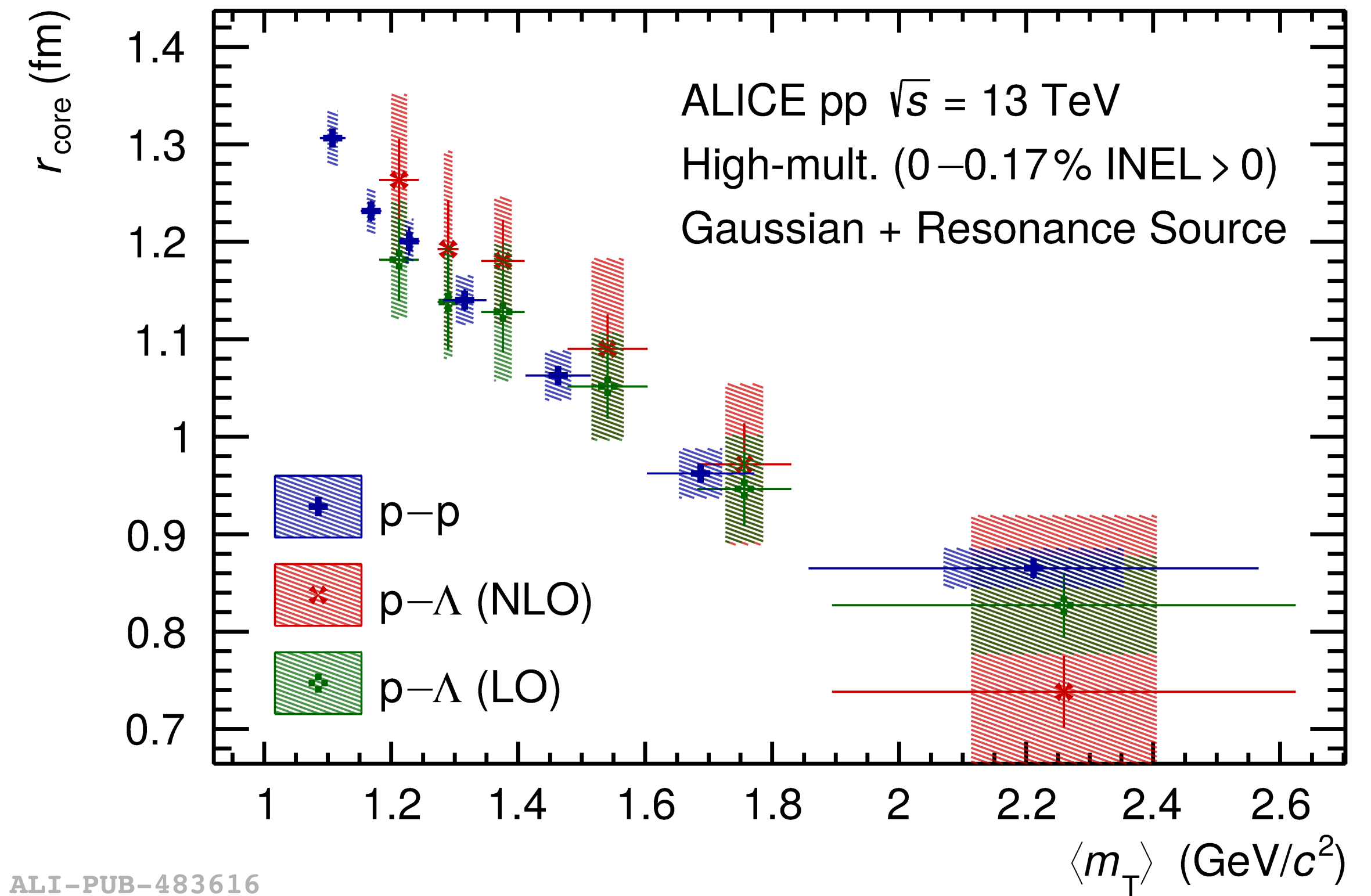
- Typical range of nuclear potential around 1-2 fm
 - ➔ study of strong interaction among hadrons not possible with larger sources
 - ➔ proton–proton and proton–nucleus collisions are the ideal laboratory to study the strong interaction

● Without considering resonances

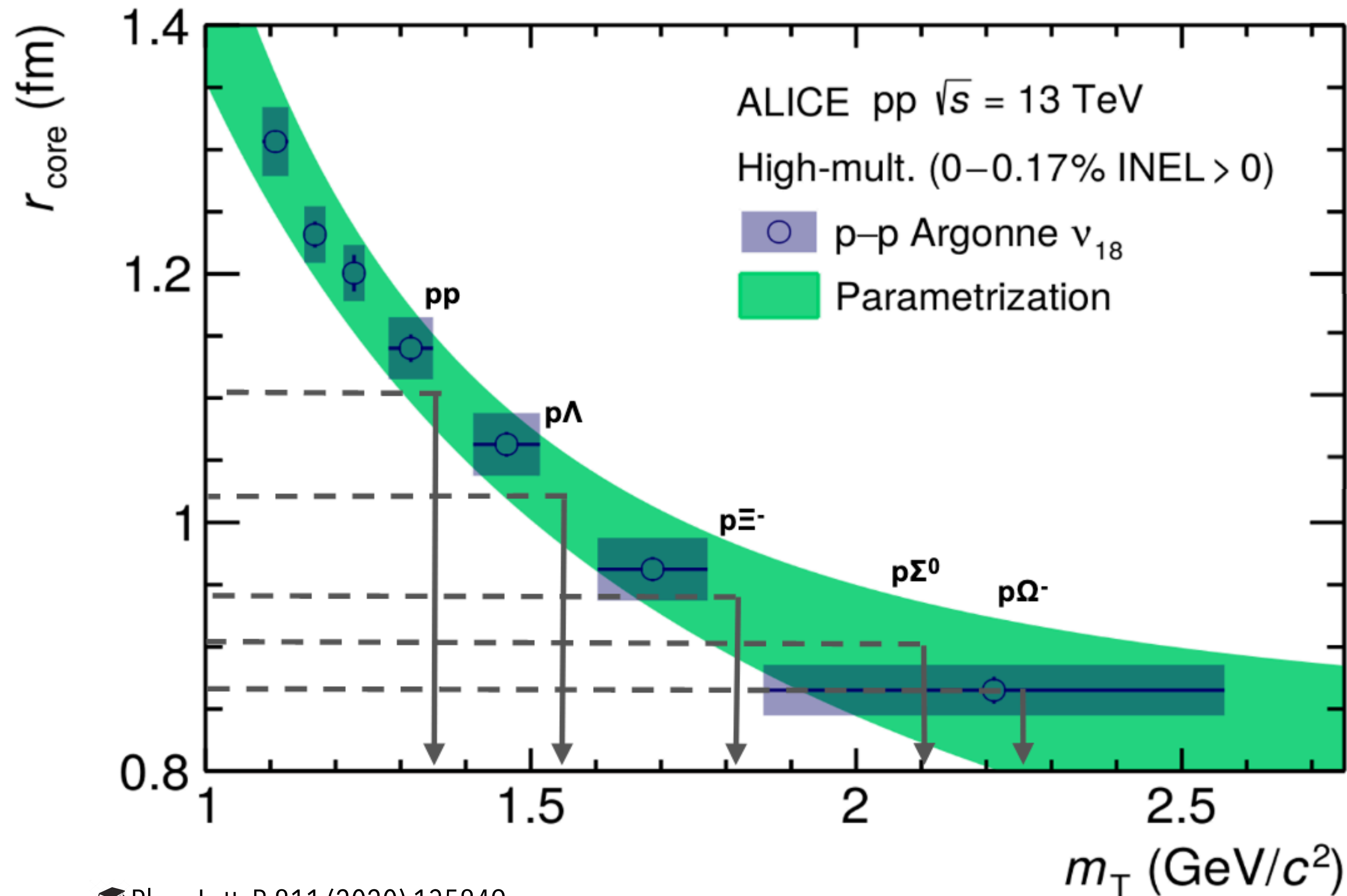


ALI-PUB-483601

● Considering resonances



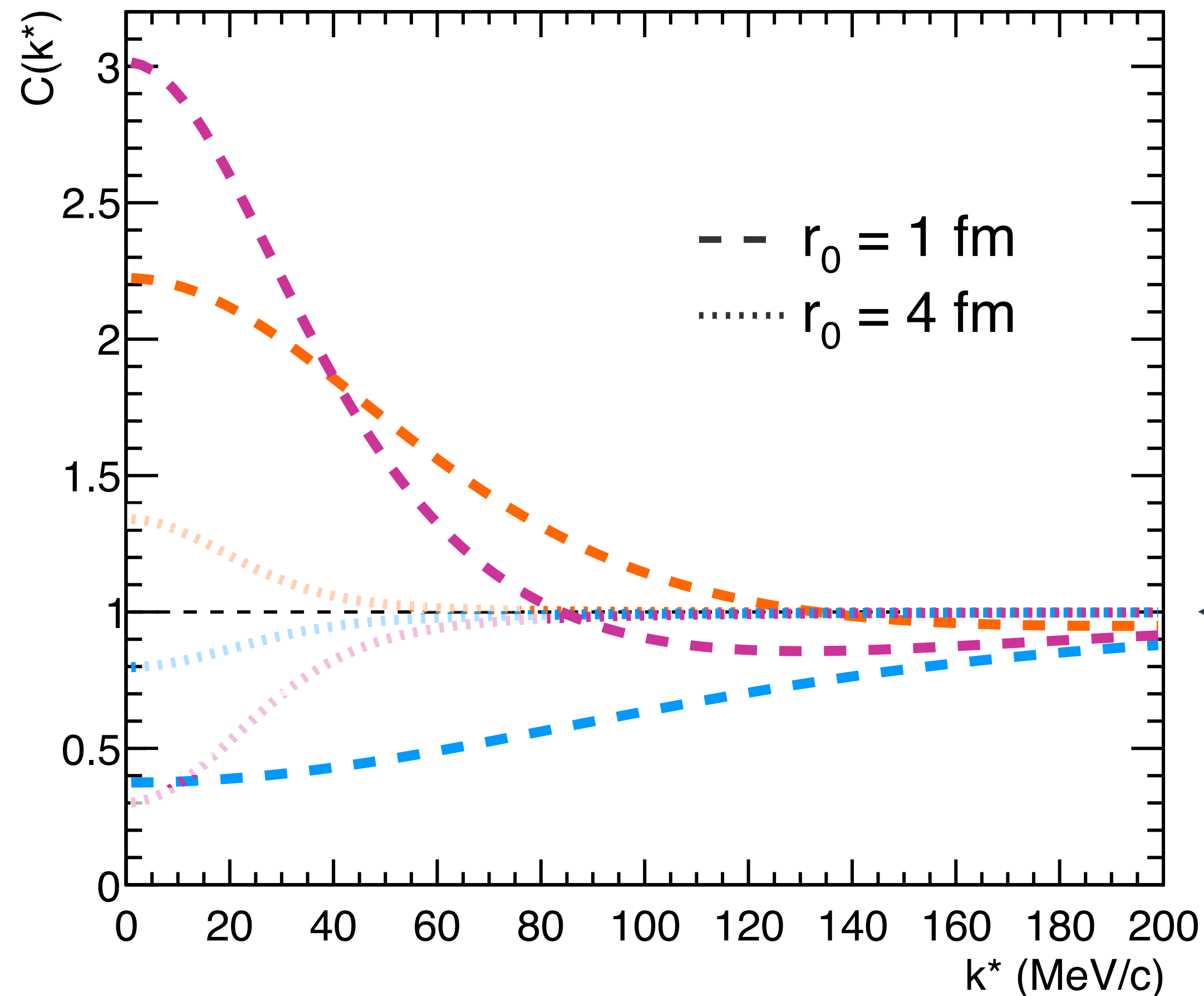
ALI-PUB-483616



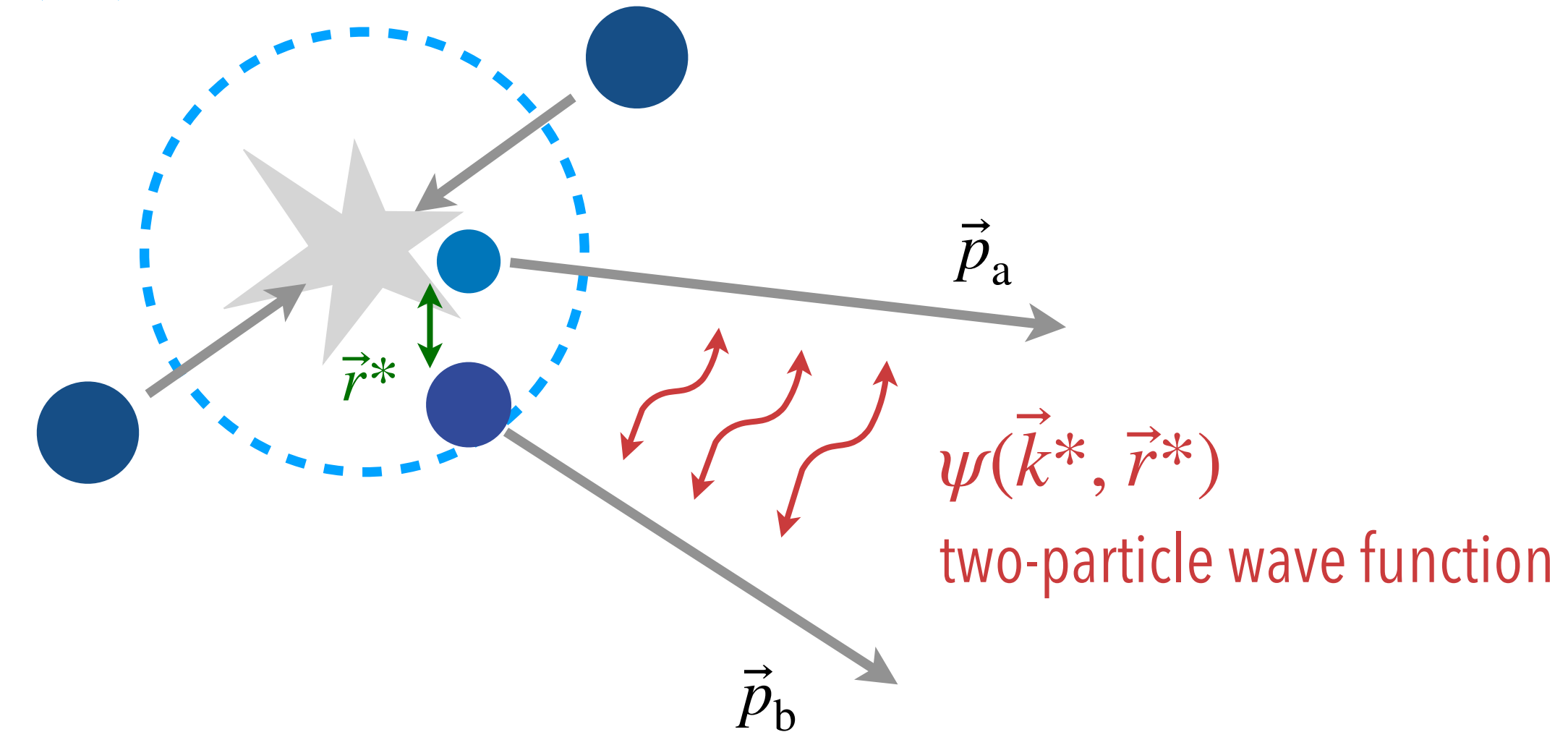
- Measurement of source radius obtained from p–p correlation used to obtain the values for other baryon species

$$C(\vec{k}^*) = \int S(\vec{r}^*) |\psi(\vec{k}^*, \vec{r}^*)|^2 d^3 r^*$$

→ Relative wave function sensitive to interaction potential



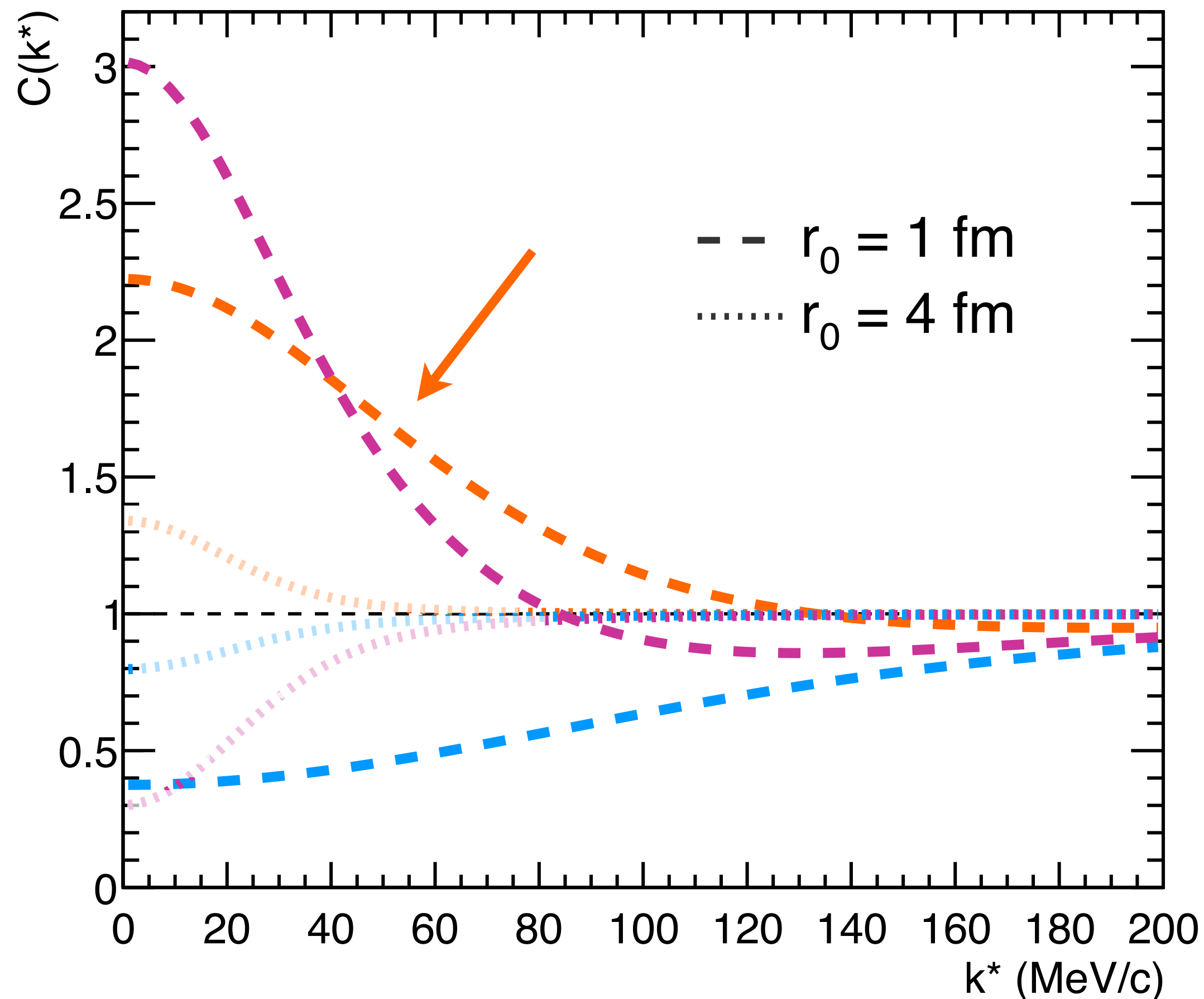
$S(\vec{r}^*)$ source function



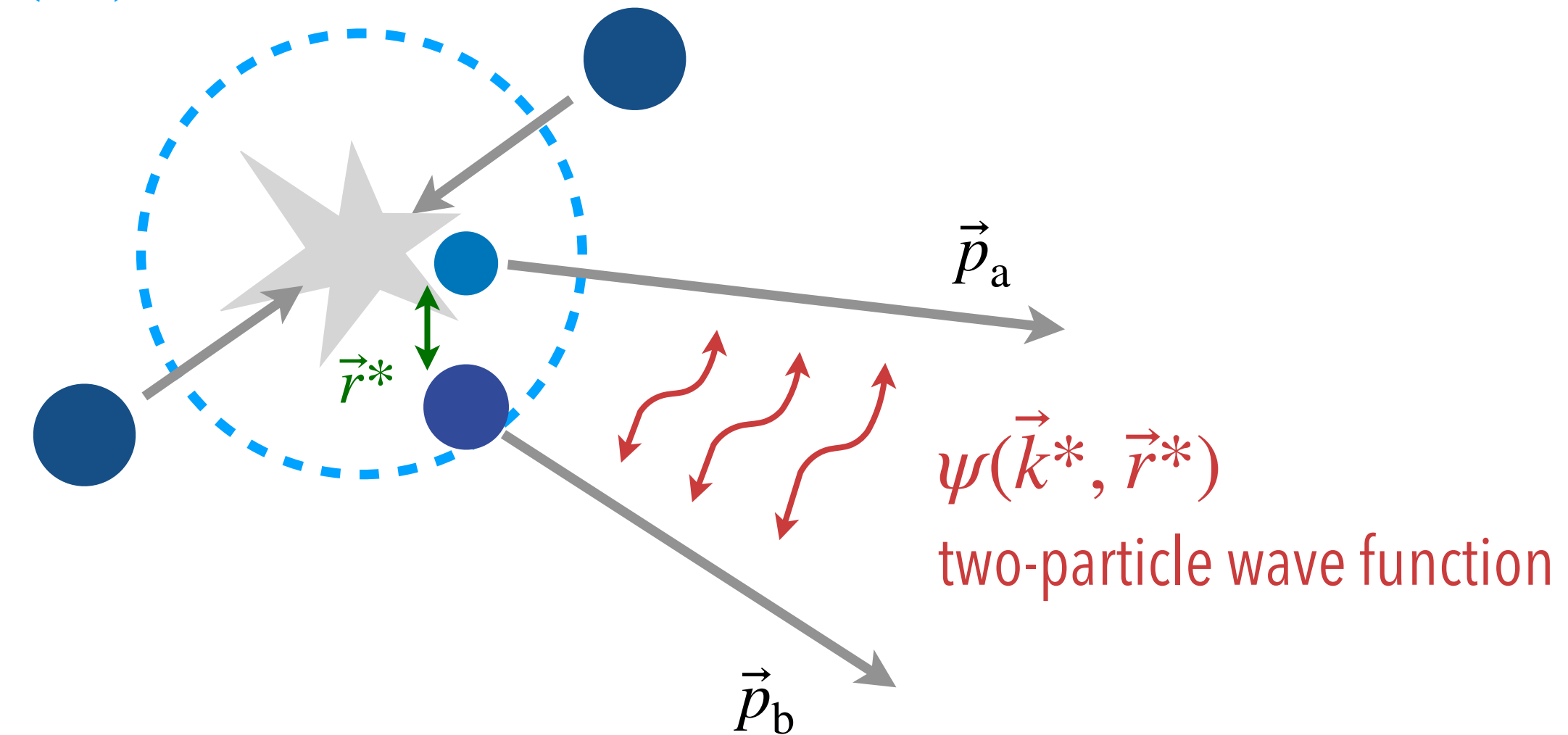
→ Absence of interaction $C(k^*) = 1$

$$C(\vec{k}^*) = \int S(\vec{r}^*) |\psi(\vec{k}^*, \vec{r}^*)|^2 d^3 r^*$$

→ Relative wave function sensitive to interaction potential



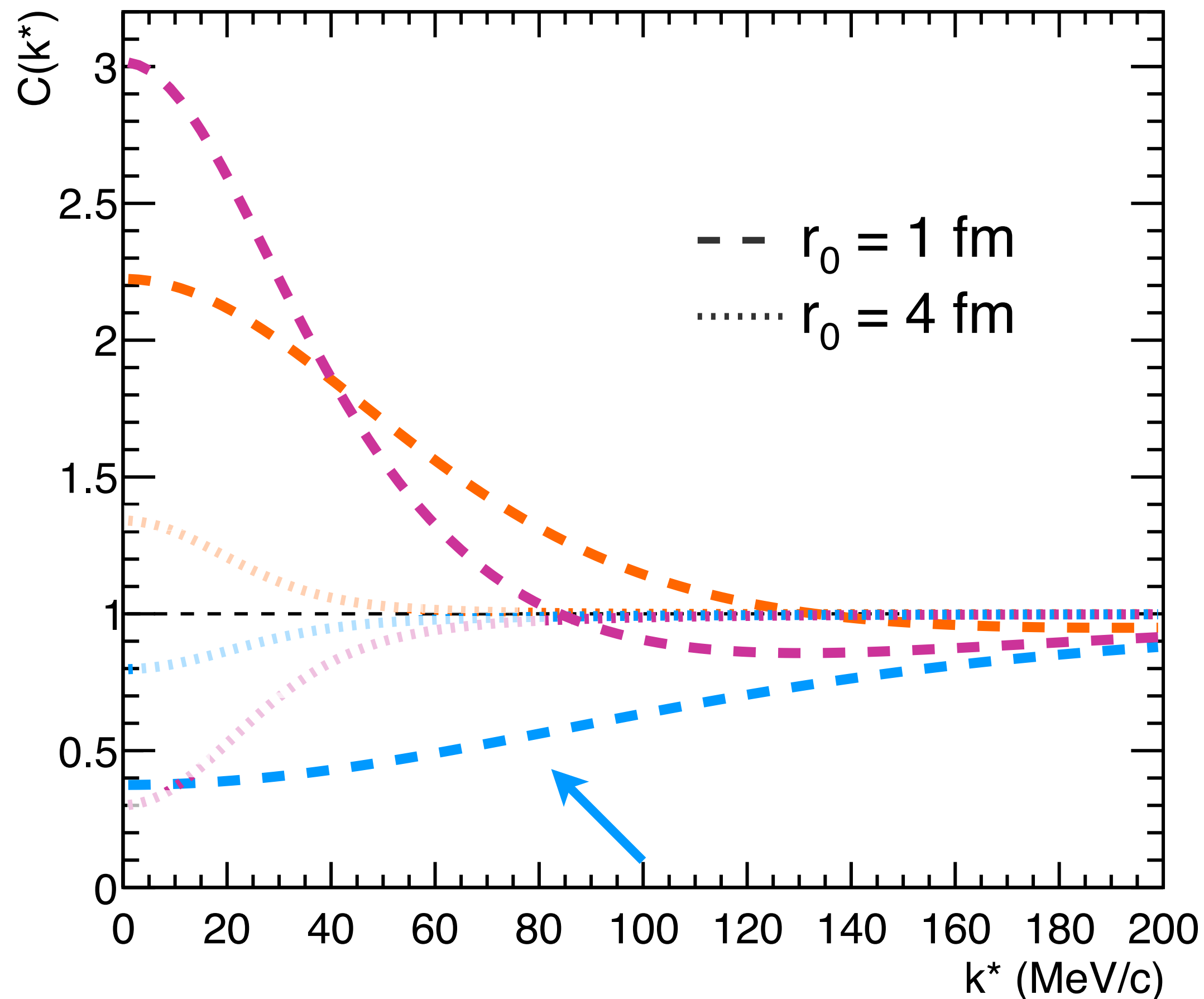
$S(\vec{r}^*)$ source function



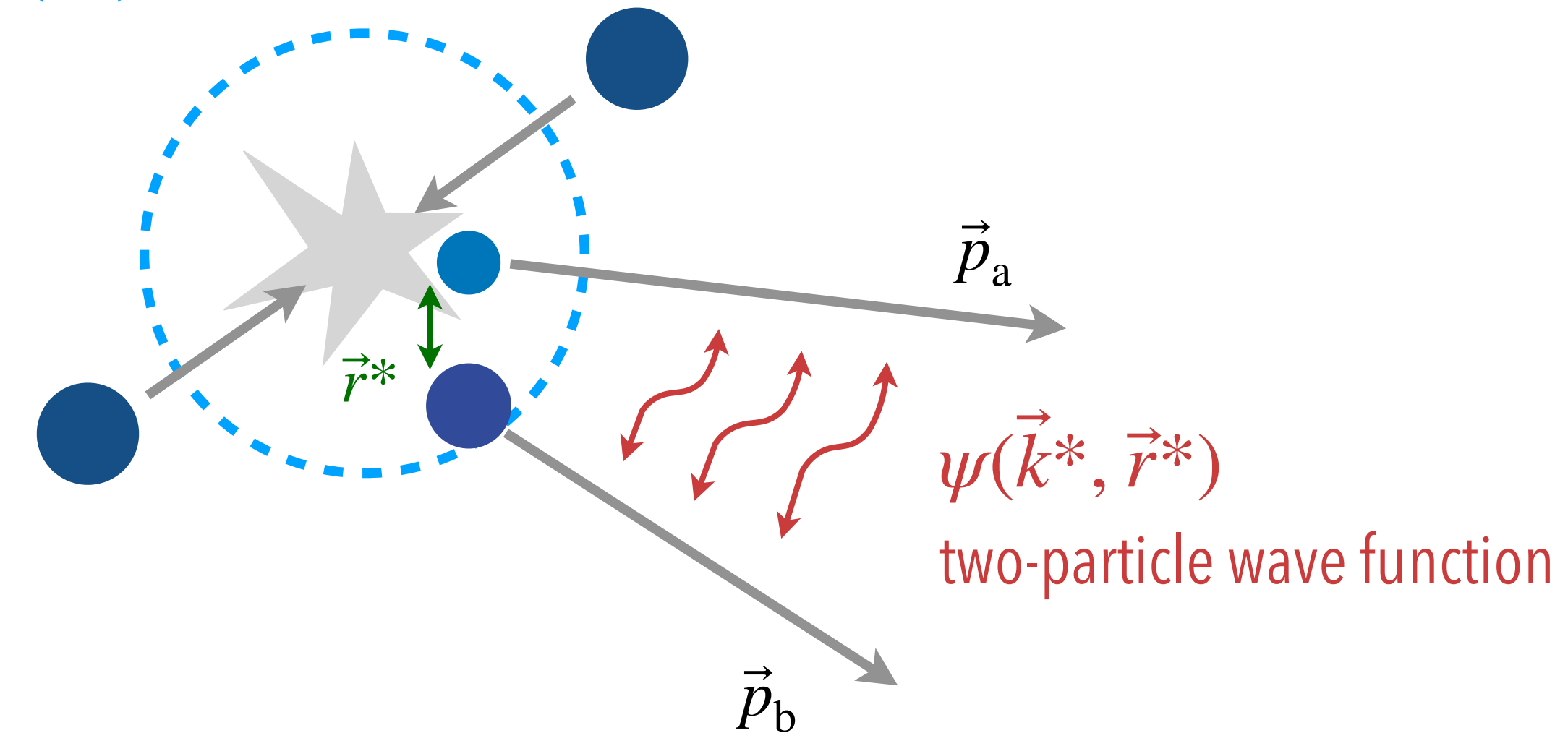
- Absence of interaction $C(k^*) = 1$
- Attractive potential $C(k^*) > 1$

$$C(\vec{k}^*) = \int S(\vec{r}^*) |\psi(\vec{k}^*, \vec{r}^*)|^2 d^3 r^*$$

→ Relative wave function sensitive to interaction potential



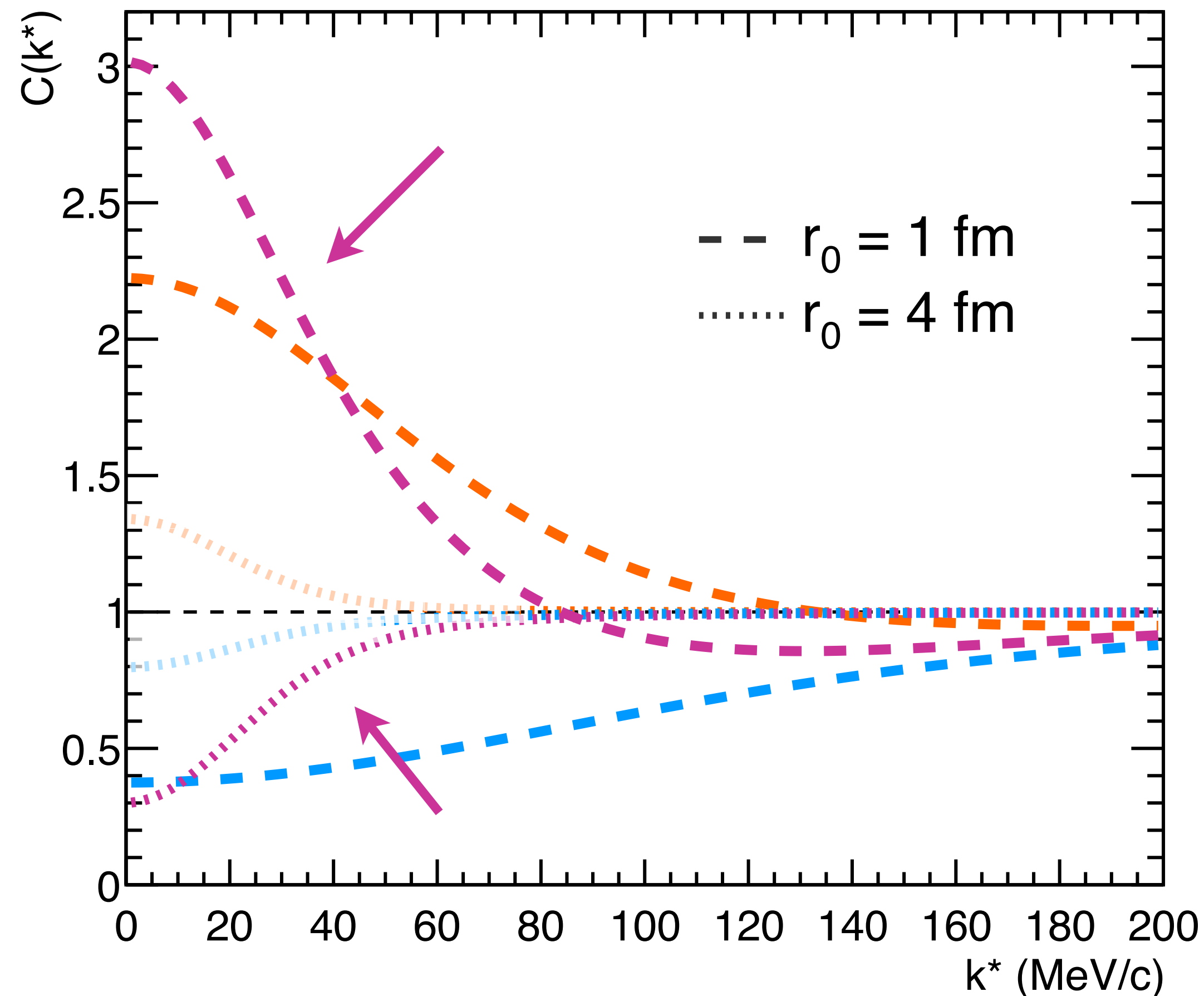
$S(\vec{r}^*)$ source function



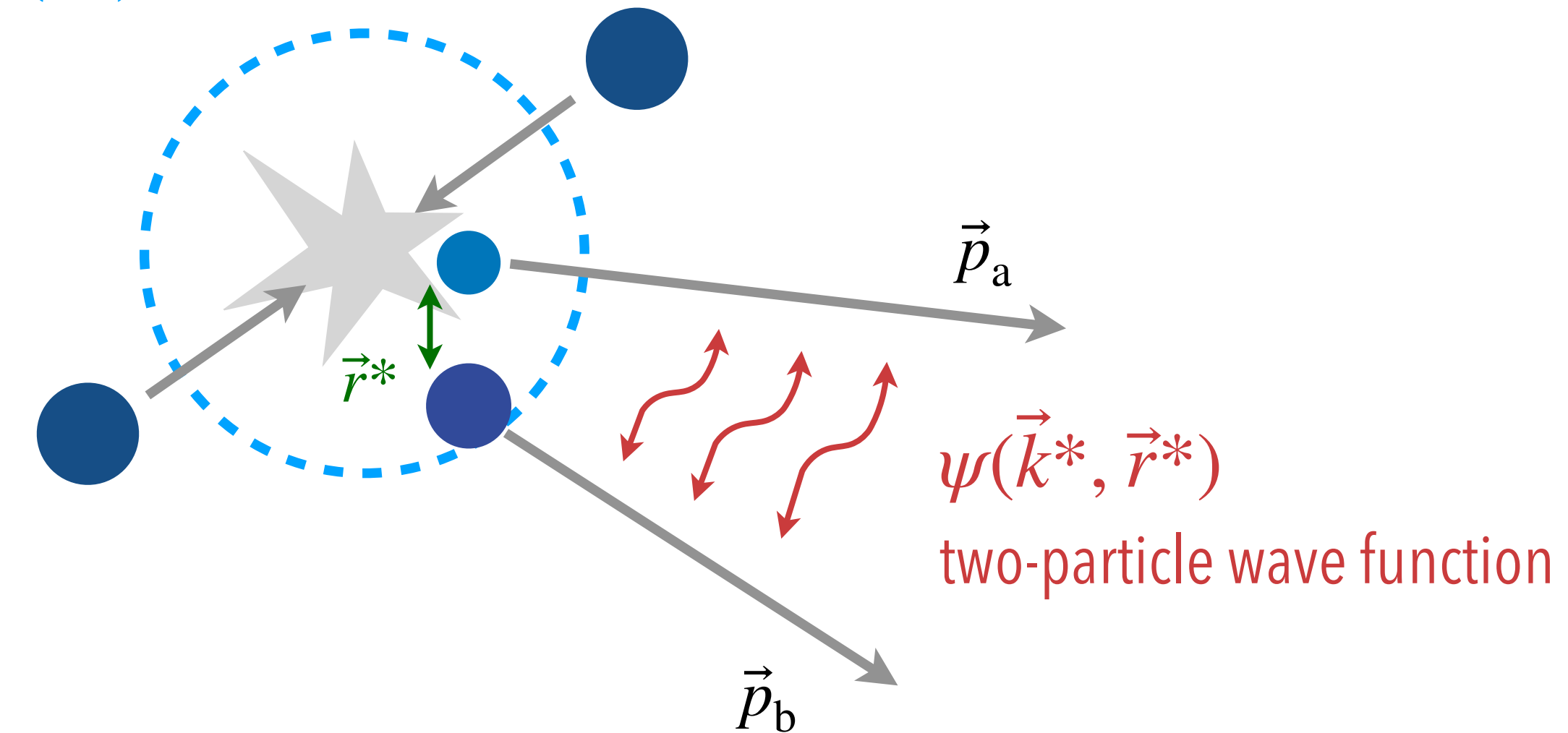
- Absence of interaction $C(k^*) = 1$
- Attractive potential $C(k^*) > 1$
- Repulsive potential $C(k^*) < 1$

$$C(\vec{k}^*) = \int S(\vec{r}^*) |\psi(\vec{k}^*, \vec{r}^*)|^2 d^3 r^*$$

→ Relative wave function sensitive to interaction potential



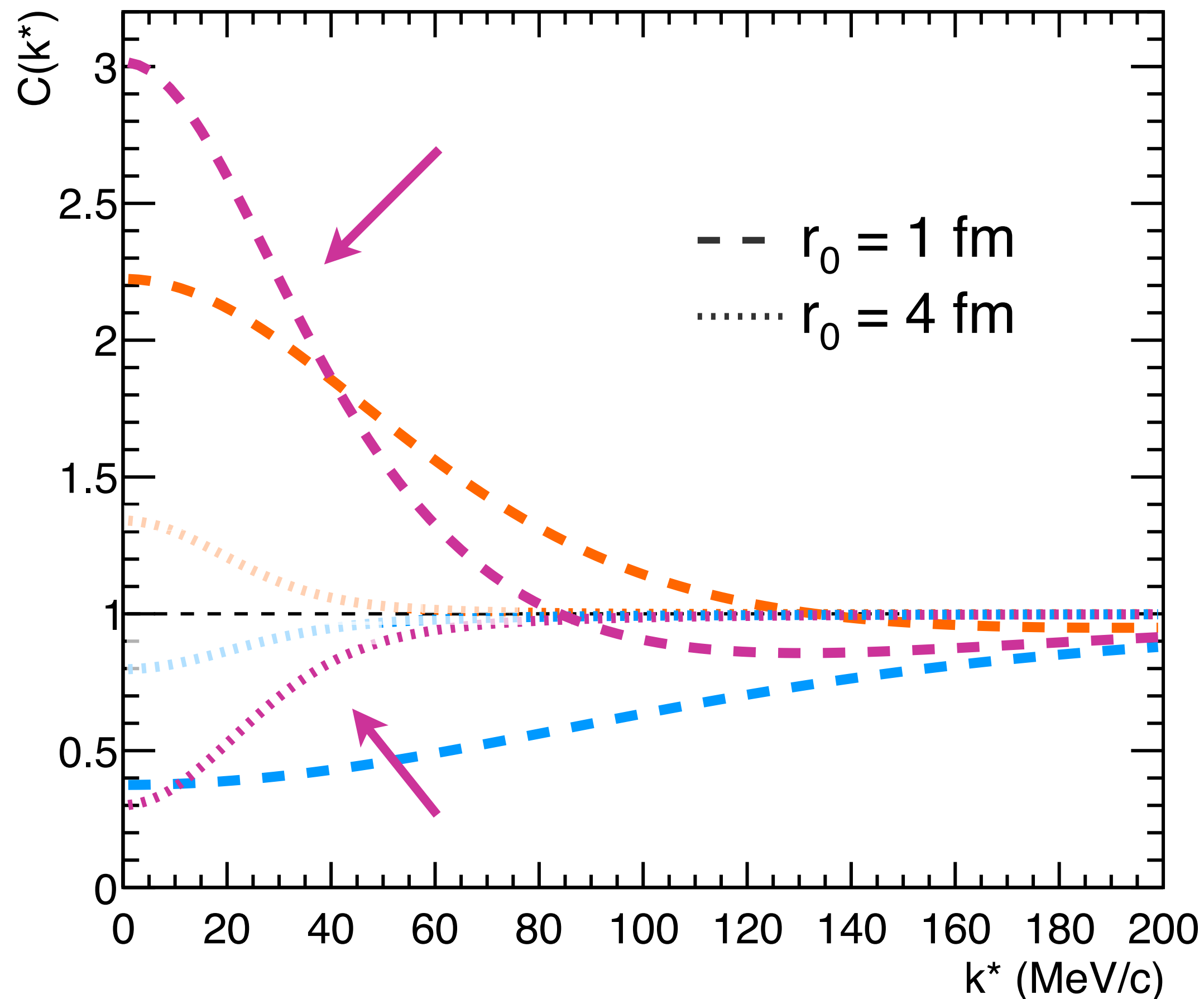
$S(\vec{r}^*)$ source function



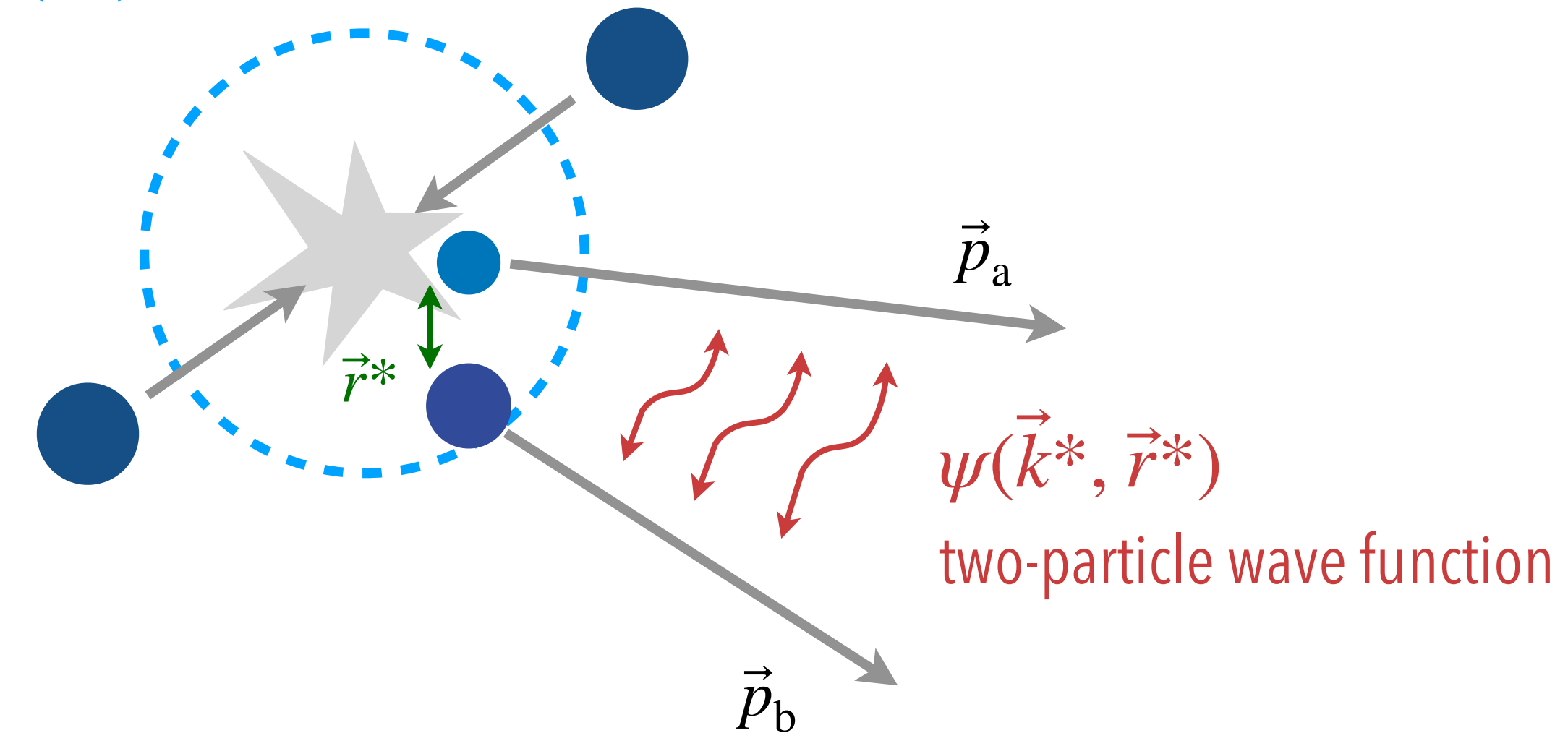
- Absence of interaction $C(k^*) = 1$
- Attractive potential $C(k^*) > 1$
- Repulsive potential $C(k^*) < 1$
- Bound-state formation $C(k^*) < > 1$

$$C(\vec{k}^*) = \int S(\vec{r}^*) |\psi(\vec{k}^*, \vec{r}^*)|^2 d^3 r^*$$

→ Relative wave function sensitive to interaction potential



$S(\vec{r}^*)$ source function



- Absence of interaction $C(k^*) = 1$
- Attractive potential $C(k^*) > 1$
- Repulsive potential $C(k^*) < 1$
- Bound-state formation $C(k^*) \ll 1$